DOCTORAL DISSERTATION

IN-PLANE SEISMIC BEHAVIOR OF FIBER CONCRETE FILLED MASONRY BRICK WALLS

Reza Amiraslanzadeh Mamaghani

July 2014

DOCTORAL DISSERTATION

IN-PLANE SEISMIC BEHAVIOR OF FIBER CONCRETE FILLED MASONRY BRICK WALLS

Graduate School of Natural Science and Technology, Kanazawa University

Major subject: Earthquake Engineering

Course: Ph.D

Student registration No: 1123142411

Name: Reza Amiraslanzadeh Mamaghani

Chief advisor: Masakatsu Miyajima

博　士　論　文

IN-PLANE SEISMIC BEHAVIOR OF FIBER CONCRETE FILLED MASONRY BRICK WALLS

ファイバーコンクリート充填煉瓦壁の地震時面内挙動

金沢大学大学院自然科学研究科

環境科学専攻

環境計画講座

Student registration No: 1123142411

Name: Reza Amiraslanzadeh Mamaghani

Chief advisor: Masakatsu Miyajima

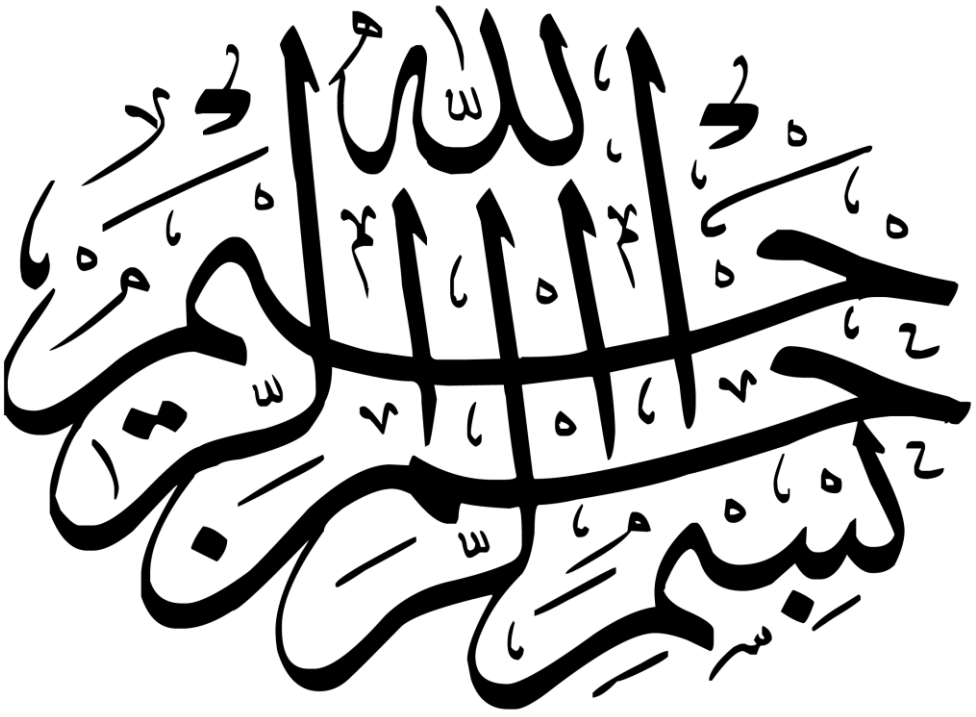

In The Name Of God, Most Gracious, Most Merciful.

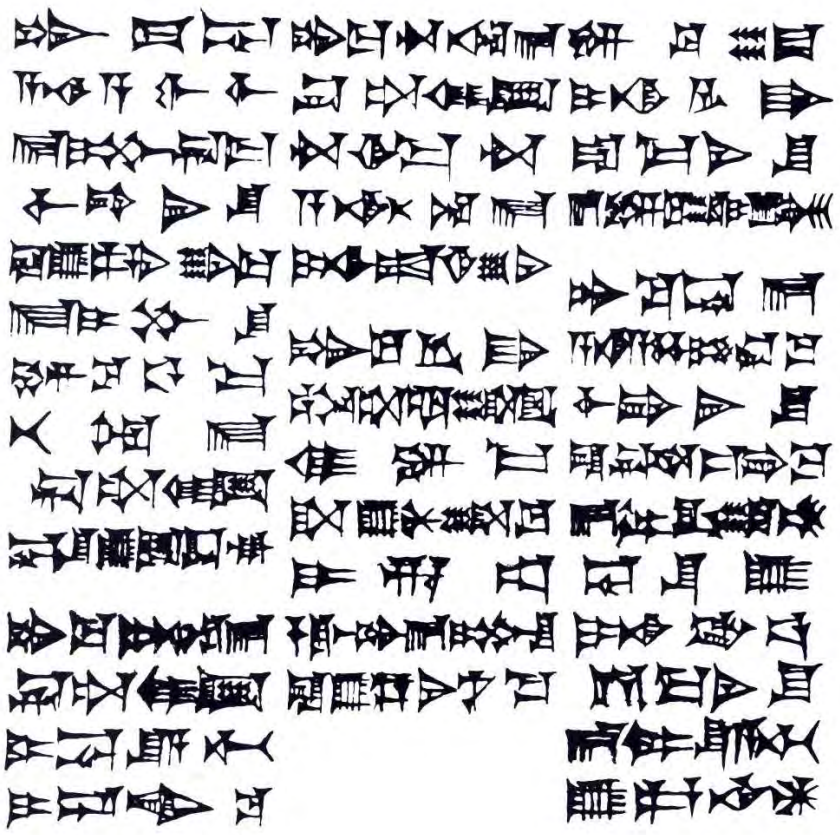

Translation:
If a builder builds a house for a man and does not make its construction firm and the house collapses and causes the death of the owner of the house, that builder shall be put to death. If it causes the death of a son of that owner, they shall put to death the son of that builder. If it causes the death of a slave of the owner, he shall give to the owner a slave of equal value. If it destroys properly, he shall restore whatever it destroyed and because he did not make the house firm, he shall rebuild the house which collapsed at his own expense. If a builder builds a house and does not make its construction meet the requirements and a wall falls in, that builder shall strengthen the wall at his own expense.

FROM THE CODE OF HAMMURABI (2200 B.C.)
(**Source:** بReinforced Masonry Engineering Handbook (Clay and CONCRETE MASONRY)پ, James E. Amrhein, Fifth Edition, Masonry Institute of Americaand CRC Press, New York, 1998).

SUMMARY

Present study deals with determination of shear and seismic parameters of reinforced and unreinforced masonry brick walls assembled with head-straight texture order. This kind of bearing walls in addition to having beautiful feature in both sides, demonstrates appropriate fastening and interlocking among the masonry units. In process of construction using this technique because of special arrangement of bricks, some regular interval voids appear all at the height of the wall. For reinforcement of this kind of walls these voids can be filled by high performance fiber concrete. In this study through filling the holes using steel fiber concrete, we tried to study the roles of these regular slim concrete columns on seismic performance and failure modes of masonry walls. Motivating above mentioned reasons this type of URM construction were introduced and eight full scale specimens were constructed and tested under diagonal compression and cyclic horizontal loads. Experimental tests carried out on triplets in order to define shear parameters of brick mortar interface, and diagonal compression test in order to define shear strength of masonry panels. According to various interpretations of the results of diagonal compression test, comparison between mentioned values and those obtained by laboratory tests on shear triplets are presented. It is concluded that filling the voids of head-straight texture masonry walls using steel fiber concrete, significantly increase shear parameters of these walls. In order to determine seismic parameters same as diagonal test four specimens (two panels without concrete cores and two panels with fiber concrete cores) with different level of pre-compression vertical load, have been designed and cyclic loading test were carried out according to evaluate in-plane shear behavior and identification of shear strength, ductility, energy dissipation and stiffness degradation of aforementioned panels. Observations following of past earthquakes have shown that piers between openings are the most vulnerable part of a masonry building. Therefore in this study height to length ratio of specimens was considered one in order to synchronizing the behavior of the model with seismic response of unreinforced and reinforced masonry piers that exhibit a flexural mode of failure. The results showed that all the specimens failed due to development of horizontal cracks from sides to the middle in the first layer from the bottom of the specimen. Comparisons were made among the results of seismic analysis of two types of masonry panels. The results evidence that existing of fiber concrete columns despite having positive effect on the shear resistance of the walls, causes significant influence of the seismic performance such as ductility and energy dissipation.

ACKNOWLEDGMENTS

The author wishes to acknowledge all those who have contributed to achieving this research work. First and foremost I offer my sincerest gratitude to Professor Masakatsu Miyajima, for accepting me in his laboratory and his supports during my study with his patience, encouragement and knowledge. I would like to express my deepest gratitude to Dr. Toshikazu Ikemoto for his heartily supports and helpful advices during my research in Earthquake Engineering Laboratory in Kanazawa University. I would also like to thank Dr. Akira Murata for his great support and valuable advices. I would like also to thank committee members of this dissertation: Professors Masakatsu Miyajima, Hiroshi Masuya, Kentaro Yamaguchi, Saiji Fukada and Toshikazu Ikemoto for their critical reading and helpful argue. I owe my deepest gratitude to Dr. Abdolhossein Fallahi for introducing and Professor Masakatsu Miyajima for accepting me as member of his Laboratory.

Acknowledgement is also toward the master and bachelor students Kazuki Akimoto, Shogo Hori, Kazuki Yamaguchi and Yoshihiro Nakashima for their valuable helps during the execution of the experimental program.

I owe a lot to my family for everything they did, and are still doing for me and specially my wife Sara, who had to put up with a lot of inconvenience during my study in Japan. I can say with confidence to my wife and my family that, I would not be who I am today without you.

Reza Amiraslanzadeh

July 2014

Table of Contents

LIST OF PHOTOS

CHAPTER 1

CHAPTER 2

CHAPTER 3

CHAPTER 4

LIST OF TABLES

CHAPTER 1

CHAPTER 2

CHAPTER 3

CHAPTER 4

LIST OF FIGURES

CHAPTER 1

CHAPTER 2

CHAPTER 3

CHAPTER 4

Chapter 5

Chapter 1. INTRODUCTION

The experience of developed and under developed countries from past earthquakes in the last decade (e.g. Loma Prieta-USA (1989), Kobe-Japan (1995), L'Aquila-Italy (2009), Bam-Iran (2003), Skopje-Macedonia (1963)) demonstrates that modern structures, built with masonry, reinforced concrete or steel, according to the present codes, might still suffer important damage or collapse due to different causes. Structural and earthquake engineers should learn from the past lessons in order to design and built structures with adequate economy and safety levels. Nevertheless, experience has demonstrated that, in general, unreinforced masonry exhibits poor performance when subjected to seismic excitations. In earthquake hazardous areas, the use of unreinforced masonry is only recommended for low-rise buildings with specific limitations. On the contrary, reinforced masonry (masonry in which bars or mesh, usually of steel, are embedded in mortar or grout so that all materials act together in resisting forces) seems to exhibit excellent behavior with respect to seismic actions [1, 2]. The most important part of masonry structures that tolerate gravity and lateral forces is load bearing walls. In brick masonry for construction of bearing walls there are special arrangement of brick units that can be used in order to obtain elegant appearance and desired thickness toward the walls. Among the methods of construction of load bearing walls the type which seems to be more appropriate (considering thickness, appearance and masonry unit fastening) is Head-straight texture order. Mentioned masonry bearing walls due to special arrangement of bricks contain internal holes that are conventionally filled with rubble material. Head-straight masonry walls due to component materials are considered as unreinforced construction that unquestionably recognized as the type of construction most vulnerable to earthquakes.

As is available in the literature review in recent decade many innovative and creative approaches have been proposed and a lot of researches have been performed in order to find out a suitable solution for strengthening and reinforcement of brick masonry construction. Some proper remedies have been provided and offered from researchers to reinforcement of brick masonry that as well as have some drawbacks and disadvantages. In this research an attempt was made to propose a suitable, effective and applicable method of reinforcement for Head-straight brick masonry walls in order to strengthen and

improve performance of this type of construction system and offer a new type of reinforced load bearing masonry wall.

1.1 An overview on historical masonry construction

Masonry construction is an age-old material that have been used since the earliest times of mankind for about at least 10,000 years in a variety of structures, homes, private and public buildings and historical monuments. This kind of construction material represents a performance of feature that was attractive for human beings. Stone as the first kind of masonry unit was used to constructs structures such as the Egyptian Pyramids, the Colosseum in Rome, India's Taj Mahal and the Great Wall of China that are some of the world's most significant architectural achievements have been built with masonry (**Photos 1.1-1.3**) [3]. Through civilization, architects and builders have selected masonry construction material for its beauty, versatility, and durability. For an instant the Egyptian pyramids were built around 2500 B.C. in Giza and over the years has remained intact. Lime-stone veneer which once clad the pyramids can now only be seen at the top of the great pyramid, Cheops, since much of limestone facing was later removed and used by the citizens [4]. Masonry is the oldest construction substance that is still used in the building industry. The most important characteristic of this type of construction is its simplicity. Laying the pieces of stone or brick units on top of each other dry or by the means of cohesive like mud or mortar has revealed its simplicity though adequate technique that has been successful ever since remote ages.

Photo 1.1 Egyptian pyramids**.**

Photo 1.2 Colosseum in Rome and Taj Mahal in India.

Photo 1.3 China great wall.

Occasionally, the masonry is also used to refer to the brick units themselves. Masonry is considered a durable construction method, and brick is one of the most common types of masonry used in industrialized nations.

1.2 Earthquake and masonry constructions

Failure of masonry structures in earthquakes causes a great loss of human and financial resources around world. Past earthquakes such as ones occurred in Pakistan (2009), China (2008) and Iran (2003) [5,6] have shown high seismic vulnerability of this kind of construction. As a tragic example, the worst death toll from an earthquake in the past century occurred in 1976 in China (T̤ang Shan province) where it was estimated that 240,000 people lost their lives [7]. Evidence from the recent earthquakes has confirmed that the overall performance of URM buildings is dependent on parameters such as the wall stability, type of roof system, quality of mortar and geometrical features [8].

As we know structures in seismically active regions should be designed and constructed in such a way that local or general collapse are prevented. "Heavy and large walls, built perpendicular and with good foundations, return to its original position, always... and suffer less damage if well connected". These preliminary observations of Pirro Ligorio in the 16th century demonstrate the concern of safety with respect to seismic actions [4,9].

As mentioned before the effect of earthquakes on structures, depends on aspects such as magnitude and dynamic characteristics of the earthquake, location of the construction, geological conditions of the soil, shape of construction, foundations, construction material, adequate design provisions, detailing of the structural elements, etc. despite this the main influence factors are: (a) regularity in plan and elevation, and (b) use of

materials adequate to provide the necessary resistance to the seismic action. In case of unreinforced masonry regrettably, numerous constructions do not comply with the above requirements. In Portugal, in 1755, the most famous earthquake of Lisbon illustrated the effects of a shake of large intensity and leads to the development of a new type of ductile and reinforced construction "the Pombaline cage"[4].

1.3 Seismic vulnerability of masonry

1.3.1 Damage classification and vulnerability of masonry buildings

European Macroseismic Scale classified the buildings in strict details as shown in **Table 1.1** and **Table 1.2** in case of earthquake vulnerability class and definition of damage level of masonry.

Table 1.1 Classification of masonry structures vulnerability based on EMS regulation [9].

TYPE OF STRUCTURE		VULNERABILITY CLASS					
		A	B	C	D	E	F
MASONRY	RUBBLE STONE, FIELDSTONE	O					
	ADOBE (EARTH BRICK)	O	—				
	SIMPLE STONE	···	O				
	MASSIVE STONE		—	O	···		
	UNREINFORCED, WITH MANUFACTURED STONE UNITS	···	O	···			
	UNREINFORCED, WITH RC FLOORS		—	O	···		
	REINFORCED OR CONFINED			···	O	—	
O	MOST LIKELY VULNERABILITY CLASS						
—	PROBABLE RANGE						
···	RANGE OF LESS PROBABLE, EXCEPTIONAL CASES						

1.3.2 EMS intensity degrees definition

According to the EMS (European Macroseismic Scale) seismic intensities are defined in twelve classes which are issued under the MSK scale modification [7]. In this new classification, the intensity definitions are based on the effects on the humans, the objects, nature and on the damage to buildings as follows [4]:

Intensity level I: **Not felt**

a) Not felt, even under the most favorable circumstances.

b) No effect.

c) No damage.

Level II: **Scarcely felt**

a) The tremor is felt only at isolated instances (<1%) of individuals at rest and in a specially receptive position indoors.

b) No effect.

c) No damage.

Level III**: Weak**

a) The earthquake is felt indoors by a few. People at rest feel a swaying or light trembling.

b) Hanging objects swing slightly.

c) No damage.

Level IV: **Largely observed**

a) The earthquake is felt indoors by many and felt outdoors only by very few. A few people are awakened. The level of vibration is not frightening. The vibration is moderate. Observers feel a slight trembling or swaying of the building, room or bed, chair etc.

b) China, glasses, windows and doors rattle. Hanging objects swing. Light furniture shakes visibly in a few cases. Woodwork creaks in a few cases.

c) No damage.

Level V: **Strong**

a) The earthquake is felt indoors by most, outdoors by few. A few people are frightened and run outdoors. Many sleeping people awake. Observers feel a strong shaking or rocking of the whole building, room or furniture.

b) Hanging objects swing considerably. China and glasses clatter together. Small, to heavy or precariously supported objects may be shifted or fall down. Doors and windows swing open or shut. In a few cases windows panes break. Liquids oscillate and may spill from well filled containers. Animals indoors may become uneasy.

c) Damage of grade 1 to a few buildings of vulnerability class A and B.

Level VI: **Slightly damaging**

a) Felt by most people indoors and by many outdoors. A few persons lose their balance. Many people are frightened and run outdoors.

b) Small objects of ordinary stability may fall and furniture may be shifted. In few instances dishes and glassware may break. Farm animals (even outdoors) may be frightened.
c) Damage of grade 1 is sustained by many buildings of vulnerability class A and B; a few of class A and B suffer damage of grade 2; a few of class C suffer damage of grade 1.

Level VII: **Damaging**
a) Most people are frightened and try to run outdoors. Many find it difficult to stand, especially on upper floors.
b) Furniture is shifted and top-heavy furniture may be overturned. Objects fall from shelves in large numbers. Water splashes from containers, tanks and pools.
c) Many buildings of vulnerability class A suffer damage of grade 3; a few of grade 4. Many buildings of vulnerability class B suffer damage of grade 2; a few of grade 3. A few buildings of vulnerability class C sustain damage of grade 2. A few buildings of vulnerability class D sustain damage of grade 1.

Level VIII: **Heavily damaging**
a) Many people find it difficult to stand, even outdoors.
b) Furniture may be overturned. Objects like TV sets, typewriters etc. fall to the ground. Tombstones may occasionally be displaced, twisted or overturned. Waves may be seen on very soft ground.
c) Many buildings of vulnerability class A suffer damage of grade 4; a few of grade 5. Many buildings of vulnerability class B suffer damage of grade 3; a few of grade 4. Many buildings of vulnerability class C suffer damage of grade 2; a few of grade 3. A few buildings of vulnerability class D sustain damage of grade 2.

Level IX: **Destructive**
a) General panic. People may be forcibly thrown to the ground.
b) Many monuments and columns fall or are twisted. Waves are seen on soft ground.
c) Many buildings of vulnerability class A sustain damage of grade 5. Many buildings of vulnerability class B suffer damage of grade 4; a few of grade 5. Many buildings of vulnerability class C suffer damage of grade 3; a few of grade 4. Many buildings of

vulnerability class D suffer damage of grade 2; a few of grade 3. A few buildings of vulnerability class E sustain damage of grade 2.

Level X: **Very destructive**

c) Most buildings of vulnerability class A sustain damage of grade 5. Many buildings of vulnerability class B sustain damage of grade 5. Many buildings of vulnerability class C suffer damage of grade 4; a few of grade 5. Many buildings of vulnerability class D suffer damage of grade 3; a few of grade 4. Many buildings of vulnerability class E suffer damage of grade 2; a few of grade 3. A few buildings of vulnerability class F sustain damage of grade 2.

Level XI: **Devastating**

c) Most buildings of vulnerability class B sustain damage of grade 5. Most buildings of vulnerability class C suffer damage of grade 4; many of grade 5. Many buildings of vulnerability class D suffer damage of grade 4; a few of grade 5. Many buildings of vulnerability class E suffer damage of grade 3; a few of grade 4. Many buildings of vulnerability class F suffer damage of grade 2; a few of grade 3.

Level XII: **Completely devastating**

c) All buildings of vulnerability class A, B and practically all of vulnerability class C is destroyed. Most buildings of vulnerability class D, E and F are destroyed. The earthquake effects have reached the maximum conceivable effects.

Table 1.2 Damage levels definition of masonry structures based on EMS [9].

Classification of damage to masonry buildings	
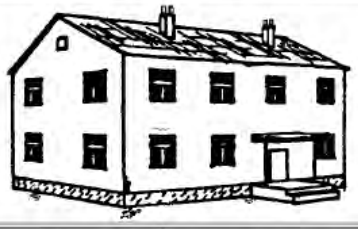	**Grade 1: Negligible to slight damage (no structural damage, slight non-structural damage)** Hair-line cracks in very few walls. Fall of small pieces of plaster only. Fall of loose stones from upper parts of buildings in very few cases.
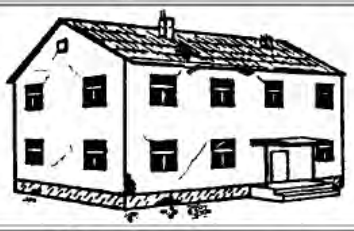	**Grade 2: Moderate damage (slight structural damage, moderate non-structural damage)** Cracks in many walls. Fall of fairly large pieces of plaster. Partial collapse of chimneys.
	**Grade 3: Substantial to heavy damage (moderate structural damage, heavy non-structural damage)** Large and extensive cracks in most walls. Roof tiles detach. Chimneys fracture at the roof line; failure of individual non-structural elements (partitions, gable walls).
	**Grade 4: Very heavy damage (heavy structural damage, very heavy non-structural damage)** Serious failure of walls; partial structural failure of roofs and floors.
	**Grade 5: Destruction (very heavy structural damage)** Total or near total collapse.

1.4 Brief description of some masonry construction systems

1.4.1 Adobe buildings

The Arg-e Bam (Persian: ارگ بم) was the largest adobe building in the world, located in Bam, a city in the Kerman Province of southeastern Iran (See **Photo 1.4**). It is listed by UNESCO as part of the World Heritage Site. The origin of this enormous citadel on the Silk Road can be traced back to the Achaemenid period (6th to 4th centuries BC) and even beyond. On 26th of December 2003, this unique structure was almost completely destroyed by an earthquake [10].

Specification of adobe buildings for a simple one story structure are: foundation made of stone and mud, bearing walls made of adobe, mud and chaff and roof made of timbers that covered by a blanket of stick woods and a layer of mud for isolation (**Photo 1.5**). This kind of construction is very popular in rural are of Middle East developing counties like Iran. As we described Adobe buildings, these structures are brittle and they cannot be persistent in case of strong ground motion. In accordance to the past earthquake reports, most of the people how injured or even dead was in an adobe building in rural area.

Failure modes in most of adobe buildings are separating bearing walls from each other in the corners and falling down surrounding walls and collapse of roof.

Based on field investigations of Ahar twin earthquakes on 11th August 2012 in East-Azerbaijan province of NW Iran most weak points of these structures are as follows [11]:

1. Lack of any effective connection between bearing walls and roof (**Photo 1.6**).

2. Lack of any effective connection between roof timbers that allows them to behave separately (**Photo 1.7 a**).

3. Decay of the timbers (main beam of roof) that are very potential for collapse even under the gravity loads (**Photo 1.7 b**).

4. Thick layer of mud on the roofs (for isolation) that increases earthquake effective force to the structure (**Photo 1.8**).

Photo 1.4 Arg-e bam in Iran was destroyed in 26th December 2003.

Photo 1.5 Description of adobe building.

Photo 1.6 Lack of effective connection of the roof to the timbers.

Photo 1.7 a: Lack of effective connection among timbers **b**: Decay of the roof to the timbers.

Photo 1.8 Thick layer of mud on the roof.

1.4.2 Stone masonry

Stone has been used in building construction all over the world since ancient times because of its durable and locally available. There are huge numbers of stone buildings in the country, ranging from rural houses to royal palaces and temples. This kind of construction can be divided into three types as follows:

1.4.2.1 Rubble stone masonry

Rubble masonry is rough, uneven building stone set in mortar, but not laid in regular courses. This method of construction is the most traditional constructions in which undressed stones are used as the basic building material, usually with poor quality mortar, leading to buildings which are heavy and have little resistance to lateral loading. Floors are typically of wood, and provide no horizontal stiffening [4]. Structure may appear as the outer surface of a wall or may fill the core of a wall which is faced with unit masonry such as brick or cut stone.

1.4.2.2 Simple stone masonry

This kind of construction is different from fieldstone construction in that the building stones have undergone some dressing prior to use. These hewn stones are arranged in the process of construction of the building according to some techniques to improve the strength of the structure, using larger stones to tie in the walls at the corners [4].

1.4.2.3 Bulk stone masonry

Bulk stone masonry is a construction in which very large stones used. This method of construction is usually restricted to monumental constructions, castles, large civic buildings, etc. Special buildings of this type such as cathedrals or castles would not normally be used for intensity assessment because in the case of a row of buildings in an urban block, it is often those structures at the end of a row or in a corner position that are worst affected. One side of the structure is anchored to a neighbor while the other is not, causing an irregularity in the overall stiffness of the structure which will lead to increased damage. However, some cities contain areas of 19th century public buildings of this type

which could be used for intensity assessment. These buildings usually possess great strength, which contributes to their good vulnerability class [4 ,7].

1.4.3 Brick masonry buildings

In brick masonry building walls are made of fired clay bricks and the roof is made of steel beams and brick arches or reinforced concrete floor. This type of construction is very common type of in the archetypal "B" type of building in the European Macroseismic Scale (EMS). It worth noting that Eurocode 8 referred such construction is to under the heading of "manufactured stone units". It is characteristic of this building type that no special attempts have been made to improve the horizontal elements of the structure, floors being typically of wood and therefore flexible. In general, the vulnerability is affected by the number, size and position of openings. Large openings, small piers between openings and quoins as wells as long walls without perpendicular stiffening contribute to a more vulnerable building [4].

1.4.4 Confined brick masonry buildings

In case of confined brick masonry the walls are confined by concrete tie beams and columns to improve in-plane and out-of-plane ductility and energy dissipation. In this kind of structure at first walls are made by considering the places of tie columns. After that by reinforcing, molding and placing concrete to the columns this procedure is finished. Then tie beams are made on the top of the walls to make good integration between the components. Evidence of past earthquake showed that unlike brick masonry, confined masonry buildings do not experienced severe damage or total collapse except large numbers of serious cracks and detachments on the walls and wall-roof connections.

1.5 Literature review of current researches on brick masonry

The earlier research works on brick masonry can be classified into two different categories: first being the study of unreinforced brick masonry and its assemblages and second the effect of reinforcement on mechanical parameters as well as in-plane seismic behavior of the brick masonry wall. In this part some recent reports of the performance of unreinforced and reinforced brick masonry is presented and discussed.

Brick masonry wall

M.Rosa et al [12] suggested a strengthening method based on the attachment of steel bars in the bed joints. It is particularly suitable for regular brick masonry showing a critical crack pattern due to high compressive loads. Experimental investigation and numerical analyses indicated that the existence of the bars allowed control of the cracking phenomena, keeping the structure in the preferred safety conditions. Both experimental and numerical analyses showed that the most significant result concerns the reduction of the tensile stresses in the bricks and of the dilatancy of the wall.

X. Jianzhuang et al [13] developed cyclic loading test on three new types of sandwich masonry walls. The walls were classified into three categories denoted by A, B and C according to their masonry cohesion patterns and construction details, and they were laid up by three types of bricks, respectively. The following measures were taken in the construction of the walls to ensure cooperation between the two leaves. A header course was added to every three stretcher courses in Category A, a prefabricated steel mesh composed of two longitudinal bars connected by diagonal bars was embedded in the mortar of every three bed joints in Category B, and the bricks in Category C overlapped each other. Apparently, the header courses in Category A and the steel meshes in Category B worked as transverse connectors, and the distinctive masonry bond pattern of Category C helped the two leaves of the wall work together. Five specimens were constructed and tested. The results showed that the specimens failed mainly due to slippage along the bottom cracks or the development of diagonal cracks, and the failure patterns were considerably influenced by the aspect ratio. Comparisons were made between the experimental results and the calculated results of the shear capacity. It is concluded that the formulas in the two Chinese codes (GB 50011 and GB 50003) are suitable for the calculation of the shear capacity for the new types of walls, and the formula in GB 50011 tends to be more conservative.

Gabor [14] studied the shear behavior of hollow brick masonry panels. The panels were subjected to horizontal loading and the out of plane failure and the diagonal tensile failure was studied. Finite element modeling was done with the elasto-plastic properties of the mortar joints cohesion, and residual friction was studied. It was concluded that finite element modeling approaches with a good accuracy with respect to the behavior of masonry panels, ultimate loads, ultimate strains, plastic strain evolution and failure modes.

N. Sathiparan et al [15] conducted a series of diagonal compression tests and out-of plane tests using non-retrofitted and retrofitted wallettes by polypropylene (*PP*) band meshes. The retrofitted wallettes achieved 2.5 times larger strengths and 45 times larger deformations than the non-retrofitted wallettes did. In out-of plane tests, the effect of mesh was not observed before the wall cracked. After cracking, the presence of mesh positively influenced the behavior wallettes. In the retrofitted case, although the initial cracking was followed by a sharp drop at least 45% of the peak strength remained. After this, the strength was regained by readjusting and packing by PP band mesh. The final strength of the specimen was equal to 1.2kN much higher than initial strength of 0.6kN. The retrofitted wallettes achieved 2 times larger strengths and 60 times larger deformations than the non-retrofitted wallettes.

P. Agarwal and Thakkar [16] demonstrated the differences in the behavior of brick masonry model subjected to either shock table motion or quasi-static loading. The shock model responds with a significantly higher initial strength and stiffness as compared to the quasi-static model subjected to equivalent lateral displacements. Severity of damage was greater in quasi-static test due to increased crack propagation. The shock test suggested that at low levels of excitation at the base, acceleration gets amplified at the roof, with an almost elastic behavior of the model. Marked reduction in both strength and stiffness has been observed when the model was loaded statically rather than dynamically. The crack patterns obtained under both the test methods were nearly similar.

Turco et al [17] reported the results of an experimental program under three phases; in the first phase mechanical properties of the materials used were determined. Then, the fiber reinforced polymer bars technique was used to strengthen unreinforced masonry walls to resist out-of-plane forces (second phase) and in-plane forces (third phase). Basically, glass and carbon FRP bars, having a rectangular and circular cross-section, and with a smooth or twisted sand-coated finish, were used as reinforcement. They were mounted vertically or horizontally into two different embedding materials: latex modified cementitious paste and an epoxy-based paste. Two kinds of masonry type, built with clay and concrete masonry units, were also considered. The walls exhibited the following modes of failure: (1) de-bonding of the fiber reinforced polymer reinforcement and (2) shear failure in the masonry near the support. The specimens were diagonally loaded and tested in a closed loop fashion. The force was applied to the wall by steel shoes placed at the top corner, and transmitted to similar shoes at the bottom corner through high strength steel bars. Linear variable displacement transducers were placed diagonally along the wall

to monitor deformations. The failure of the control wall was brittle, controlled by bonding between the masonry units and mortar. Some materials came loose after reaching the ultimate load. Strength and pseudo-ductility substantially increased; the capacity by a factor of up to 2.5 in the case of shear strengthening and by 4.5-26 times in the case of flexural strengthening. The glass fiber reinforced polymer in spite of its low elastic modulus, had proved to be a good material for masonry strengthening: often the performances were better than those obtained using the carbon fiber reinforced polymer.

N. Ismail et al [18] developed some experimental test on unreinforced masonry wallets strengthened using twisted steel bars. The in-plane shear behavior of URM wallettes strengthened using near surface mounted high strength twisted stainless steel reinforcement was investigated and in particular, the effectiveness of the reinforcing schemes to restrain the diagonal cracking failure mode was studied. A total of 17 URM wallettes, each being 1.2 m × 1.2 m in size, were tested in induced diagonal compression. Several parameters pertaining to the in-plane shear behavior of strengthened URM walls were investigated, including failure modes, shear strength, maximum drift, pseudo-ductility, and shear modulus. From this research it was inferred that as-built tested wallettes exhibited sudden post-peak strength degradation and failed along a stepped diagonal joint crack, whilst strengthened wallettes failed along distributed diagonal cracks in a more ductile fashion and exhibited a shear strength increment ranging from 114% to 189%.

Agbabian et al [19, 20] 1984; Abrams 2001 discovered that rocking piers in unreinforced masonry (URM) walls have been largely recognized as deformation-controlled ductile elements in comparison to more brittle shear-critical masonry piers. They found that rocking mechanism is more suitable for medium height buildings, with low density of walls where rocking of piers allows larger displacement of the building without significant damage to the pier and is regarded as a reliable system to provide a desired level of performance. They demonstrate that in rocking process the system has a much lower equivalent stiffness than before the starting of the rocking which helps to reduce the inertial forces as the response is shifted to a less demanding portion of the acceleration spectra.

M. Elgawady et al [21] demonstrated preliminary comparisons between the test results of the dynamic and static cyclic tests. The test specimens are half-scale specimens built using half-scale hollow clay masonry units and weak mortar. The specimens, before and

after retrofitting, are subjected to a series of either synthetic earthquakes or static cyclic test runs. The tests showed that the composites improve the cracking and ultimate load of the retrofitted specimen by a factor of 3 and 2.6, respectively. The lateral resistance of the reference specimen measured in the static cyclic tests is 1.2 times the lateral resistance of the similar reference specimen measured in the dynamic test. In spite of relatively poor mortar, the specimen friction coefficient exceeded 1.0. However, after heavy damage and a drift of about 2% the specimen coefficient of friction reduced to 0.7. The initial stiffness for the reference and retrofitted specimens was approximately the same in the static cyclic and dynamic tests. The lateral resistance of the reference specimen in the static cyclic test is approximately 20% higher than the lateral resistance in the dynamic test.

1.6 Research gap

As mentioned before the main concern of current studies in masonry field is promotion and upgrading the performance of unreinforced masonry. Too many suggestions have been made in order to enhance mechanical properties of this kind of construction system but each of mentioned procedures has its own disadvantages and limitations due to component material shape and properties, expected thickness of the walls and structural contribution of masonry part on load bearing of all structure. In brick masonry bearing walls are the most important part of masonry structures that tolerate gravity and lateral forces. For construction of bearing walls there are special arrangement of brick units that can be used in order to obtain beautiful appearance and desired thickness toward the walls (See **Figure 1.1**). For load bearing walls the thickness of masonry is typically larger than the length of the unit. On the other word, two masonry units are used on the width of the wall leading to some unique types of brick order. Previous studies in this regard (brick masonry construction) have not considered the thickness and available texture arrangement of bricks that is suitable for ordinary brick masonry construction.

Among the methods of construction of load bearing walls the type which seems to be more appropriate (considering thickness, appearance and masonry unit fastening) is Head-straight texture order. Using this order thickness of the wall, varies between 30 to 40 cm depended on the unit length. For construction of brick walls via mentioned technique, each header is centered on the stretcher above and below. In other words, bond, consisting of alternate headers and stretchers in each course is constructed. In front side at first brick by length of three-quarters is placed straight along the wall stretches. Then next unit is placed perpendicular to the head joint of the first unit. This procedure

continues along the wall stretches using full size brick units and will again end to a three-quarters straight brick unit. Back side of the wall has a simple head-straight order but using full size bricks. The order of front and back side of the wall in next layer has the inverse order of first layer (**Figure 1.2**).

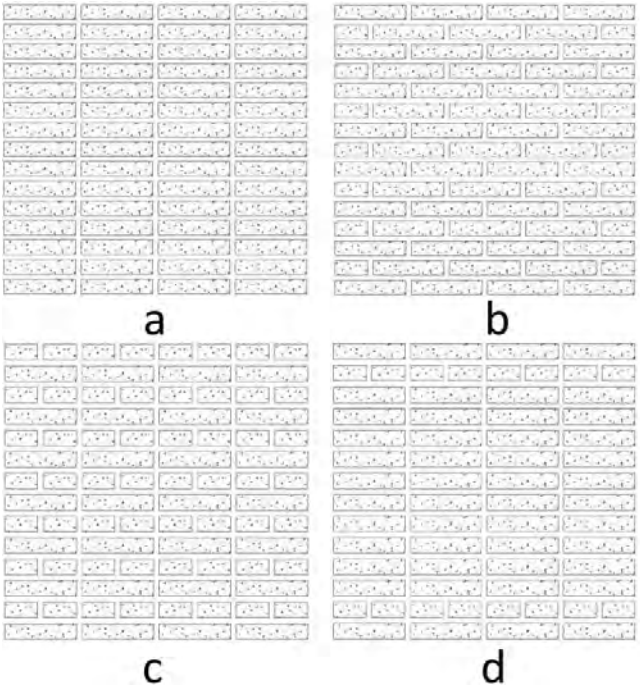

Figure 1.1 Various types of texture orders for brick masonry: (a) stack bond, (b) stretcher bond, (c) English (or cross) bond, (d) American (or common) bond.

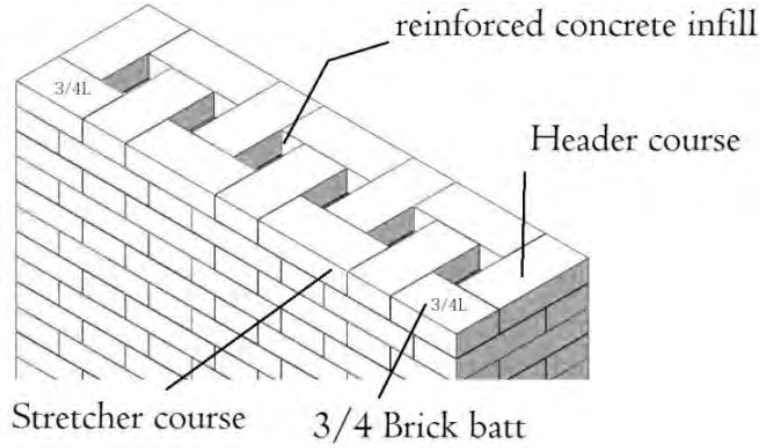

Figure 1.2 Head-straight texture order of brick wall.

As mentioned more studies have been implemented in recent decades in order to evaluate and characterize seismic behavior and performance of this structural element [12, 22] but a few of these empirical programs was considered thickness of the wall and texture order

corresponded to a load bearing walls width. As it is obvious this kind of bearing walls in addition to having beautiful feature in both sides, demonstrates appropriate fastening and interlocking among the masonry units. Like other types of brick masonry walls due to brittle behavior and low amount of tensile strength, Head-straight ordered walls considered as unreinforced masonry category, which involving the restrictions and limitations for construction in earthquake prone area. As mentioned due to special arrangement of bricks some interval voids appears all at the height of the walls that counts as the unique feature of mentioned walls which can be exploited as a proper place for reinforcement. In this study by filling mentioned holes using steel fiber concrete, we tried to study the roles of these regular slim concrete columns on strengthening, seismic performance and failure modes of masonry walls.

1.7 Research Objective

For reinforcement of Head-straight texture order masonry walls, the internal voids of mentioned masonry (that were produced due to the arrangement of brick units) can be filled by high performance fiber concrete. Motivating above mentioned reasons, experimental program have been established and specimens were classified into two categories denoted by URM (for the walls were laid up by Head-straight order without in-filled fiber concrete cores) and CRM (for Head-straight order with inner fiber concrete cores). For investigation of mechanical properties and seismic behavior of Head-straight masonry walls diagonal compression and lateral cyclic test have been performed. Due to various types of interpretation of diagonal test, the accuracy of the mentioned results was evaluated compared with triplet test which counts as a straight forward test procedure for determination of shear parameters. For each of mentioned categories two analogous specimens were built with the same masonry cohesion pattern and construction details.

Observations following of past earthquakes and experimental programs have shown that piers between openings are the most vulnerable part of a masonry building and the failure of such piers is due in the majority of cases to flexural or diagonal tension (See **Figure 1.3**). Accordingly, in this study concerning the dimension of masonry, height to length ratio of specimens was considered one in order to synchronizing the behavior of the model with seismic response of unreinforced and reinforced masonry piers that exhibit a flexural mode of failure.

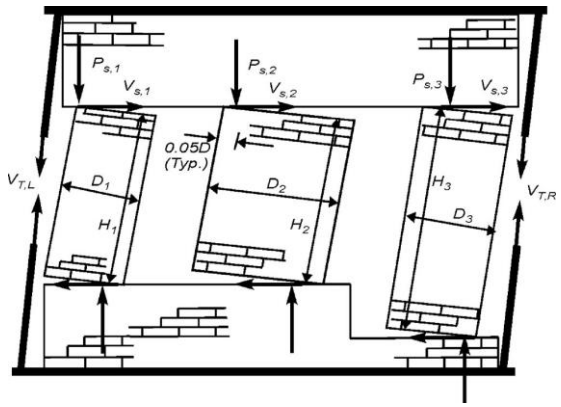

Figure 1.3 Shear behavior of rocking piers.

With regard to cyclic test for performing a foundation, all specimens were placed on a mold with certain dimensions including a prefabricated mesh rebar. The foundation concrete was placed until the second layer of the wall from the bottom. Ultimately loading concrete beam (with two holes to install loading utilities) was mounted on the top of the wall.

Experimental results were obtained, including failure modes, force-displacement hysteresis curves, shear behavior and envelope curves of force-displacement diagrams. Through experimental data analysis, a monographic investigation was performed to characterize seismic performance of mentioned walls, such as energy dissipation, pseudo-ductility and stiffness degradation.

1.8 Thesis Organization

This dissertation was organized in five chapters based on the steps followed during the research period.

A general overview on historic masonry buildings, a brief description of types of masonry construction and its seismic vulnerability in line with literature review of recent investigations on brick masonry walls were introduced in Chapter 1.

Chapter 2 discusses in detail about brick masonry construction type, material properties and mechanical behavior of masonry component in line with plane masonry characteristics failure modes and required standard.

Chapter 3 deals with the structural behavior of unreinforced masonry brick wall. In particular, in-plane mechanical characteristic and failure modes of unreinforced brick walls were investigated based on previous experimental studies and earthquake experiences. Furthermore the retrofit policies and available conventional rehabilitation

techniques for unreinforced masonry based on the structural effectiveness and other remarkable parameters of retrofitting techniques, performance of them was compared to each other and provided in this chapter.

Chapter 4 illustrates the experimental results of all performed tests and analysis conducted in the current study based on the introduced strategies in this chapter. The outcome of conducted experimental program and discussion of obtained results were explained in this chapter

The summary, major finding and conclusion remarks of this research were described in Chapter 5. Also, recommendations for future studies were mentioned in this section.

1.9 References

[1] Bezelga, A.A.: ،Housing characterization and technical-economical estimation، UTLINCM, (1984).

[2] Eurocode 6.: ،Desi gn of masonry structures. part 1-1. : General rules for buildings. Rules for reinforced and unreinforced masonry، ENV1996-1-1: 1995, (1995).

[3] D. Oliveira "experimental and numerical analysis of blocky masonry structures under cyclic loading" PhD Thesis, University of Minho, Portugal (2002).

[4] A. Bourzam, Shear capacity prediction of confined masonry walls subjected to cyclic lateral loading, PhD thesis, Kanazawa University, Japan (2009).

[5] Mostafaei, H., Toshimi, K. (2004). Investigation and analysis of damage to buildings during the 2003 Bam earthquake. Bull, Earth, Res, Inst, Univ. Tokyo, Vol.79, pp. 107-132.

[6] Shibaya, A., Ghayamghamian, M., Hisada,Y. Building damage and seismic intensity in Bam city from the 2003 Bam, Iran, earthquake. Bull, Earth, Res, Inst, Univ. Tokyo, Vol.79, pp. 81-93 (2004).

[7] EMS-98: ،European Macroseismic Scale, Gr ىnthal، G. (ed.), European Seismological Commission, (1998).

[8] G. Zamani Ahari, "Structural in-plane behavior of masonry walls externally retrofitted with fiber reinforced materials" PhD thesis, Kyushu university, Japan (2013).

[9] Ligorio, P.: ،Mea sures for the safety of buildings against earthquakes، quoted in Latina, C., Load bearing masonry walls (in Italian), Laterconsult, (1994).

[10] http://en.wikipedia.org/wiki/Arg-%C3%A9_Bam.

[11] R.Amiraslanzadeh, M. Miyajima, A.Fallahi, A. Sadeghi and S.Karimzadeh ،Re port of 11th August 2012 Ahar twin earthquakes in East-Azerbaijan province of NW Iran، International Symposium on Earthquake Engineering, JAEE, Vol.1, Tokyo, Japan (2012).

[12] Maria Rosa, Valluzzi , Luigia Binda, Claudio Modena, Mechanical behaviour of historic masonry structures strengthened by bed joints structural repointingپ Construction and Building Materials, 19, pp 63ت73 , (2005).

[13] X. Jianzhuang, P. Jie and H. Yongzhong, Experimental study on the seismic performance of new sandwich masonry walls Vol.12, No.1 Earthquake Engineering and Engineering Vibration (2013).

[14] Gabor A, Ferrier E, Jacquelin E and Hamelin P, Analysis and modeling of the in-plane shear behavior of hollow brick masonry panel. Construction and Building materials, 20, pp 308 ت321(2006).

[15] N. Sathiparan, P. Mayorco, K. N. Guragain and K. Meguro, Experimental study on In-plane and Out-of-plane behaviour of masonry walletes retrofitted by PP Band meshes, Seisan Kenkyu, 57(6), pp 530- 533(2005).

[16] Pankaj Agarwal and Thakkar S K, A comparative study of brick masonry house model under quasi-static and dynamic loading, ISET Journal of Earthquake Technology, 38, pp 103 ت122 , (2001).

[17] Turco, V., بThe NSM GFRP Bars Method for Strengthening of Masonry Walls: Experimental Analysis on the Influence of the Embedding Materialپ, Degree Thesis, Department of Construction and Transportation, University of Padua, Italy, October 2002.

[18]N. Ismail, R. B. Petersen, M. J. Masia, J. M. Ingham, Diagonal shear behavior of unreinforced masonry wallettes strengthened using twisted steel bars, Construction and building materials, No. 25 pp. 4386-4393, (2011).

[19] Abrams, D. P بPer formance-based engineering concepts for unreinforced masonry building structures.پ Prœ. Struct. Eng. Mater., 4(3), 320ت331 (2001).

[20] Agbabian, M. S., Barnes, S. B., and Karioitis, J. C بMethodology for mitigation of seismic hazards in existing unreinforced masonry buildings: The methodology.پABK-TR-08, National Science Foundation, Washington, (1984).

[21] Mohamed Elgawady, Pierino Lestuzzi, Marc Badoux, Dynamic Versus Static Cyclic Tests of Masonry walls before and after Retrofitting with GFRP, 13th World Conference on Earthquake Engineering, Vancouver B C , Canada, August 1-6, Paper No 2913 (2004).

[22] Deyuan Zhou, Zhen Lei, Jibing, In-plane behavior of seismically damaged masonry walls repaired with external BFRP Wang, Composite Structures 102 9ت19 (2013).

Chapter 2. Material and masonry mechanical properties

2.1 Introduction

Brick masonry essential materials are almost composed of brick units and mortar. These materials are assembled into a quasi-homogeneous structural system. As we know a wide variety of masonry materials are exist in around the world leading to numerous mechanical properties of mentioned materials. Therefore it is very important to classify and characterize specifications and mechanical behavior of all masonry units. On the other point of view, understanding the behavior of mentioned masonry is vital and essential due to realize the behavior of a masonry structure.

2.2 Masonry materials requirements

As mentioned before a wide variety of masonry types around the world are used for construction, from traditional types (adobe and stone masonry) to the modern ones, using high quality bricks or block masonry units. This kind of construction system further subdivide into, (a) Unreinforced masonry, consisting of mortar and masonry units, (b) Confined masonry, consisting of masonry units, mortar, reinforcing steel and concrete, and (c) Reinforced masonry, composed of masonry units, mortar, reinforcing steel and grout or concrete infill [1].

2.2.1 Brick units

Brick is a block unit of a kneaded clay soil, sand and lime, or concrete material, fire hardened or sun dried, used in masonry structures. This type of construction material can be produced in numerous types, materials, and sizes which vary with region and time period. Two most basic categories of brick are fired and non-fired brick. The most numerous kind of bricks are fired brick that are laid in courses together to make a durable structure. Fired brick are one of the longest lasting and strongest construction materials sometimes referred to as artificial stone and have been used since around 5000 BC. Sun dried bricks have a history much older than fired bricks, are known by the synonyms mud brick or adobe units, and have an additional ingredient of a mechanical binder such as chaff [2].

Normally, brick contains the following ingredients:

1. Alumina (clay) ت20% to 30% by weight
2. Silica (sand) ت50% to 60% by weight
3. Lime ت2 to 5% by weight
4. Iron oxide ت≤ 7% by weight
5. Magnesia تless than 1% by weight [3].

Masonry brick units exist in different forms as illustrated in **Figure 2.1.** Appearance and the quality degree of brick units are usually defined by national standards or codes, which different among the countries that limit the use of the masonry units, depending on the seismic zone and brick types.

With regard to the differences in various national codes, only some general requirements concerning the use of different units in earthquake prone areas will be presented.

Bricks are produced in various classes. With regard to the appearance, size and total volume of holes, volume of each hole, area of any hole as summarized in **Table 2.1**, European Committee for Standardization chapter 6 (Eurocode 6) classifies brick units into four classes.

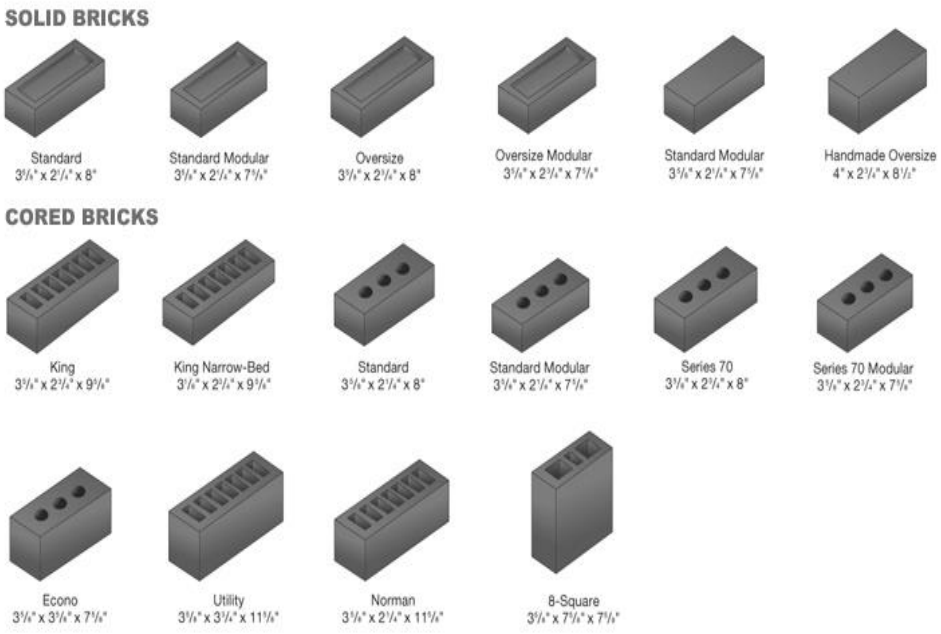

Figure 2.1 Regular shape and size of masonry brick and blocks.

Table 2.1 Classifying masonry units and requirement according to Eurocode 6.

	Group of masonry units			
	1	2a	2b	3
Volume of holes (% of the gross volume)[1]	≤25	>25-45 for clay units, >25-50 for concrete aggregate units	>45-55 for clay units, > 50-60 for concrete aggregate units[2]	≤70
Volume of any holes (% of the gross volume)	≤12.5	≤12.5 for clay units, ≤25 for concrete aggregate units	≤12.5 for clay units, ≤25 for concrete aggregate units[2]	Limited by area (see below)
Area of any hole	Limited by volume (see below)	Limited by volume (see below)	Limited by volume (see below)	≤2800 mm^2 except units with a single hole should be ≤18000 mm^2
	≥37.5	≥30	≥20	No requirement

Notes:
1. Holes may consist of formed vertical holes through the units or frogs or recesses.
2. If there is national experience, based on tests, that confirms that the safety of the masonry is not reduced unacceptably when a higher proportion of holes is incorporated, the limit of 55 % for clay units and 60 % for concrete aggregate units may be increased for masonry units that are used in the country with the national experience.
3. The combined thickness is the thickness of the webs and shells, measured horizontally across the unit at right angles to the face of the wall.

As mentioned before the size of bricks varies among the countries but typically size is summarized and shown in **Table 2.2**. The "nominal size" is that the "work size" of the brick plus the nominal thickness of the mortar joint, usually 10 *mm* [1].

Table 2.2 Nominal and working size of masonry blocks.

Coordinating size [1] (length × height) (*mm*)	Work size (length × height) (*mm*)	Work size (Thickness) (*mm*)
225 × 112.5[2]	215 × 102.5	65
400 × 200	390 × 190	60, 75, 90, 100, 115, 140, 150, 190, 200
450 × 150	440 × 140	60, 75, 90, 100, 140, 150, 190, 200, 225
450 × 200	440 × 190	60, 75, 90, 100, 140, 150, 190, 200, 220
450 × 225	440 × 215	60, 75, 90, 100, 115, 125, 140, 150, 175, 190, 200, 215, 220, 225, 250
450 × 300	440 × 290	60, 75, 90, 100, 140, 150, 190, 200, 215
600 × 150	590 × 140	75, 90, 100, 140, 150, 190, 200, 215
600 × 200	590 × 190	75, 90, 100, 140, 150, 190, 200, 215
600 × 225	590 × 215	75, 90, 100, 125, 140, 150, 165, 200, 215, 225, 250

Notes:
1. Coordinating size = Work size + 10 *mm*
2. Brick units

Beside this, Eurocode 8 (European guideline for design of structures for earthquake resistance) provides further requirements for hollow units used for earthquake resistant masonry construction as below:

1- The brick units have less than 50% holes (in % of gross volume)
2- Minimum thickness of shells is 15 *mm*
3- The vertical webs in hollow and cellular units extend over the entire horizontal length of the unit.

2.2.2 Mechanical properties of brick units

Minimum value of compressive strength of masonry units according to Eurocode 8 is 2.5 *MPa*. This amount is determined about 7.5 *MPa* for hollow clay units and concrete blocks. Normalized compressive strength is suggested by Eurocode 6 for design purpose. Normalized compressive strength is the mean value that determined by testing of at least ten air dried equivalent specimens by the dimension of 10×10 cm that cut from masonry brick units. Beside the mentioned values for compressive strength, BS EN 771-1-6 standard (specification for Masonry Units) for various types of masonry brick units gives the minimum values of compressive strength as follows:

· Clay units: min σ_b=2.5 *MPa*
· Calcium silicate units: min σ_b =5.0 *MPa*
· Concrete units: min σ_b =1.8 *MPa*
· Autoclaved aerated concrete units: min σ_b =1.8 *MPa*

Above mentioned values are realized for standard masonry specimens. If the strength is obtained by testing full sized brick the value of strength should multiply by the shape factor Δ, which takes into account the actual dimensions of the unit. **Table 2.3** demonstrates the value of shape factor for various brick unit dimension.

Table 2.3 The value of shape factor for various masonry unit dimensions.

Height (mm)	Least horizontal dimension (mm)				
	50	100	150	200	>250
50	0.85	0.75	0.7	-	-
65	0.95	0.85	0.75	0.7	0.65
100	1.15	1.00	0.90	0.80	o.75
150	1.30	1.20	1.10	1.00	0.95
200	1.45	1.35	1.25	1.15	1.10
>200	1.55	1.45	1.35	1.25	1.15

2.2.3 Mortar

Mortar for masonry construction is a workable paste used to bind construction blocks together and fill the gaps between them. This word comes from Latin mortarium meaning crushed. Mortar may also be used to bind masonry blocks of stone, brick, cinder blocks, etc. Mortar becomes hard when it sets, resulting in a rigid aggregate construction. Modern mortars are typically made from a mixture of sand, a binder such as cement or lime, and water. Mortar can also be used to fix, or point, masonry when the original mortar has washed away [4].

The principal function of mortar is to bond masonry units into a monolithic structure. Conversely, mortar keeps the units apart, filling all the cracks and crevices and providing a uniform structure. Bonding must be accomplished in such a way that the structural properties of the units are consolidated, at the same time ensuring a barrier to the entry of wind-driven rain. If it is successful, the wall will possess sufficient durability to withstand exposure to the elements.

Sometimes some kinds of additives can be added to mortar to improve its workability or for different reasons [1].

It should be note that, the description of a mortar always includes the type of binder and the amount of binder and aggregate. The amounts of binder and aggregate should always be expressed as parts by weight. For example LC 50/50/650 means 50 kg lime, 50 kg cement and 650 kg sand. Also as an alternative the components can be expressed in volumes. For example that is LC 2:1:12 which means 2 parts lime by volume, 1 part cement by volume, and 12 parts sand by volume [5].

Several types of mortar can be used for masonry walls according to the specification used in Eurocode 6 as follows [6]:

1- General purpose mortar, used in joints with thickness greater than 3 *mm* and produced with dense aggregate.

2- Thin layer mortar which is designed for use in masonry with nominal thickness of joints 1-3*mm*.

3- Lightweight mortar which is made using perlite, expanded clay, expanded shale etc. Lightweight mortars typically have a dry hardened density lower than 1500 kg/m^3.

Typical composition of general purpose mortar mixes and expected mean compressive strength are shown in **Table 2.4**.

Table 2.4 Typical prescribed composition and strength of general purpose mortars.

Mortar type	Mean compressive strength	Approximate composition in part of volume		
		Cement	Hydrated lime	Sand
M2	2.5 MPa	1	1.25-2.50	2.25-3 times cement and lime
M5	5 MPa	1	0.50-1.25	
M10	10 MPa	1	0.25-0.50	
M20	20 MPa	1	0-0.25	

In earthquake regions mortars used in masonry construction should comply with Eurocode 8. According to mentioned regulation for the construction of masonry structures, the minimum compressive strength of mortar is set to 5 *MPa*. EN1015-11 suggests determining mechanical properties of mortar by testing mortar prisms 40×40×160 *mm* [7]. The compressive strength of the mortar is calculated after averaging the strength values of six specimens. The thickness of bed and head joints is recommended to be in the range 8-15 *mm* and all head joints should be fully filled with mortar [1].

2.3 Masonry prisms properties and required standards

In order to estimation the strength and load bearing of masonry walls or any masonry structure subjected lateral loads, some important masonry mechanical characteristics should be known such as:

· The masonry compressive strength and the modulus of elasticity,

· The stress-strain relationship

· The masonry shear strength and the shear modulus

· The tensile strength

Masonry mechanical characteristics can be determined by testing standard specimens of masonry prisms and walls according to a set of known standards.

2.3.1 Compression test of masonry prisms

Compressive strength of masonry in the direction normal to the bed joints is generally considered as the main design property of masonry. The most common method for obtaining this property is to perform uniaxial compression test on masonry prism specimens. Compressive strength of masonry can be determined by testing either small wallets of at least 1.5 units length and 3 units height, or walls of 1.0-1.8*m* long and 2.4-2.7m high. It should be note that still there is not a general agreement on reliability of this method among researchers it is the suggested method in several design codes [8]. The test configuration is illustrated in **Figure 2.2** [9].

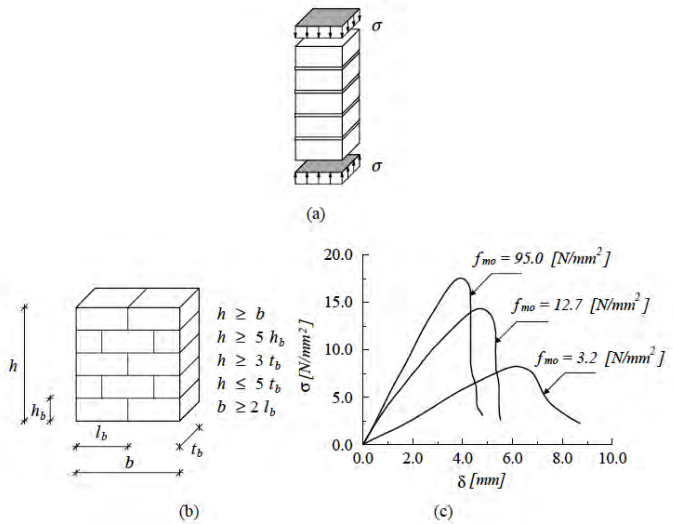

Figure 2.2 Uniaxial compressive tests on masonry prisms (a) Stacked bond prism (b) Schematic representation of RILEM test specimen (c) Experimental stress-displacement diagrams for prisms made of mortar with various compressive strength [10].

As we know the properties of the masonry units depends on the properties of component materials unit and the mortar. Therefore it is not easy to predict their characteristics before testing. Masonry design standards therefore specify low design values for compression strength unless prism tests are carried out to confirm higher values. Because of the massive of typical masonry prisms, the tests are difficult and expensive to perform, and most designers use the low strength as a default option. For tasting the prisms specimens are placed in a compressive testing machine, and the vertical load is applied at a uniform rate so that the failure occurs after 15-30 minutes after the beginning of testing. In order to take into account the slenderness if the wall is slender (height/thickness ratio greater than 20), lateral displacements at the mid-height of the wall are measured. If δ is the displacement just before the attainment of maximum vertical load, and t is the thickness of the wall, the test value can be increased by a shape factor (α) of $t/(t-\delta)$, provided that the increase is not greater than 15%. The main trigger for failure of masonry prism in axial loading is the difference in elastic properties of the unit and mortar [11]. In ASTM C 67 standard, a reduction factor is proposed for the calculation of compressive strength in masonry prisms with h/t ratios less than five. As the test illustrated, in low height specimens, failure started from a series of vertical tensile cracks and ultimate compressive load bearing capacity of the specimen achieved when the compressive stress in mortar exceed the allowable amount [1].

Several parameters alter the compressive strength of brick masonry walls. Considering the anisotropic characteristics of masonry, the geometry feature such as the brick laying technique plays an important role. Generally, the compressive strength of masonry is dependent on the mechanical properties of brick and mortar and their interaction which took place in their interface. Therefore, a wide range of quantitative and qualitative factors contribute to the compressive behavior of the masonry wall [10].

The compressive behavior of masonry in the direction parallel to the bed joints still have not been studied properly. The ratio between the uniaxial compressive strength parallel and normal to the bed joints varies from 0.2 to 0.8. Mentioned ratios were obtained from tests on the masonry samples of solid and perforated clay units, calcium silicate units, lightweight concrete units and aerated concrete units. [12].

Three identical specimens should be tested and the results should be evaluated according to EN 1052-1. The mean compressive strength of masonry is adjusted if the compressive strength of masonry units and mortar deviate from the design mean values within ± 25 % of the specified strength. The characteristic compressive strength of masonry f_k is determined as the smaller value of either $f_k = f/1.2$ or $f_k = f_{min}$ [1].

In order to determine the compressive strength of masonry structures some analytical models [31-35] have been proposed. Mentioned models try to obtain the compressive strength of the brick and mortar combination, from theoretical principles, starting from a series of mechanical hypotheses and applying equilibrium and compatibility equations. Although most of these models hypothesized that the bond between bricks and mortar remains undamaged if either brick or mortar fails, it has been shown that this is not completely approved. The models are also highly complex, require a variety of parameters (geometry, brick and mortar compressive strengths, elasticity modulus and Poisson coefficient) and obtain expressions in which some of the factors are interrelated [10, 13].

The value of compressive strength of unreinforced masonry made with general purpose mortar if no test data are available, could be calculated on the basis of the normalized compressive strength of masonry units f_b and compressive strength of mortar f_{mor} using the Eq 2.1 [1];

$$f_k = k\,(f_b^{0.65} \times f_{mor}^{0.2}) \quad (\text{in } MPa) \qquad (2.1)$$

In which f_{mor} should not be greater than 20 *MPa* or greater than $2f_b$ which is the smaller. According to the quantity of k Eurocode 6 recommends that the constant k may be taken as:

- 0.60 for group1 masonry units in a wall without longitudinal mortar joint,
- 0.55 for group 2a masonry units in a wall without longitudinal mortar joint,
- 0.50 for group 2b masonry units in a wall without longitudinal mortar joint and for group1 masonry units in a wall with longitudinal mortar joint.
- 0.45 for Group 2a masonry units in a wall with longitudinal mortar joint,
- 0.40 for Group 2b masonry units in a wall with longitudinal mortar joint and for Group 3 masonry units.

The compression strength of the masonry units may vary from as low as 5 *MPa* for low quality limestone blocks to over 100 *MPa* for high-fired ceramic clay units. As mentioned before there is a wide variation in the compression strength of the various constituents of masonry. A minimum strength of about 12.5 *MPa* is typically required by design codes.

2.3.2 Determination of modulus of elasticity

Expected values for elastic modulus of masonry in compression shall be measured using one of the following two methods:

1. Test prisms shall be made or extracted from an existing wall and tested in compression. Stresses and deformations shall be measured to determine modulus values (secant method).

2. By empirical method in which number of researchers have correlated the modulus of elasticity of masonry to its compressive strength on an empirical basis. Still there is a lack of unanimity as to the appropriate relationship between modulus of elasticity and masonry compression strength.

a) Secant method

Powell and Hodgkinson [14] proposed the secant method that was confirmed by Turnsek and Cacovic [15]. Modulus of elasticity from the stress-strain curve of masonry compression test can be determined as illustrated in **Photo 2.1:**

- Chord modulus for a line joining the curve at 5% of *f'm* to 33% *f'm*
- Chord modulus for a line joining the curve at 5% of *f'm* to 35% *f'm*

Since this region of the mentioned diagrams usually lies well within the reasonable linear part of the curve is ignored because it often represents a relatively closing up of the interface between the mortar and the units [1].

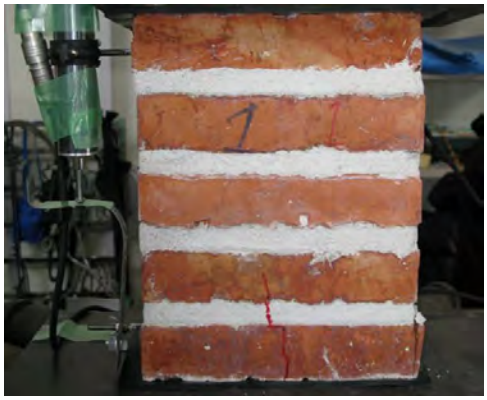

Photo 3.1. Masonry prism compression test according to LUM B1.

b) Empirical method

In order to evaluate the amount of modulus of elasticity a number of researchers have associated the modulus of elasticity of masonry to its compressive strength (*f'm*) as follows:

$E=2116\sqrt{f_m}f$ (Schubert, 1982)

$E = 1180\, f'_m{}^{0.83}$ (Sinha and Pedreschi, 1983)

$E = 750\, f'_m$, 20.5 *GPa* (maximum) (MIA, 1998)

$E = 1000\, f'_m$ (*EC 6* and *CIB* (Bull, 2001)

It is very important and advisable to assume conservatively high values for modulus of elasticity to assure that lateral seismic design load are not underestimated [1].

2.4 Shear parameters of masonry prisms

Among methods and standards that are provided to evaluate shear strength of masonry unit, two most famous standards BS EN 1052 [16] and ASTM E 519 [17] will be presented and discussed in this study. Despite both of these tests can be implemented for new structures, for existing masonry structures only diagonal test can be performed. For determination of mechanical parameters of brick mortar interface (cohesive value and friction coefficient) it is mandatory to perform triplet test with various amounts of pre-compression load.

2.4.1 Triplet shear test

Triplet test can perform in order to obtain shear strength as well as mechanical parameters of masonry interface such as cohesive value and friction coefficient. In this method specimens are composed of three number of masonry units that are stuck together from their bed joint by two layer of mortar. According to the BS standard the specimen prisms are placed longitudinally under the load that applies to the head of the middle masonry unit (**Photo 2.2**). This experiment can be done with or without lateral confining load, but for determination of friction coefficient it is mandatory to perform both experiments.

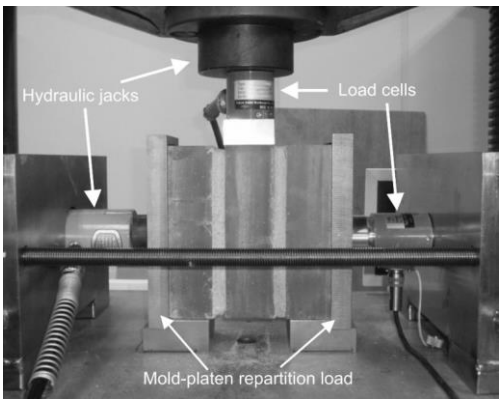

Photo 3.2. Triplet test apparatus and arrangement of measurement devices [1].

2.4.1.1 Failure modes of masonry prisms under shear triplet test

Depending on the strength of mortar, pre-compression load level, properties of brick and mortar and bond strength of brick-mortar interface five different kinds of failure are expectable (**Figure 2.3)**. Referring to first two modes (A1 and A2), due to the weakness of the brick-mortar interface, the failure occurs with the separation of the mortar from the brick. Failure mode B can be expected in case of low strength mortar. The use of high strength mortar with good adhesive property can lead to the failure type C and D. The higher level of pre-compression can also be lead to failure type D in which the specimen fails due to cracks passing through one or both bricks.

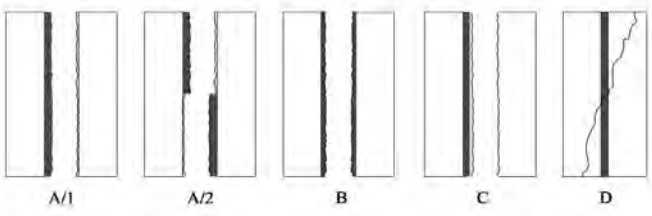

Figure 2.3 Expected failure modes for masonry prisms subjected to triplet test according to EN 1052-3 [18].

In contrast to the results of diagonal test that are subjected to various interpretations, the data of triplet test can be directly attained according to BS EN 1052 unique formulation. So shear strength of each specimen can be calculated as:

$$f_{voi} = \frac{F_{i,\max}}{2A_i} \qquad (2.2)$$

In which $F_{i,\max}$ is the maximum vertical load and A_i is the area of brick-mortar interface and f_{voi} is maximum shear strength of masonry interface . Ultimately characteristic shear strength for brick mortar interface f_{vok} is calculated as:

$$f_{vok} = 0.8 \times f_{vo} \qquad (2.3)$$

In which f_{vo} is the mean value of shear strength for specimens by same pre-compression load level.

2.4.2 Diagonal tension test

Diagonal compression test procedure calls for testing of square masonry piers with height to length (H/L) ratio of 1 subjected to a compressive load *P* applied on one of its diagonals (**photo 2.3**). Failure of the panel is generally associated with the development of a crack starting from its center. This crack may pass prevailingly through mortar joints (assuming the shape of a "stair-stepped" path in the case of a regular masonry pattern) or even through the units.

Photo 3.3. Diagonal compression test on full scale masonry panel.

The results of ASTM standard are exposed to various kinds of interpretations [19,20], which involve different formulation. In the standard interpretation, shear strength of masonry τ (by adopting an isotropic linearly elastic model) can be achieved by assuming that the panel fails if the principal tensile stress σ_I at the center reaches to its maximum amount [21,22]. Therefore in most standards and codes [23,24], shear strength is calculated by assuming a pure shear stress state ($\sigma_I / \sigma_{II} = -1$) (**Figure 2.4**).

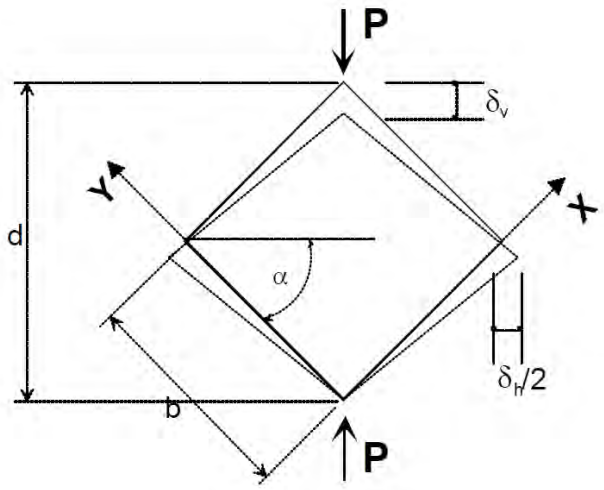

Figure 2.4 Definition sketch of shear stress and strain in diagonal compression test.

ASTM E519 suggest following formulation using mentioned hypothesis to determine shear strength τ, shear strain γ and shear elastic modulus G for masonry panels can be evaluated as follows:

$$\tau=\sigma_t = P_{Max}/\sqrt{2}\,A_n \qquad (2.4)$$

In which P is applied load and A_n is net gross section of the masonry panel. It is worth noting that often diagonal tensile strength of masonry σ_t is erroneously assimilated to the local cohesion (c) of the mortar/block interfaces [25]. As well shear strain and modulus of rigidity according to E519 standard, can be calculated using following formulas:

$$\gamma = \tan\alpha + \frac{1}{\tan\alpha}\left(\frac{\delta_v + \delta_h}{2d}\right) \qquad (2.5)$$

$$G = \frac{\tau}{\gamma} \qquad (2.6)$$

Where γ is shearing strain, d is vertical gage length, δ_V and δ_h are respectively vertical shortening and horizontal extension of panel during the test and G is modulus of rigidity.

Some researchers discovered that this interpretation is reliable, since in non-linear range the stress redistribution occurring in the panel does not significantly affect the value of σ_I computed by the elastic isotropic solution [25]. As can be proved by a finite element analysis [26-28], the elastic solution provides that: although principal directions are considered coincide with the two diagonals of the panels, the stress stated at the center of the specimen is not a pure shear state which was supposed on ASTM E 519 and RILEM TC 76 formulation. Consequently using mentioned hypothesis stress state at the center of specimen can be calculated as: $\sigma_x = \sigma_y = -0.56\ P_{Max}/A_n$, $\sigma_I = 0.5\ P_{Max}/A_n$, $\sigma_{II} = 1.62\ P_{Max}/A_n$, corresponding to a ratio $\sigma_I/\sigma_{II} \approx -0.3$ (**Figure 2.5** shows the relative Mohr's circles). Ultimately evaluating the shear strength of masonry panels employing this stress state has two interpretations: in the first one the shear strength at the middle of the panels supposed to be equal with the principal tensile stress:

$$\tau = \sigma_I = 0.5\frac{P_{\max}}{A_n} \qquad (2.7)$$

In the other interpretation, the value of shear strength can be determined by adopting the Turnaşek-Cacovic criterion to the tensile principal stress [29]:

$$\tau = \frac{1}{1.5}\sigma_I = 0.33\frac{P_{\max}}{A_n} \qquad (2.8)$$

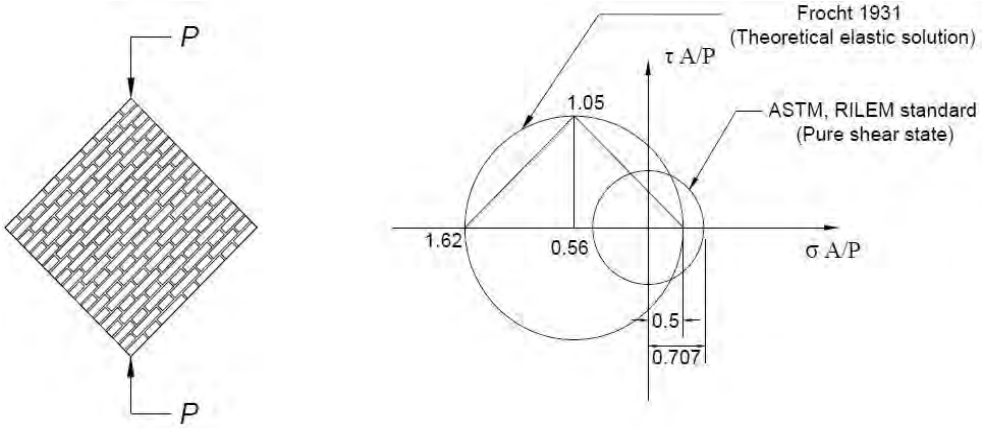

Figure 2.5 Mohr's representation of stress state at the center of masonry panel in diagonal compression test.

Development of computer technology has improved the resolution of experimental measurements providing an understanding of the material properties at a finer scale. One of the fundamental equations of mechanics for an isotropic material is:

$$G = \frac{E}{2(1+\nu)} \qquad (2.9)$$

Where *G*,*E* and *ν* are respectively the shear modulus, Youngبsmodulus and Poissonي ratio. A simple design assumption using a Poissonبsratio of 0.25 (A mid-range value which is a reasonable starting point for design), gives the usual isotropic equation for the shear modulus as $G = 0.4E$ (Lekhnitskii 1963). This ratio is also presented in almost all national masonry building codes, including the latest draft of the Eurocode 6 stating بـ *In the absence of a more precise value, it may be assumed that the shear modulus, G, is 40% of the elastic modulus E"*(Eurocode 1995)[30].

2.5 References

[1] A. Bourzam, Shear capacity prediction of confined masonry walls subjected to cyclic lateral loading, PhD thesis, Kanazawa University, Japan (2009).

[2]http://en.wikipedia.org/wiki/Brick

[3] Punmia, B.C.; Jain, Ashok Kumar, Basic Civil Engineering, Firewall Media, pp. 33, ISBN 978-81-7008-403-7 (2003).

[4] http://en.wikipedia.org/wiki/Mortar_(masonry)

[5] K. Sandin, "Mortars for Masonry and Rendering Choice and Application" Building Issues Vol7 پ Number 3 (1995).

[6] Eurocode 6.Design of masonry structures Part1-1: General rules for reinforced and unreinforced masonry structures. EN1996-1-1:2005,CENBrussels; (2005).

[7] BS EN 1015-11:1999 Methods of test for mortar for masonry. "Determination of flexural and compressive strength of hardened mortar", November (1999).

[8] Mann, W., Betzler, M., Investigations on the effect of different forms of test samples to test the compressive strength of masonry. In: Proc 10th Intl. Brick/Block Masonry Conf. Calgary, Canada, pp. 1305-1313 (1994).

[9] Chuang, S.W, Seismic Retrofitting Techniques for Existing Unreinforced Masonry, PhD Thesis, University of South Australia (2004).

[10] G. Zamani Ahari, "Structural in-plane behavior of masonry walls externally retrofitted with fiber reinforced materials" PhD thesis, Kyushu university, Japan (2013).

[11] Hilsdorf, H.K. Investigation into Failure Mechanism of Brick Masonry Loaded in Axial Compression. Proc. of Int. Conf. on Masonry Structural Systems, Gulf Pub. Col., Houston, Texas, pp.34-41(1969).

[12] Hofmann, G., Schubert, P. x. Compressive strength of masonry parallel to the bed joints, Proc. 10th Int. Brick and Block Masonry Conf., Ed. N.G. Shrive and A. Huizer, Calgary, Alberta, pp.1453-1462 (1969).

[13] Roca, J.G., Marco, C.O., Adam, J.M, Compressive strength of masonry made of clay bricks and cement mortar: Estimation based on Neural Networks and Fuzzy Logic. Engineering Structures, Vol. 48, pp. 21ت27 (2013).

[14] Hendry, A.W.: بStructural masonryپ, 2 ndEd., Macmillan Press, (1998).

[15] Turnجek, V. and Cacovic, F.: بSo me experimental results on the strength of brick masonry wallsپ,Proc. 2nd Int. Brick-Masonry Conf. (British Ceramic Society, Stokeon-Trent, 1971), pp. 149-156, (1971).

[16] EN 1052-3. Methods of test for masonry. Part 3: Determination of initial shear strength. European standard; (2007).

[17] ASTM E 519-2010. Standard test method for diagonal tension (shear) in masonry assemblages. American Society for Testing Material, (2010).

[18] Alecci V, Fagone M, Rotunno T, De Stefano M. Shear strength of brick masonry walls assembled with different types of mortar. Constr Build Mater,40:1038-1045 (2013).

[19] L. Binda, G. Cardani, G. Castori, M. Corradi, A. Saisi, C. Tedeschi, Procedure sperimentali per la determinazione delle caratteristiche della muratura, In: Borri A, editor. Manuale delle murature storiche ت vol. I. Roma, Tipografia del Genio Civile, 316ت8 (2011).

[20] S. Chiostrini, L. Galano, A. Vignoli, On the determination of strength of ancient masonry walls via experimental tests, In: Proc. 12th world conference on earthquake, (2000).

[21] V. Alecci, M. Fagone, T. Rotunno, M. De Stefano, Shear strength of brick masonry walls assembled with different types of mortar, Construction and Building Materials 40, 1038-1045 (2013).

[22] C. Calderini, S. Cattari, S. Lagomarsino, The use of the diagonal compression test to identify the shear mechanical parameters of masonry, Construction and Building Materials 24 5, 677-685 (2010).

[23] ASTM Committee E519 / E519M - 10, Standard test method for diagonal tension (shear) in masonry assemblages, American Society for Testing Material (2010).

[24] RILEM TC 76-LUM, Diagonal tensile strength of small walls specimens, RILEM Publications SARL (1994).

[25] C. Calderini, S. Cattari, S. Lagomarsino, The use of the diagonal compression test to identify the shear mechanical parameters of masonry, Construction and Building Materials 24 5,, 677-685 (2010).

[26] F.Y. Yokel, S.G. Fattal, Failure Hypothesis for Masonry Shear Walls, Journal of Structural Division, ASCE Vol.102 (3) 515ت532 (1976).

[27] M.M. Frocht, Recent advances in photoelasticity, ASME Trans 55 135ت53 (SeptemberتDecember 1931).

[28] A. Brignola, S. Frumento, S. Lagomarsino, S. Podesta, Identification of shear parameters of masonry panels through the in-situ diagonal compression test, International Journal of Architectural Heritage 31, 52ت73 (2009).

[29] V. Turnaچek, F. Cacovic, Some experimental results on the strength of brick masonry walls, In: Proc. of the 2nd international brick masonry conference United Kingdom Stoke-on-Trent, 149ت56 (1971).

[30] Vlatko Z. Bosiljkov, Yuri Z.Totoev and John. M. Nichols. "Shear modulus and stiffness of brickwork masonry: An experimental perspective" Journal of structural engineering and mechanics, Pages 21-43 DOI: 10.12989/sem.2005.20.1.021 (2005)

[31] Hilsdorf, H.K, Investigation into the failure mechanism of brick masonry loaded in axial compression. Designing, engineering and constructing with masonry products, Gulf Publishing Company. pp. 34ت41(1969).

[32] Binda, L., Fontana, A., Frigerio, G, Mechanical behavior of brick masonries derived from unit and mortar characteristics. Proc. of the 8th international brick/block masonry conf, Dublin, pp. 205ت216 (1988).

[33] Atkinson, R.H., Noland, J.L., Abrams, D.P, A deformation theory for stack bonded masonry prisms in compression. Proc. of 7th intl. brick masonry conf., Melbourne University, Melbourne, pp. 565ت576 (1982).

[34] Francis, A.J., Horman, C.B., Jerrems, L.E, The effect of joint thickness and other factors on the compressive strength of brickwork. In: West HWH, Speed KH, editors.

Proc. of the 2nd int. brick masonry conf. Stoke-on-Trent, UK: British Ceramic Research Association, pp. 31ت37 (1971).

[35] Khoo, C.L., Hendry, A.W, A failure criterion for brickwork in axial compression. Proc. 3rd intl. brick masonry conference. pp.139ت145 (1973).

Chapter 3. Strengthening methods and seismic analysis of brick walls

3.1 Introduction

Unreinforced masonry (URM) buildings represent a large portion of the buildings around the world. Many attributes make brick a practical and popular construction choice. In addition to the inherent beauty of brickwork, it is also thought to create the impression of solidity and permanence, so brick homes often sell for higher prices. Brick is almost maintenance-free, never needs to be painted or stained, and resists damage from wind, fire, and water. It also offers both noise and thermal insulation, so structures created from it generally stay cooler in the summer and warmer in the winter [1].

Despite this kind of constructions demonstrates acceptable compression strength, it can scarcely bear shear and tensile stress therefore, known as no-tension material. Nevertheless, masonry buildings are constructed in many parts of the world where earthquake occurs [2].

As we know earthquakes impose lateral force to the structures which produce shear and tension stress among the elements of structural components that makes this kind of construction more vulnerable. Hence moderate to strong earthquakes can devastate complete cities or villages, resulting in massive death toll and cause extensive losses. For this reason in the last decade researchers around the world have been interested toward both experimental and analytical studying of masonry constructions. Although experimental studies are almost always time consuming and more onerous, its results are more confident and reliable. Also, despite the great improvements and developments on numerical procedures and finite element methods, the accuracy of obtained outcomes are always depend on the correct identification and characterization of mechanical properties of materials that is required to characterize masonry numerical models [3].

Although several studies (both experimental and numerical) have been conducted in last decade to characterize and understand the behavior of masonry brick walls as available in literature [4-12] nevertheless, because of complexity and crucial influence of masonry and texture type on the behavior of this kind of structure it is essential and vital to perform more studies and investigations.

3.3 Behavior of brick masonry walls against earthquake

As discussed despite masonry brick walls have acceptable strength in case of compressive and shear loads, they can scarcely bear tension and torsion stresses. It was proved by past earthquakes that, this kind of construction technique demonstrate various types of performance as the direction of load change. Generally in-plane and out of plane behaviors have been defined in the past decades in order to simplify understanding the performance of the masonry walls in case of seismic lateral loads.

The stability of masonry buildings needs to be verified only for vertical gravity loads, if no any unusual natural disaster is expected in the region, in particular earthquake. In case of an earthquake, however, the structure will be subjected to a series of cyclic horizontal actions, which will often cause high additional bending and shear stresses in structural walls, exceeding the elastic range of the behavior of masonry materials. Structural walls, which are the basic resisting element to seismic loads, will be damaged, and, if they had not been properly designed and detailed to withstand inelastic deformation and to dissipate energy, the induced inertia forces might cause heavy damage or even collapse of the building. Since the ground motion is tridirectional, both vertical and horizontal inertia forces are induced, changing in time, and resulting in tridimensional vibration of the structure. In addition, due to the distributed mass of masonry walls, inertia forces perpendicular to the planes of the walls are also induced, resulting in the out-of-plane vibration of structural and non-structural walls. Because of typical structural configuration and reserve in strength of masonry materials with regard to carrying vertical gravity loads, there is generally no need to verify the load carrying capacity of masonry walls and floors for vertical seismic action. Also, because of uniform distribution of walls in both orthogonal directions, geometric requirements for shear walls (effective height, size and position of openings) and connection between walls and floors, out-of-plane resistance to seismic action is usually not critical [15].

The major types of masonry failure modes have been identified as:

3.3.1 In-plane cracking

Masonry walls express high strength and stiffness in line with its in-plane force reaction that causes high load resistance capacity. The produced in-plane load led to the in-plane cracks in a pattern that depends on H/L ratio of the wall, vertical pre-stress load, masonry mechanical properties and foundation or support condition. In plane masonry wall crack types are as follows:

3.3.1.1 Tension diagonal cracks: because of developing of tension stresses in the wall subjected to in-plane lateral loads. Because of reversal nature of the seismic loads, this kind of cracks emerges as symmetrical crossed cracks on the surface of the wall. It worth noting that, this kind of cracks causes a significant decrease on the load resistance capacity of the masonry walls.

3.3.1.2 Shear cracks: due to the shear stresses in the interface of the brick-mortar this kind of cracks develop in the masonry walls with a ladder shape pattern.

3.3.1.3 Corner crushing cracks: this kind of cracks arises due to stress concentration on the edge corners of the masonry walls.

3.3.1.4 Flexural (bending) cracks*:* if the value of aspect ratio of masonry wall (H/L) was higher than 1.0, the in-plane behavior of the wall becomes flexural and in consequence horizontal bending cracks appears at the down margin of the wall. Mentioned flexural cracks develop due to low tension strength of masonry in the stretching area. Because of reversal nature of the seismic loads, this kind of cracks emerges as symmetrical crossed cracks on the surface of the wall.

Figure 3.3 demonstrate mentioned failure behavior of unreinforced masonry wall subjected to in-plane lateral load.

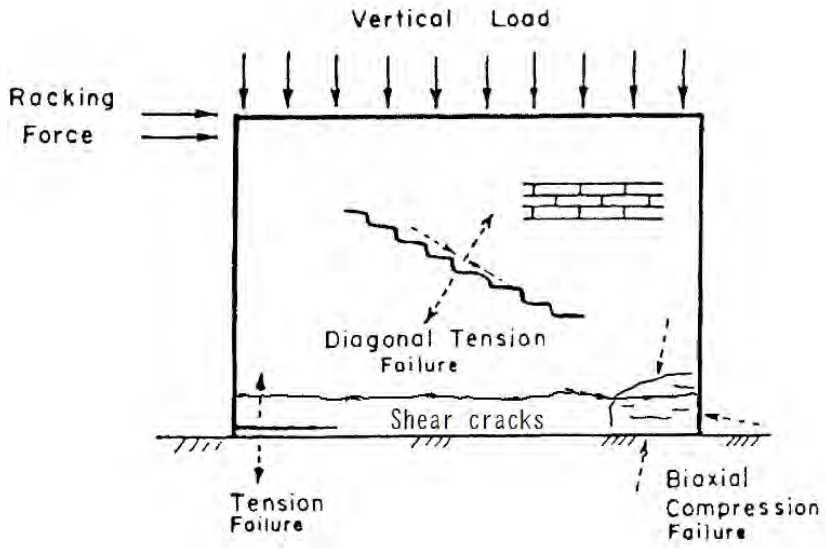

Figure 3.1 Modes of failure of masonry wall.

Photo 3.1 demonstrate an example of in-plane diagonal cracks in a building that was suffered from 11th of August Ahar earthquake in northwest of Iran.

Photo 3.1. Tension diagonal cracks of masonry wall [16, 17].

3.3.2 Separation of adjacent walls

Due to weakness in the connection corner of masonry walls this region in highly vulnerable in case of seismic loads. The most reason of this failure is due to stress concentration resulting from both lateral masonry walls. **Photo 3.2** demonstrates some examples of this type of masonry wall failure.

Photo 3.2. Separation of adjacent walls in masonry building.

3.3.3 Out-of-plane wall collapse

This failure type is common when the main direction of the seismic shake is perpendicular to the masonry walls and these have insufficient transversal supports. This failure type is becomes more likely when connections between the walls fail as observed in **Photo 3.3**. If the connection between walls is weak, due for example to a poor block or brick stacking, it can easily fail. As a result each of the connecting walls becomes an independent structure, which is the worst-case scenario is only supported at the bottom. An out-of-plane failure type is extremely possible to occur under these conditions.

Photo 3.3 Out of plane behavior of masonry walls in case of seismic orthogonal loads.

3.3.4 Cracking due to stress concentrations around openings (doors and windows)

This type of failure is the most common cracking type in the masonry structures that is due to stress concentration around the opening. At the corners of the openings, tension cracks may appear due to the reverse cyclic stress induced by lateral loading. The mentioned cracks start from the corners and tend to develop down and up side of the wall. Until the shear cracks become excessively severe, the gravity load carrying capacity of the walls is not jeopardized.

3.4 Strengthening methods of brick masonry walls

As we know large numbers of masonry structures have not been designed for seismic loads and structural walls of these buildings were principally designed to resist gravity loads. Therefore moderate to strong earthquakes can devastate complete cities or villages resulting in massive death toll and cause extensive losses. Hence strengthening of these structures and improving their strength, is significant and vital. There are various methods in this regard in different categories, and some of them are under research and being experimented. Application of these methods to URM structures is expected to increase strength and ductility of the structure. However, sometimes the cost of reinforcement is not reasonable, or advanced technology is needed and therefore isn't suitable for developing countries (that need to retrofit buildings), especially in rural regions. The most suitable methods in case of URM brick walls are introduced below.

3.4.1 Surface Treatment

Surface treatment is a common method which has largely developed through experience. Since this approach covers the surface of masonry walls, sometimes it is not suitable for historical buildings with architectural value. Recent methods in this category are introduced below.

3.4.1.1 Bamboo-Band Technique

Bamboo-band strengthening technique is simple enough to be understood and applied by layman without any prior special expertise. Bamboo-band mesh techniques enhance the seismic capacity of the adobe masonry building significantly. This retrofitting system consists of vertical and horizontal bamboo used as external reinforcing. At first bamboo band mesh prepare on a square grid in a way that one band crosses over another band in

different layers at subsequent crossing points. This process was quite similar to the basket weaving process. Straws place at approximately 200 *mm* pitch. Holes can be prepared by drilling through the wall. The prepared mesh is then installed on both outside and inside of the wall and wrapped around the comer of the house. The inside and outside meshes are connected by the Polypropylene strings (PP strings) which were passed through the hole.

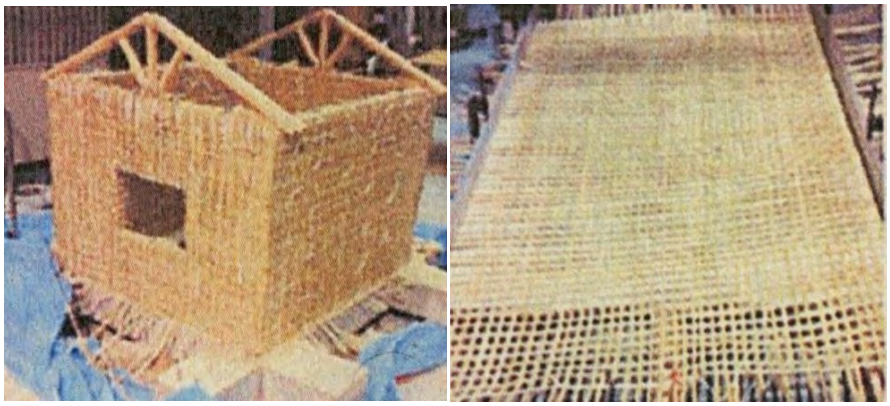

Photo 3.4. Preparing Bamboo-band mesh and application [18].

Experiments have shown that the retrofitted masonry building by this method could withstand over twice larger input energy than what non-retrofitted specimen can do. However, bricks surrounding the bamboo cannot provide proper protection of bamboo meshes.

Low cost and no need for special workers are considers as the main advantages of this method.

3.4.1.2 Shotcrete

Shotcrete is a covering method of masonry walls reinforced by mesh of bars, with sprayed concrete. This method is more convenient and less costly than the other strengthening methods. The thickness of a shotcrete layer can be adapted to the seismic demand. In general, the overlay thickness is at least 60 *mm*. The shotcrete overlay is typically reinforced with a welded wire fabric at about the minimum steel ratio for crack control. In order to transfer the shear stress across shotcrete-masonry interface, shear dowels (6-13 *mm* diameter @ 25-120 *mm*) are fixed using epoxy or cement grout into

holes drilled into the masonry wall. This method involves the removal of wythes of bricks and subsequently filling the void with pneumatically applied concrete [19,20].

Photo 3.5. Applying Shotcrete on a masonry wall.

This method of retrofitting consists of:

1- Cleaned surface, watered and grinded
2- Shear dowels @25-250mm
3- Shrinkage control reinforcement
4- Wall surface sprayed under 7 Mpa pressure on wall surface.

Experiments showed that retrofitting using Shotcrete is very effective in increasing both strength and ductility of URM walls. Also this method significantly increases the ultimate load of the retrofitted walls. Abrams and Lynch (2001), in a static cyclic test, increased the ultimate load of the retrofitted specimen by a factor of 3. Also the stiffness of the retrofitted specimens at the peak lateral force is approximately 3 times the stiffness of the unreinforced one. Moreover, Shotcrete increases the flexural strength of unreinforced masonry walls and dissipates high-energy due to successive elongation and yield of reinforcement in tension.

Shotcrete typically adds considerable weight to the structure, which results in larger inertia forces during an earthquake and may require foundation adjustments.

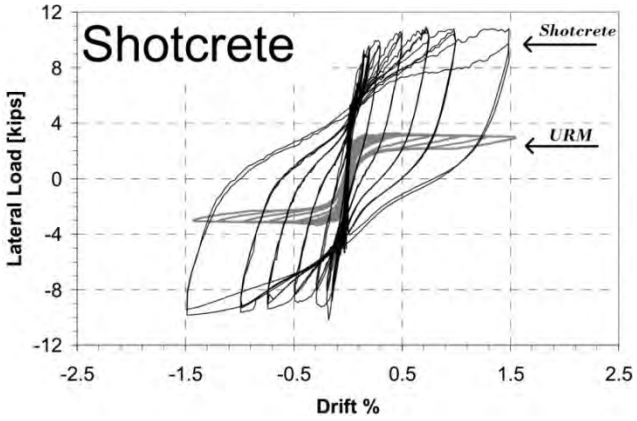

Figure 3.2 Hysteretic curves for a specimen before and after retrofitting using shotcrete (Abrams and Lynch 2001[25]).

3.4.1.3 FRP

FRP (also fiber -reinforced polymer) is a composite material made of a polymer matrix reinforced with fibers. Fibers are usually glass, carbon, aramid, and also other fibers. This material is lightweight and non-corrosive. Applying FRP method to a URM wall increases both the in-plane and out-of-plane strength of the wall. Schwegler conducted full scale tests on URM walls retrofit with an epoxy bonded carbon FRP. Results showed that both the in-plane and out-of-plane strength were significantly increased as a result of the retrofit. Kolsch showed that the use of a carbon fiber cement matrix composite is very effective in increasing the out-of-plane flexural strength of URM walls. Triantafillou tested several URM walls retrofitted with strips of epoxy-bonded carbon FRP in both in-plane and out-of-plane flexure. Retrofitted walls displayed approximately nine times the capacity of not retrofitted walls in both out-of-plane and in-plane bending. Also under static cyclic loading test, using FRP improved the lateral resistance by a factor of 1.7 to 5.9. However, in some cases debonding occurred at lateral load levels ranging from 50% to 80% of the ultimate load resistance. Some other studies showed that FRP overlays improve the shear resistance of the wall by a factor of 1.3 to 2.9. However, due to the coverage of the surface this method is not appropriate for historic structures with architectural value [21].

Photo 3.6. FRP retrofitting method.

3.4.2 Post-Tensioning

Post-tensioning has been used extensively in order to enhance the tensile and flexural capacity of URM walls. This method is applied by core drilling from the top of the masonry walls and vertically post-tensioning the walls to the foundation. Post-tensioning method involves a compressive force applied to masonry walls. This force counteracts the tensile stresses resulting from lateral loads. Experiments showed that this method can improve the lateral strength of URM walls bay a factor of 2. Al-Manaseer and Neis compared out-of-plane flexural behavior of reinforced masonry wall panels with post-tensioned masonry wall panels. Results showed that the post-tensioned walls displayed a similar level of ductility and an increase in both initial flexural stiffness and strength. While this method is somewhat costly, it has advantages in that it does not alter the appearance of the structure (especially important for historical structures) and that the occupants of the structure need not be disturbed during application [22].

Photo 3.7. Applying Post-tensioning method.

3.4.3 Confinement

In this retrofitting method, tie columns confine the URM wall at corners, intersections, and the border of openings. In some countries like Iran, this method applies to the new masonry construction. However, because of the minor effects of using columns alone for the confinement of walls, it is necessary to apply a horizontal element like a beam to the system. This method improves the ductility and energy dissipation of a masonry structure. The intensity of this improvement depends on the relative rigidity between the masonry and the surrounding frame and material properties.

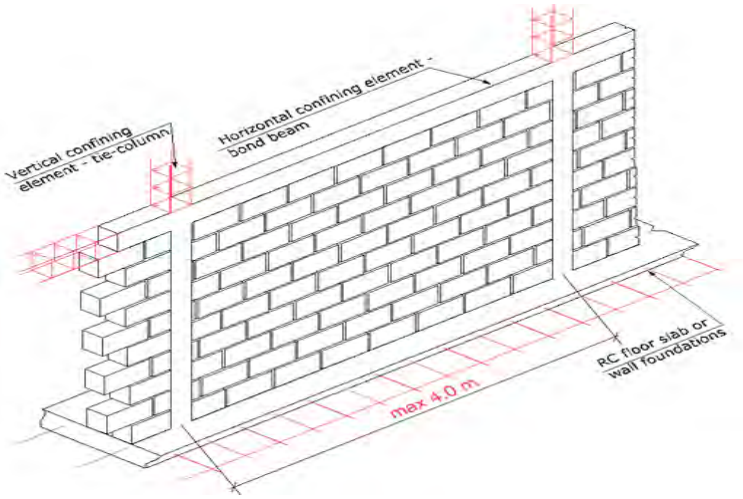

Figure 3.3 Confinement of masonry brick walls.

Scientists have done many studies about the performance of this method. Karantoni and Faradis by elastic finite element analysis showed that tie columns alone (without tie beams) do not have a significant positive effect on walls behavior. Chuxian et al discovered that confinement prevents disintegration and improves ductility and energy dissipation of URM walls, but has limited effect on the ultimate load resistance. Also Tomazevic and Klemenc proved that before cracking, the confinement effect can be neglected. Zezhen et al find that at ultimate load, the confinement increased the lateral resistance by a factor of 1.2. However, for walls with higher aspect ratio, the confinement increased the lateral resistance by a factor of 1.5. In addition, the confinement improved the lateral deformations and energy dissipation by more than 50% [23].

3.4.4 Center Core

Center Core method is advanced method for rehabilitation of masonry buildings. This method is a nondestructive method which could be achieved without evacuation of the buildings. First, vertical holes with given intervals are perforated on the walls to the footing and then reinforcing steel bars are embedded in the holes and cement grout will be injected finally to create bond strength between wall and bars. With existing technology, this core can be drilled precisely through the entire height of two or three-story masonry wall. The drilling is a dry process with the debris removal handled by a vacuum and filter system that keeps the dust to a minimum. After placing the reinforcement in the center of the hole, a filler material is pumped from the top of the wall to the bottom such that the core is filled from the bottom under pressure controlled by the height of the grout. The placement of the grout under pressure provided by the height of the core provides a beneficial migration of the grout into all voids adjacent to the core shaft. This reinforced homogeneous vertical beam provides strength to the wall with a capacity to resist both in-plane and out-of-plane loading. Grout material itself consists of a binder material (e.g. epoxy, cement, and polyester) and a filler material like sand. Abrams and Lynch proved that this technique doubles the resistance of URM wall in a static cyclic test. Although the high lateral displacement achieved during the test, the energy dissipated was limited. Some other experiments showed that ductility and out-of-plain behavior of the retrofitted wall was improved.

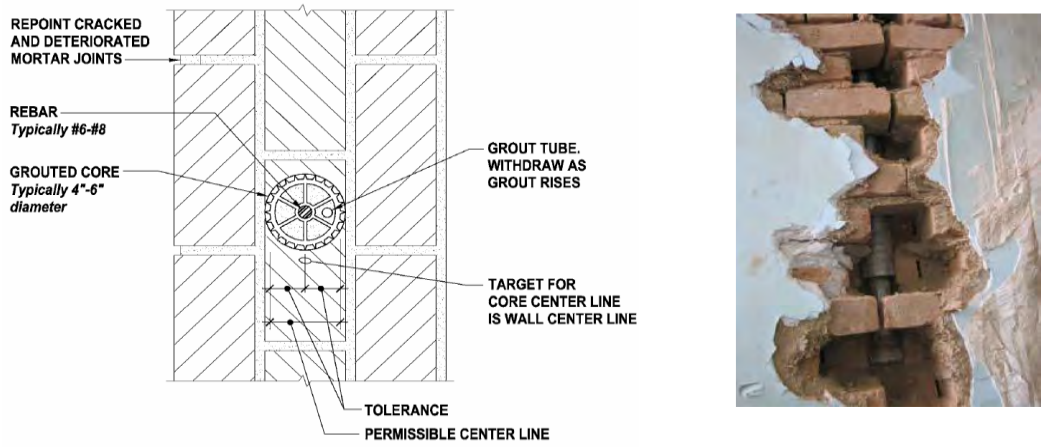

Figure 3.4 Left: Plan Detail of Center Core method in Masonry Wall Right: Applying Center Core method for existing building.

The advantage of Center Core system to the owner is the minimal site and interior disturbance and no disfiguring of the internal or external fabric to accomplish safe resistance to future ground shaking. The main disadvantage is this technique tends to create zones with widely varying stiffness and strength properties [24].

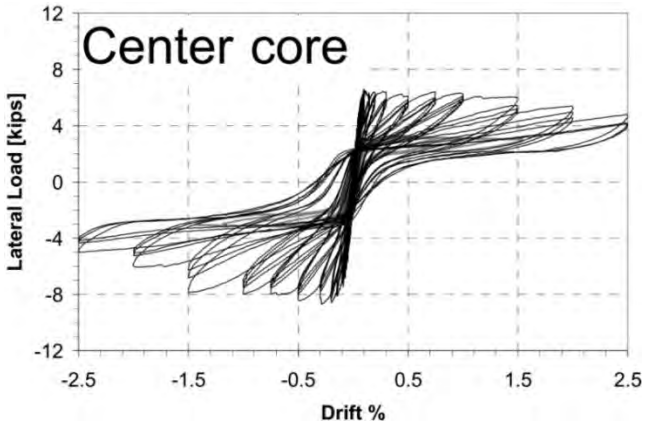

Figure 3.5 Hysteretic curves for a specimen after retrofitting using center core (Abrams and Lynch 2001[25]).

This method of retrofitting consists of:

1. A Center Core drilled down to footing (Diameter = 50-125mm)

2. Steel rebar inserted with spacers

3. Core filled with a mortar, either Epoxy sand, cement sand or Polyester sand. (Polyester mortar is recommended by researchers.)

3.4.5 Injection

Injection method is an improvement system to retrofit structures. In the case of injection into masonry walls the injection material is injected continuously via low pressure packers, which are in offset arrangement in the form of a grid. In this manner the faulty joints as well as the capillaries, pores and hollow cavities in the bricks are filled in with the injection material.

Photo3.8. Applying injection method for existing masonry brick wall.

Since this method does not affect the surface of the wall, it is popular for historical buildings with special architectural features. This technique is very useful for the purposes of improving compressive and shear strength of URM walls by restoring the initial stiffness of it. However, when injection was applied to some parts of the building, it must be proved that any partial increase of structure strength is not dangerous for other parts or the whole wall. For multi wythes masonry walls, injecting grout into empty collar joint enhances composite action between adjacent wythe. For injection, epoxy resin is used for relatively small cracks (less than 2 mm wide) while, cement-based grout is considered more appropriate for filling of larger cracks, voids, and empty collar joints in multi-wythe masonry walls Schuller et al. used a cement-based grout (100% type III Portland cement ASTM C150 with expansive admixture and w/c ratio of 0.75) to inject 0.08 mm wide cracks. Cement-based grout injection is capable of restore up to about 0.8 of the un-retrofitted masonry compressive strength. In addition, Hamid et al. discovered that cement-based grout injection can increase the interface shear bond of multi-wythe stonewalls by a factor of 25-40. The increment in lateral resistance ranged from 2-4 times the un-retrofitted resistance [26].

This method of retrofitting consists of:

1. Drilling the holes

2. Washing of cracks and holes with water. Inject of water (soak of the bricks), from top to bottom of the wall

3. Injection of grout with injection pressure of less than 8 to 10 psi.

3.5 Comparison of strengthening methods for URM walls

Based on the literature survey, **Table 3.1** summarizes the efficiency, advantage, and disadvantage of each technique.

Table 3.1 Comparison of different strengthening techniques.

Method	Advantages	Disadvantages
Bamboo-band	Low cost, Available materials, Low technology, Low mass, Structure could withstand twice larger input energy.	Affects architecture, Require finishing, Not suitable for historical buildings with architectural value, High disturbance.
Shotcrete	Low cost, Durable and more uniform behavior, Available materials, Improve in-plain strength by a factor of 3.6, Improves out-of-plain stability, Improves energy dissipation.	High mass, Require surface treatment, Affect architecture, Require finishing, High disturbance.
FRP	No added mass, Low disturbance, Available materials, Improves shear and flexural strength, Improves in-plain and out-of-plain behavior	Affect architecture, Require finishing, High cost.
Post-tensioning	No added mass, Low disturbance, Improves in-plain strength by a factor of 5-6, Improves out-of-plain stability, Suitable for historical buildings with architectural value.	High cost, High technology requires, Anchorage problem, Corrosion potential.
Confinement	Prevent disintegration, Improve in-plane deformability, Improves out-of-plain Stability, Improve ductility and energy dissipation.	High disturbance, High cost, Require demolition of Wall, Affect architecture
Center Core	No added mass, Low disturbance, Improves in-plain strength by a factor of 2-3, Improves out-of-plain Stability, Improves shear and flexural strength, Suitable for historical buildings with architectural value.	High cost, High technology requires, Create zones with varying stiffness
Injection	No added mass, Available materials, Low disturbance, Low cost, Can restore initial stiffness, Improves shear and compressive strength, Improves out-of-plain Stability	No significant increase in lateral resistance, Epoxy create zones with varying stiffness and strength

By comparing the strengthening methods for URM brick walls following results were achieved:

1-Applying low cost methods that are not suitably efficient are a financial risk. So it is better to carry out specific study on the economics of retrofitting methods.

2) The architectural or historical value of the building must be considered. In such types of structures, surface treatment cannot be used, and it is necessary to study other treatments like injection, Center Core, or base isolation technique.

3) Low cost or low technology cannot provide suitable efficiency, however some methods like Bamboo-band retrofitting technique have a relatively appropriate performance.

4-As we know the majority of human deaths in buildings as a result of earthquakes are caused because of out of plain corruption of unreinforced masonry walls, so the methods with high potential to improve out of plain behavior must be considered during the selection of the method of retrofitting.

5-because of the low quality of mortar and brick in rural regions, application of post tensioning methods (even for historical buildings) is not recommended.

6) High mass of URM structures is one of the most important problems that must be considered, and from this view point retrofitting methods with low additional mass are preferable.

3.6 Failure criteria of brick masonry walls

In order to realize the behavior of unreinforced masonry walls, the failure criteria of it should be understood. For a long time, the significance of joint orientation to the stress state of masonry panels has been of interest to many researchers. Johnson and Thompson [27] performed and reported diametric experiment on brick masonry discs, which generated indirect tensile stresses on joints inclined at various angles to the compressive load. Samarasinghe [28] and Samarasinghe and Hendrye [29] obtained a (σ_1, σ_2, θ) failure surface for the tension-compression principal stress range from tests on one-sixth scale brickwork. Similar observations were also made by Samarasinghe [28] on the mentioned

behavior of URM under biaxial compression-tension. Hegemier et al. [30] discovered the affect of the bed joint angle to be minimal and the behavior essentially isotropic, from a comprehensive series of biaxial tests on full scale grouted concrete masonry (both reinforced and un-reinforced). However, this isotropy could be destroyed by improper selection of block and grout strengths. Naraine and Sinha [31] investigated the behavior of URM pallets under cyclic biaxial compression and obtained that masonry under cyclic biaxial compression can exhibit three distinct stress-strain curves; they proposed a generalized interaction formula for this failure in terms of stress invariant for the range of stress ratios considered. Lourenco [32] performed a model for URM masonry that joint the modern plasticity concepts (hardening, softening, flow rule and evolution laws) with an anisotropic behavior oriented each material axis.

The non-homogeneous behavior of the unreinforced masonry walls is also as a result of its construction technique in which each unit is joined to another and consequently there is no way to ensure that every brick is placed in exactly the same way as the rest of the bricks. Also, cracking generated during the loading make more complexity to the overall behavior of URM and known as the main reason for the non-linear behavior of the wall. The main behavioral characteristics of URM can be summarized as the following facts [33]:

1) Mechanical behavior is non-homogeneous.

2) URM does not show an isotropic behavior.

3) Tensile strength is very low and in most of the cases it is close to zero.

4) Compressive response is brittle type without any yield point.

5) Stress-strain relation is neither linear nor elastic [34].

As mentioned unreinforced masonry exhibits distinct oriented properties due to the influence of the brick texture order and the mortar joints and properties, which act as planes of weakness. Its failure cannot consequently be defined plainly in terms of a criterion based on the principal stresses at any point. In various loading circumstances,

different combinations of failure pattern may be took place. Failure occurs in bed joint mortar, brick-mortar interface and bricks.

Affect of bed joint direction relative to principal stresses is the main variable that must also be taken into account. Failure can occur in the joints alone or in some form of combined mechanism depending on the direction of the joints to the applied stresses, involving mortar and the masonry unit. Thus, to completely characterize unreinforced masonry failure, a three-dimensional failure surface in terms of the principal stresses, σ_1 and σ_2, and their respective orientations to the bed joint of 0 and 90° is required [35]. The fracture modes of unreinforced brick masonry subjected to various in-plane loading conditions is shown in **Figure 3.8.** In case of biaxial compression loading, failure took place as splitting in bricks at the middle of its thickness and in a direction normal to bed joints. However, still there is not enough knowledge about the failure pattern under tension-tension biaxial combination [34].

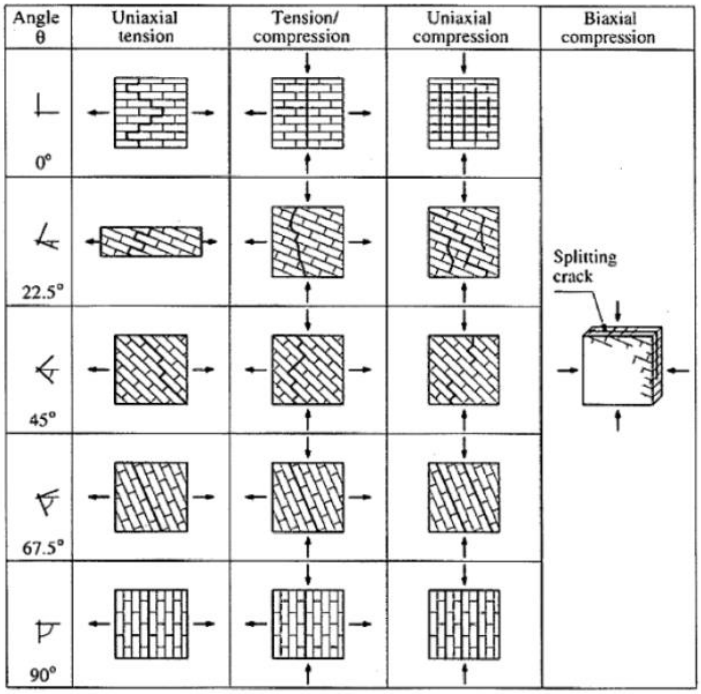

Figure 3.6 Modes of failure of URM under biaxial loading [36].

3.7 Seismic parameters of Masonry walls

3.7.1 Types of masonry wall loading in experimental program

A significant portion of our knowledge about the behavior of masonry walls impressed by external loads, have been obtained from experimental specimens on full or small scale of mentioned walls. There are four types of loading that can be used in this regard and are described as follows:

3.7.1.1 Unidirectional static loading:

In this kind of loading procedure external force applies incremental and unidirectional until failure of the specimen. The results of this kind of loading test can be used in order to compare the results obtained from other kinds of the experimental test that are better indicator of earthquake seismic loads.

3.7.1.2 Static cyclic reversal lateral loading

In this experiment type specimens are imposed to lateral cyclic loads (induced from external loads or displacements) with previously defined amplitude. In the most cases the increment of load is gradually until the fracture of the specimen. This subject is illustrated in **Figure 3.9**.

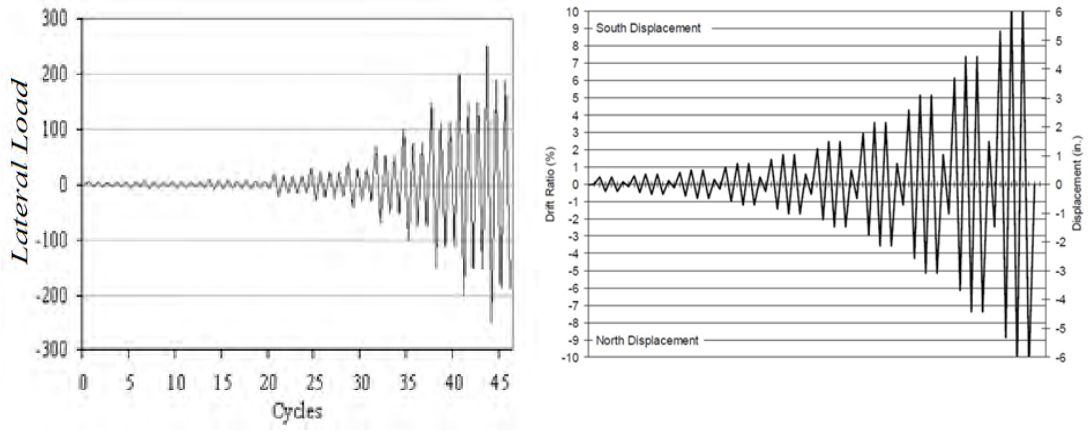

Figure 3.7 Load and displacement amplitudes in Static cyclic loading test.

As mentioned before most of the information that common design methods for seismic resistance structures are based on, are deduced form this type of experiment. In this method the reversal feature of the load that distinguishes the dynamic response of the structure from unidirectional static loading, is exist. Furthermore slowly application of the

load or displacement make possible to observe the exact behavior of the specimen under incremental load or displacement steps.

3.7.1.3 Pseudo dynamic loading

In this type of experimental procedure that has been developed in recent years, the basement of the specimen is fixed on the floor in which displacement applies to the specimens using a computer in the manner of time varying. In this kind of structural loading that mostly used in case of testing the structure verses structural components, a relatively large block of reaction slab is needed in order to absorb the reaction forces deduced from various axis of loading.

3.7.1.4 Dynamic loading test

This method that applies using a shaking table device (earthquake simulator) the specimen is subjected to input displacement with a proper scale while fixed of a shaking plate that hydraulic or electronic actuators that governs by a computer that shake the mentioned plate and simulate the real condition of an earthquake. Most of the shaking tables are able to control the displacements in horizontal and vertical directions.

Relatively rapid speed of applying load in a dynamic loading test, make impossible to inspect the specimen at the time of the test. Although with the completion of the test it becomes possible to inspect the specimen using the photos that have been taking through the test. Most of the shaking table devices are limited due to their load capacity and dimensions and therefore small scale of a structure or a structural component can be used in this kind of testing method. Difficulty of the inspection of the specimen during the test and observation of the damages imposed to the structure and limitation of the capacity of the shaking tables cased that pseudo dynamic testing method that recently has been developed be chosen as the main instrument with regard to the testing of the structural systems.

3.7.2 Hysteresis diagrams

As mentioned before cyclic reversal lateral loading procedure (pseudo static loading test) that has been developed in recent decades because of potential advantages widely is used for structural testing of construction systems in order to understand the seismic behavior (load-deflection response, strength, failure mode, ductility, energy dissipation) of masonry walls. During this loading method external force or displacement is applied to the structure with a pre-defined protocol in a cyclic reversal manner. By tracing the value of external load verses displacement of the specimen in a specified location, a distinct famous diagram (Hysteresis envelope) with close and almost symmetric reversal loops appears. Hysteresis diagrams are used in order to define the most famous seismic characteristics of structural components. The most well known features of a structure that can be specified using this method are envelope curves or skeleton curves, idealized diagram, ductility, stiffness degradation, energy dissipation capacity and equivalent viscous damping ratio. Typical shape of hysteresis diagram is illustrated in **Figure 3.10**.

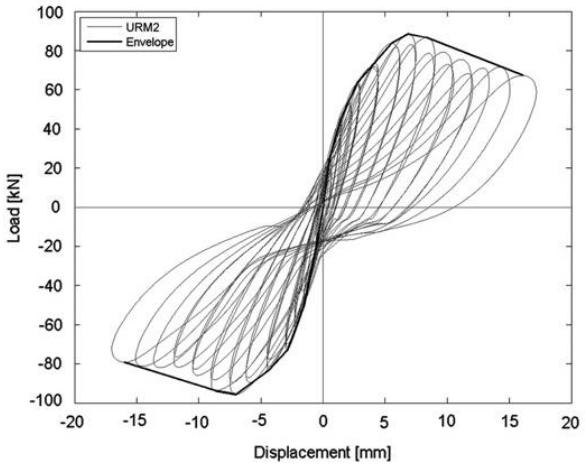

Figure 3.8 Typical shape of hysteresis envelope curve.

3.7.3 Idealization of envelope curves

To simplify design and analysis of masonry walls, concept of idealized force-displacement curves is presented by taking into account the equal energy dissipation capacity of the actual and the idealized wall [37]. Bilinear idealization for load-displacement diagrams that is suggested by Tomazevic [38] can be used in order to evaluate the in-plane seismic performance in terms of nonlinear deformability. For this purpose, elastic shear stiffness k_e was defined by the slope of the secant passing through the origin and a point on the

observed load-displacement envelope curve where the load equals 0.4 P_{peak} (As required by ASTM E 2126-02a [39]). Thereafter according to Eq.(3.1), maximum yield point (P_{yield}) of the idealized envelope is calculate considering the circumscribing an area equal to the area enclosed by observed load-displacement, between the origin, the ultimate displacement and the displacement axis.

$$P_{yield} = k_e\left(\Delta_u\sqrt{{\Delta_u}^2 - 2\,{A_{env}}/{k_e}}\right) \qquad (3.1)$$

In which A_{env} is the area under the observed load-displacement envelope curve from zero to ultimate displacement.

As suggested by Tomazevic [38] bilinear or trilinear resistance envelope can be develop for masonry shear walls as illustrated in **Figures 3.11** and **3.12** respectively in order to simplify the calculation. To idealize the experimental envelope, three limit states in the observed behavior of the tested wall are first defined:

· Crack limit, determined by displacement δ_{cr} and resistance V_{cr} at the formation of the first significant cracks in the wall, which change the slope of the envelope.

· Maximum resistance, determined by maximum resistance V_W, attained during test, and corresponding displacement δ_W.

· Ultimate state, determined by maximum displacement attained during test δ_f and corresponding resistance V_f [15].

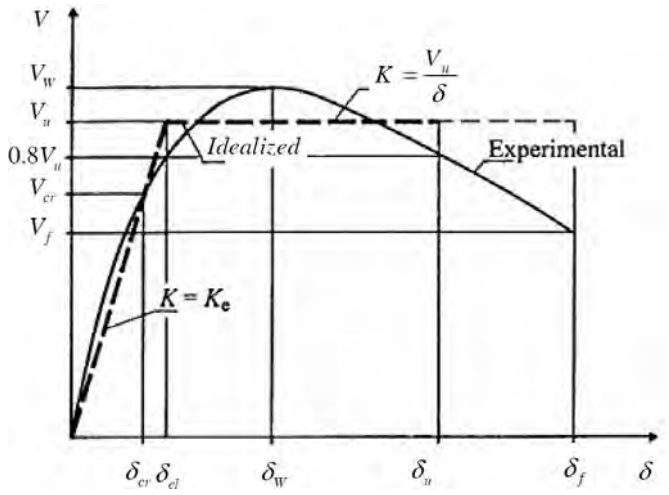

Figure 3.9 Bilinear idealization of envelope resistance curves [15, 40, 41].

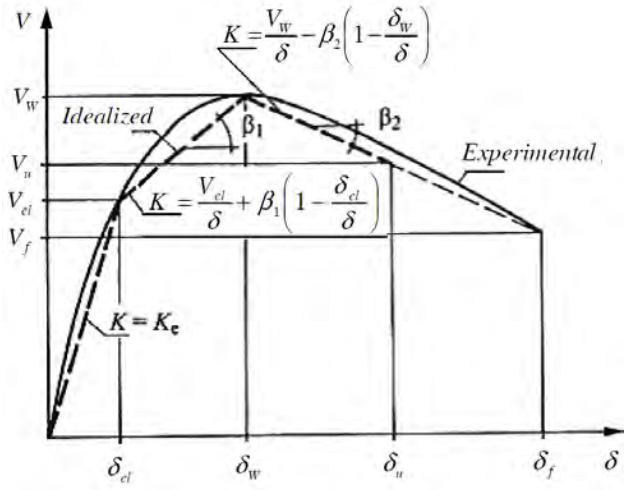

Figure 3.10 Trilinear idealization of envelope curves [15,42].

3.7.4 Pseudo-ductility

Ductility is a solid material's ability to deform under external forces; this is often characterized by the material's ability to be stretched. Ductility factor some time considered as an indicator of energy dissipation ability in structures. As we know the ductility of unreinforced masonry structures is not the ductility in a conventional sense such as the ductility of reinforced concrete which is derived from the plastic deformation of the reinforcing steel. Therefore this coefficient in case of URM structures due to special characteristics of mentioned building is very important and vital.

With the help of bilinear idealization pseudo-ductility coefficient as the most common and essential index of structures subjected to cyclic loads was calculated by the means of Eq. (3.2).

$$\mu_u = \frac{\Delta_u}{\Delta_e} \qquad (3.2)$$

Considering mentioned formulation, the pseudo-ductility it is the capacity of the specimen to deform in the inelastic range without irreparable damages or a severe degradation of the loading capacity.

3.7.5 Stiffness

Generally stiffness is the rigidity of an object, the extent to which it resists deformation in response to an applied forces [43]. The stiffness of a structural element is defined by the action effect of shear or bending moment, which causes a unit displacement or rotation of the element. The element's stiffness depends on the mechanical properties of constituent materials, the geometry and boundary restraints [15].

With regard to stiffness of the specimens in lateral cyclic loading test, the secant stiffness ($K_{s,i}$) can be calculated for each load cycles according to Eq. (3.3).

$$K_{s,i}=\frac{F_{max,i}}{\Delta_{max,i}} \qquad \text{Eq. (3.3).}$$

In which $K_{s,i}$ is the secant stiffness at the ith cycle, $F_{max,i}$ is the horizontal load at maximum displacement at ith cycle and $\Delta_{max,i}$ is relative maximum displacement.

Beside this in order to analytically determine the value of stiffness, Eq. (3.4) and (3.5) which are presented for cantilevered walls and the walls that have full restraint against rotation at the top and bottom, respectively [34].

$$K=\frac{1}{\frac{h_{eff}^3}{3I_gE_m}+\frac{h_{eff}}{G_mA_v}} \qquad (3.4)$$

$$K=\frac{1}{\frac{h_{eff}^3}{12I_gE_m}+\frac{h_{eff}}{G_mA_v}} \qquad (3.5)$$

In which:

h_{eff} wall height to the point of lateral load,

E_m elastic modulus of URM,

A_v effective shear area (assumed to be 5/6 of the gross area),

I_g the moment of inertia of the un-cracked wall cross section,

G_m the shear modulus (assumed to be $0.4E_m$).

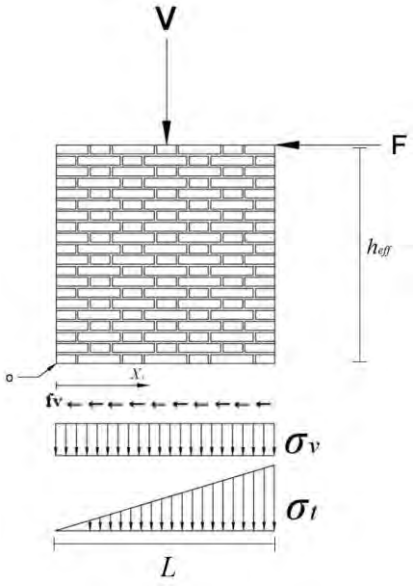

Figure 3.11 Masonry wall under horizontal lateral loading [44].

3.6 References

[1]. http://www.wisegeek.org/what-is-brick-masonry.htm

[2] Akhaveissy AH, Lateral strength force of URM structures based on a constitutive model for interface element. Lat Am J Solids Stru;8:445-461 (2011).

[3] Alecci V, Fagone M, Rotunno T, De Stefano M. Shear strength of brick masonry walls assembled with different types of mortar. Constr Build Mater;40:1038-1045 (2013).

[4]Gabor A, Ferrier E, Jacquelin E, Hamelin P. Analysis and modelling of the in-plane shear behaviour of hollow brick masonry panels. Constr Build Mater;20:308-321 (2006).

[5]Medeiros P, Vasconcelos G, Lourenغo PB, Gouveia J. Numerical modelling of non-confined and confined masonry walls. Constr Build Mater (2012).

[6] Haach VG, Vasconcelos G, Lourenغo PB. Parametrical study of masonry walls subjected to in-plane loading through numerical modeling. Engineering Structures, 33:1377-1389 (2011).

[7] Porto F, Guidi G, Garbin E, Modena C. In-Plane behavior of clay masonry walls: experimental testing and finite-element modeling, 1379-1392 (2010).

[8] Marfia S, Sacco E. Multiscale damage contact-friction model for periodic masonry walls. Comput Methods Appl Mech Engrg, 189-203 (2012).

[9] Guinea GV, Hussein G, Elices M, Planas J. Micromechanical modeling of brick-masonry fracture. Cement Concrete Res, 30:731-737 (2000).

[10] Alberto A, Antonaci P, Valente S, Damage analysis of brick-to-mortar interfaces. Engineering Procedia 10:1151-1156 (2011).

[11] Tena-Colunga A, Juعrez-Ángeles A, Salinas-Vallejo VH. Cyclic behavior of combined and confined masonry walls. Engineering Structures,31:240-259 (2009).

[12] Calderini C, Cattari S, Lagomarsino S. The use of the diagonal compression test to identify the shear mechanical parameters of masonry. Constr Build Mater, 24:677-685 (2010).

[13] X. Jianzhuang, P. Jie and H. Yongzhong, Experimental study on the seismic performance of new sandwich masonry walls Vol.12, No.1 Earthquake Engineering and Engineering Vibration (2013).

[14] Deyuan Zhou, Zhen Lei, Jibing, In-plane behavior of seismically damaged masonry walls repaired with external BFRP Wang, Composite Structures 102 9ات19 (2013).

[15] A. Bourzam, Shear capacity prediction of confined masonry walls subjected to cyclic lateral loading, PhD thesis, Kanazawa University, Japan (2009).

[16] R.Amiraslanzadeh, M. Miyajima, A.Fallahi, A. Sadeghi and S.Karimzadeh بRe port of 11th August 2012 Ahar twin earthquakes in East-Azerbaijan province of NW Iranپ International Symposium on Earthquake Engineering, JAEE, Vol.1, Tokyo, Japan (2012).

[17] M. Miyajima, A. Fallahi, A. Sadeghi, E. Ghanbari, H. Soltani, R. Amiraslanzadeh, A. Vakilazadsarabi, F. Forouzandeh and R. sheikhalizadeh, بSit e Investigation of the Ahar-Varzeghan Earthquake in NW Iran of August 11, JSCE, Disaster Report FS2013-E-0001, Japan (2012).

[18] K. Meguro, R. Soti, S. Navaratnaraj, M.Numada "Dynamic Behavior of Masonry Houses Retrofitted by Bamboo Band Meshes" 15th World Conference on Earthquake Engineering (15WCEE) Lisbon Portugal (2012).

[19] Elgawady, M. Lestuzzi, P. Badoux, M, Retrofitting of Masonry Walls Using Shotcrete. NZSEE Conference, Paper 45 (2006).

[20] Kahn, L. (1984). Shotcrete retrofit for unreinforced brick masonry, 8th WCEE, 583-590.

[21] Velazquez-Dimas, J.I. and M.R. Ehsani, Modeling Out-of-Plane Behavior of URM Walls Retrofitted with Fiber Composites. Journal of Composites for Construction. ASCE 4(4).172-181 (2000).

[22] Ganz, H.R, "Strengthening of Masonry Structures with Post-Tensioning" Sixth North American Masonry Conference. 45-655 (1993).

[23] Zezhen, N., Qi, D., Jianyou, C., Runtao, Y, A study of a seismic strengthening for multi-story brick building by additional R/C columns. 8th WCEE. 591-598 (1984).

[24] Mahdizadeh, A. Borzouie, J. Perforating the masonry walls in rehabilation of masonry buildings using center core method. 6th International conference on seismology and earthquake engineering. CD-ROM, Paper No. 11461 (2011).

[25] S. Franklin, J. Lynch, D. Abrams "Performance of Rehabilitated URM Shear Walls: Flexural Behavior of Piers" Department of Civil Engineering, University of Illinois at Urbana-Champaign Urbana, Illinois (December 2001).

[26] Schuller, M., Atkinson, R., Borgsmiller, J, Injection grouting for repair and retrofit of unreinforced masonry. 10th International brick/block masonry conference. 549-558B (1994).

[27]. Johnson, F.B. and Thompson, J.N. Development of diametric testing procedures to provide a measure of strength characteristics of masonry assemblages", Designing, Engineering and Constructing with Masonry Products, F.H. Johnson, Ed., pp. 51-57, Gulf Publishing, Houston (1969).

[28] Samarasinghe, W. "The in-plane failure of brickwork", PhD thesis, University of Edinburgh (1980).

[29] Samarasinghe, W. and Hendry, A.W. "The strength of brickwork under biaxial tension-compression", Proc. 7th International Symposium on Load Bearing Brickwork, London, pp. 129-140 (1980).

[30] Hegemier, A. et al. "Behavior of concrete masonry under biaxial stress", Proc. of the North American Masonry Conference, Boulder, University of Colorado, pp. 1-10 (1978).

[31] Naraine, K. and Sinha, S.N. "Stress-strain curves for brick masonry in biaxial compression", Journal of Structural Engineering, ASCE, 118(6), pp. 1451-1461, (1992).

[32] Lourenco, P. "Computational strategies for masonry structures", Dissertation, TU Delft, Delft, the Netherlands (1996).

[33] Zhuge, Y, Nonlinear Dynamic Response of Unreinforced Masonry under In-Plane Lateral Loads. PhD Thesis, Queensland University of Technology (1996).

[34] G. Zamani Ahari, "Structural in-plane behavior of masonry walls externally retrofitted with fiber reinforced materials" PhD thesis, Kyushu university, Japan (2013).

[35] B. Badarloo1, A.A. Tasnimi1 and M.S. Mohammadi, "Failure Criteria of Unreinforced Grouted Brick Masonry Based on a Biaxial Compression Test" Scientia iranica (transaction a: civil engineering);502-511 (2009).

[36] Dhanasekar, M, The performance of brick masonry subjected to in-plane loading. PhD Thesis, The University of Newcastle (1985).

[37] S. churilov, E. Dumova-Jovanoska, "In-plane shear behaviour of unreinforced and jacketed brick masonry walls", Soil Dynamics and Earthquake Engineering 50 85-105 (2013).

[38] Tomaževič M, Weiss P. Robustness as a criterion for use of hollow clay masonry units in seismic zones: an attempt to propose the measure. Materials and structures, 1:1ت 19, issn:1359-5997 (2011).

[39] ASTM E Committee 2126-02a Standard Test Methods for Cyclic (Reversed) Load Test for Shear Resistance of Framed Walls for Buildings, American Association State and Transportation Officials Standard (2002).

[40] Marzahn, G.: "The shear strength of dry-stacked masonry walls", LEIPZING Annual Civil Engineering Report (LACER), No. 3, Germany, (1998).

[41] Zarnic, R. and Tomazevič, M.: بAn experimentally obtained method for evaluation of the behavior of masonry infilled R/C framesپ,Proc. of the 9th World Conference on Earthquake Engrg., Tokyo-Kyoto, pp. VI-163 to VI-168, Japan (1988).

[42] Tomaževič, M. and Klemenc, I.: بSeis mic behaviour of confined masonry wallsپ, Earthquake Engrg. Struct. Dynamics, Vol. 26, pp. 1059-1071, (1997).

[43] Baumgart F, "Stiffness an unknown world of mechanical science" Injury (Elsevier) Injury Vol 31, Supplement 2 , Page 14, doi:10.1016/S0020-1383(00)80040-6 (2000).

[44] Sweeney, S.C., Horney, M.A., Orton, S.L. "Tri-Directional Seismic Analysis of an Unreinforced Masonry Building with Flexible Diaphragms. US Army Corps of Engineers, Engineer Research and Development Center (2004).

Chapter 4. Experimental program and results

4.1 Introduction

An experimental program was planned and executed in order to define masonry unit properties as well as seismic performance of masonry walls subjected to cyclic lateral loading. The experimental investigation conducted and documented in this chapter was divided in three parts. First was determination of the mechanical properties of the different components i.e. brick units, mortar and fiber concrete. The second part was spent on the experiments on mechanical properties of masonry prism such as triplet test, masonry prisms compression test and diagonal compression test. The third part of the experimental program concerned the test of four head-straight texture order brick walls under quasi static lateral loading, with two amount of vertical pre-compression load. The behavior of each specimen was discussed with emphasis on load capacity, stiffness degradation, energy dissipation, and modes of failure.

4.2 Material properties

Prior to carrying out the cyclic test on masonry panels, mechanical properties of constituent material namely bricks, mortar and fiber concrete through a set of multiple tests were obtained. Tests were conducted in line with ASTM C 109 / C109M ت12, ASTM C78 / C78M ت10, ASTM C140 ت12a, ASTM C469 / C469M ت10 [1-4] in order to determine compressive and tensile strength, module of elasticity and Poisson ratio of component materials.

4.2.1 Brick

Considering quality and high strength of Japanese bricks (having compressive strength of about 50 *MPa*) and regarding to the quality of brick units in Middle East countries we preferred to import medium strength units from china. The bricks employed were solid baked clay bricks by nominal size of 50×110×240 mm^3.

All bricks were entirely saturated before construction. In order to define mechanical properties of the bricks in line with ASTM C 67 - 12 [5], uniaxial compression tests on four specimens of 50×110×110 mm^3 size, obtained by cutting common bricks were

performed. In order to obtain the stress strain curve, Poisson ratio and Young modulus, two horizontal and vertical gauges was pasted on each specimen (See **Photo 4.1**). The results are summarized in **Table 4.1** and **Figure 4.1**. The stress-strain curves of compression tests for brick units discovered basically linear failure. No ductility was observed.

Photo 4.1. Bricks specimen for compression test.

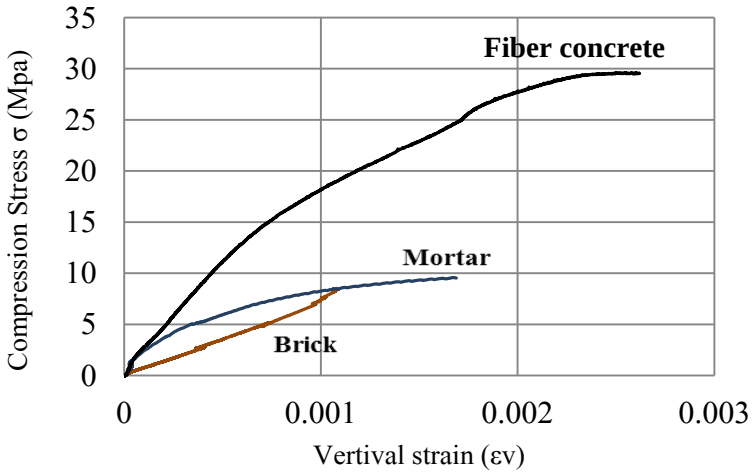

Figure 4.1 Stress-strain curves of bricks and mortar compression test.

4.2.2 Mortar

Mortar was used to join the brick units made from a pre-mix based on Portland cement, fine sand and water. Composition of component materials for mortar mixture according to ASTM C 144 - 11 [6] is reported in **Table 4.2**. The amount of water was decided to produce suitable workability. In order to evaluate compressive strength of mortar four cylindrical specimens by dimension of 50×100 were made by the same mortar as used to build the masonry prisms and masonry walls. All compressive test specimens were tested at an age of the standard 28 days. It is worth noting that masonry prisms and walls were

also tested practically at the same age. For curing, the mortar specimens were placed on water by degree of 21˚C after three days from molding until 28 days. **Photo 4.2** shows test setup and failure mode of mortar specimens.

Table 4.1 exhibits the results in terms of elastic modulus and ultimate strength, and **Figure 4.1** shows the pattern of the stress-strain curve.

Photo 4.2. Mortar compression test and failure mode.

4.2.3 Steel fiber concrete

In case of fiber concrete, component materials were mixed together by gradually adding the amount of water until the achievement of optimum consistency. Thereafter steel fibers with the length of 35 mm (see **Figure 4.3**) were gradually added to the concrete to avoid bunching in the mix. The yield and ultimate stress of the fibers were respectively 600 and 900 *MPa*. For exploring the tensile strength of fiber concrete as required by ASTM C 1609/C 1609M ت05 [7] three prismatic specimens of 100×100×400 mm^3 were produced and after 28 days of curing, were subjected to bending tests on three points

In **Table 4.2** average values of above mention experiments for all types of masonry elements are reported.

Table 4.1 Mortar and fiber concrete composition materials.

	Cement (kg/m3)	*Water (kg/m3)*	*W/C*	*Lime (kg/m3)*	*Sand (kg/m3)*	*Grave (kg/m3)*	*Steel fiber (% of cement weigth)*	*Super plastisizer (kg/m3)*
Mortar	*208*	*325*	*1.56*	*237*	*1025*	-	-	-
Fiber concrete	*270*	*177*	*0.66*	-	*935*	*900*	*51.5%*	*2.7*

Photo 4.3. Prismatic specimens prepared for rupture test.

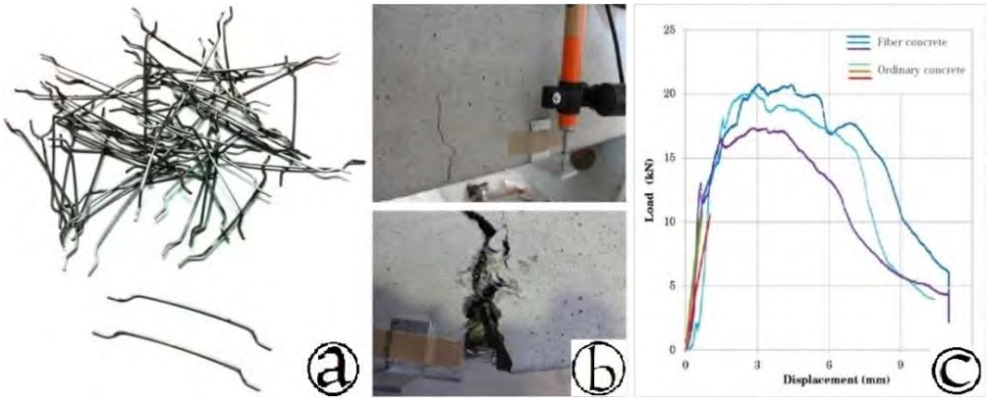

Figure 4.2 a: Steel fibers with double end hook, b: Rupture test on fiber concrete prisms, c: load displacement diagram in rupture test.

Table 4.2 Mechanical properties of masonry components.

	$\sigma_{c\ (MPa)}$	$\sigma_{f\ (MPa)}$	$E_{\ (GPa)}$	υ	*Density (kg/m³)*
Brick	8.02	0.73	9.2	0.15	1709
Mortar	10.6	0.75	28.7	0.2	1760
Fiber concrete	27	4.7	12.3	0.17	2380

4.3 Preliminary tests on masonry

4.3.1 Compressive strength of masonry

Masonry compressive strength was tested on three stack bonded prisms of five bricks each, under axial compressive loading. The main purpose was to determine mechanical characteristics of combined brick-mortar prisms and compare them with recommended value of relative standards. All prisms were performed in accordance to the code LUM B1, RILEM, 1994b [8]. The joints were kept uniform thickness of about 15 *mm* and filled with mortar. Each specimen was cured for 28 days at the ambient temperature of the laboratory with the head-straight texture order masonry walls in order to simulate the same practical condition, which was a sufficient time for hardening of the lime mortar.

In each specimen at one side, axial LVDT (Linear Variable Displacement Transducer) was placed in order to measure vertical displacement of masonry. After embedding the prisms in the jaw apparatus the axial load was applied under displacement control protocol in order to record all load displacement history.

After the test axial strain of each specimen was defined dividing the average axial displacement by initial axial length. Also the compressive stress of the prisms was calculated as the axial load divided by the initial cross section area perpendicular to the axial load direction.

Photo 4.4 and **Table 4.3** present the specimen test setup, failure mechanism and the obtained mechanical properties of masonry. The ratio of modulus of elasticity in compression was approximately 945, which was slightly (5%) less than the recommended value in EN 1996 Eurocode 6 [9].

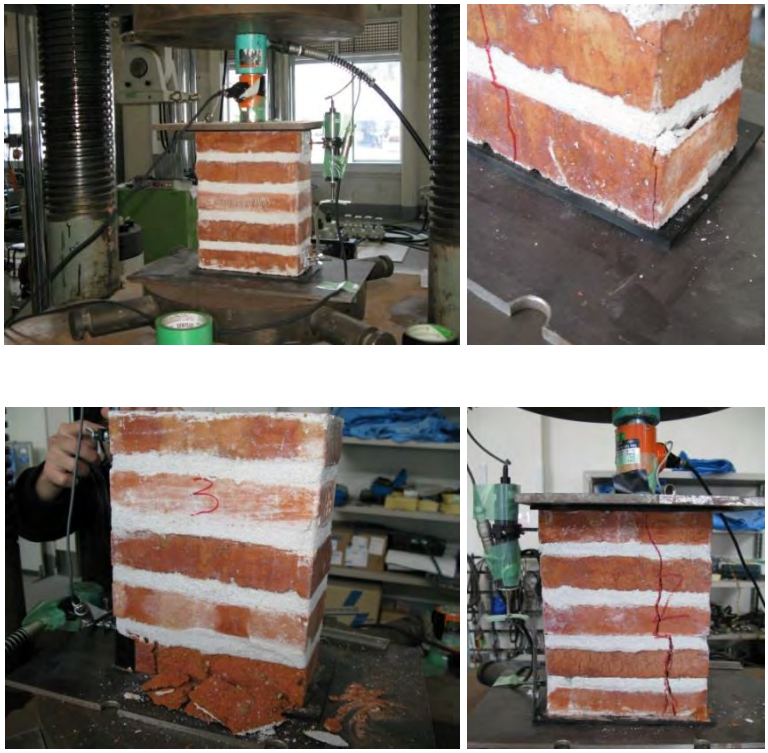

Photo 4.4. Compression test on masonry prisms.

Table 4.3 compressive strength of masonry prisms.

Sample	Max Load (kN)	Compressive strength *f* (kg/cm^2)	Modulus of elasticity *E*(kg/cm^2)	Ratio *E/f*
1	9064.1	34.3	30725	895
2	8289.9	31.4	31421	1001
3	8102.6	30.7	28811	940
	Mean *f*	32.1	30364	945
	$f_k=f/1.2$	26.8		

4.3.2 Flexural bond strength test of masonry

The main purpose of flexural bond test is to determine tensile strength among masonry units and mortar. This parameter has crucial effect on governing the failure type in masonry construction. Two methods have been provided by ASTM E 518 [24] for performing tests on flexural beams of masonry. Specimens of both methods is consists of five layer masonry wallets that should be loaded as a beam element. Method A uses concentrated loads at 1/3 points of the span (see Figure. x a). Method B uses a uniform loading over the entire span (see Fig. b) by the means of an air bag. In this study method

A was applied on three masonry wallets that have been constructed and cured for 28 days at the ambient temperature of the laboratory with the head-straight texture order masonry walls in order to simulate the same practical condition. The joints of wallets were kept uniform thickness of about 15 *mm* and filled with mortar. After embedding the prisms in the jaw apparatus for application of load two roller beams was used in order to prevent producing any shear and moment stress in the specimen. The out of plane load was applied under displacement control protocol in order to record all load displacement history. After the test and as suggested by E 518 [24], tensile strength of each specimen was defined by the means of equation xx.

$$R=\frac{(P+0.75\,P_s)l}{bd^2} \qquad \text{Eq. 4.3.2}$$

In which R is gross area modulus of rupture (MPa), P is maximum applied load indicated by the testing machine (N), P_s is weight of specimen (N), l is span, (*mm*), b is average width of specimen (*mm*), d is and average depth of specimen (*mm*).

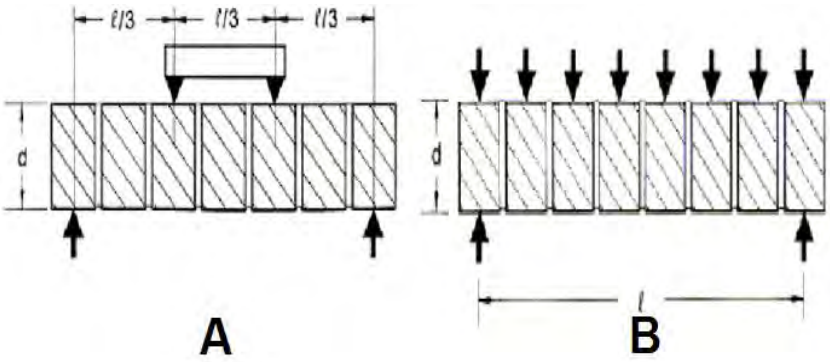

Figure 4.3 ASTM E518 Method A and B Setup.

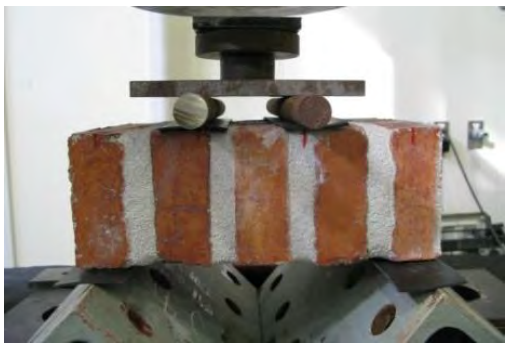

Photo 4.5 Specimen test setup for flexural bond test.

Photo 4.5 and **Table 4.4** present the specimen test setup and the results of the experimental test program. In this table, the values of flexural bond strength, *R*, were derived using Eq.4.3.2. The table shows that the values of bond strength calculated using method A are in good agreement with those tabulated in BS 5628 (0.2 MPa) [25].

Table 4.4 Specimens characteristics and results of flexural bond test.

No of specimens	Max load (N)	specimen weight (N)	specimen length (*mm*)	specimen depth (*mm*)	specimen width (*mm*)	*R* (Mpa)
1st	1680	142.688	311	240	109.7	0.19
2nd	830	142.296	310.5	235	110.1	0.10
3rd	3970	138.964	309.5	240	109.8	0.43
Mean						0.24

4.3.3 Triplet test results

In this experimental campaign triplet test with nine level of pre-compression load were performed and for each level of load, three specimens were produced and after performing recommended conditions for curing, specimens were subjected to different level of lateral and vertical loads. At first after specimen prisms are placed longitudinally in the loading position. Then lateral load was applied gradually to the bed joints of the specimen until reaching desired pre-compression stress level. End unit of specimens was supported using two sheets of steel plates to ensure a uniform load distribution (See **Photo 4.5**). Nine different pre-compression load levels were adopted (0 kN, 1 kN, 3 kN, 5 kN, 10 kN, 15 kN, 20 kN, 30 kN and 40 kN) and were kept constant, as much as possible, during the tests. This load was applied by the means of a small mobile hydraulic jack and a load cell that was embedded in the opposite side of the specimen. Then vertical load was applied to the head joint of the middle masonry unit until failure of the specimen. Displacements were imposed at a uniform rate until the failure. The use of a displacement control device allowed observation of whole loading history. A universal testing machine with a maximum loading capacity of 1000 *kN* was used to apply vertical load. Shear parameters of masonry prisms was calculated using formula 2.2 and 2.3. Values for the shear strength of the units represent average of three specimens that was vertically loaded in same pre-compression stress level. Results of triplet tests are summarized in **Table 4.4**. In this table the mean value of shear strength, maximum vertical load, pre-compression stress, and mode of failure are reported.

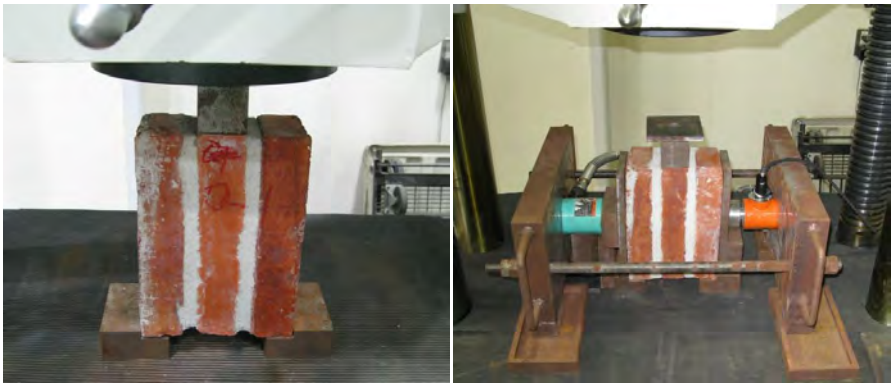

Photo 4.6. Triplet test setup for shear test on masonry prisms.

Table 4.5 Results of triplet tests.

Specimen code	Maximum vertical Load (kN)	Shear strength (MPa)	Pre-compression stress (MPa)	Failure mode
TPC-0	8.14	0.1542	0	A1
TPC-1	18.56	0.3515	0.0379	A1-A2
TPC-3	26.05	0.4934	0.1136	A1-A2
TPC-5	27.42	0.5193	0.1894	A1-A2
TPC-10	29.36	0.5561	0.3788	A1-A2
TPC-15	43.98	0.8330	0.5682	A1-A2
TPC-20	48.75	0.9233	0.7576	A1-A2-D
TPC-30	64.88	1.2288	1.1364	D
TPC-40	77.13	1.4608	1.5152	D

The failure behavior of masonry prisms under shear stress with various pre-compression stress levels as described in BS EN 1052 [10], can be represented by the Coulomb friction law, which establishes a linear relationship between the shear strength τ and the normal stress σ, using following formula:

$$\tau = \sigma \tan\phi + c \qquad (4.3)$$

Figure 4.4 shows the relation between the contact pressure and the shear strength for all performed triplet tests, as well as a linear regression carried out with the average shear strength for each series of tests. The intercept of linear regression indicates cohesion value (c), equal to 0.36 MPa and slope of the linear regression ($\tan\phi$) that indicates friction coefficient equal to 0.72. In standard masonry, the value of the friction angle seems to range between 0.7 and 1.2, according to different combinations of units and mortars [18]. The value obtained can therefore be considered acceptable. The correlation coefficient of the linear regression (R^2) is 0.967, which indicates an excellent correlation.

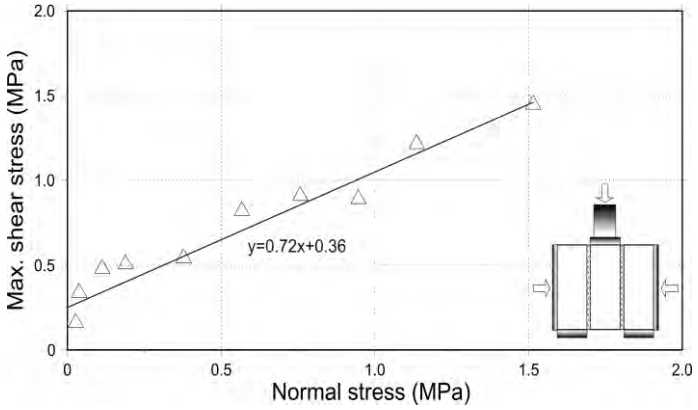

Figure 4.4 Maximum values of shear stresses in function of lateral pre-compression stress.

As described in section 2.2 failure mode of masonry in triplet test depends on pre-compression load, properties and characteristics of brick and mortar and bond strength of brick-mortar interface. Last item in turn, depends on bonding strength of mortar, specification of brick surface such as roughness and smoothness and water absorption of brick units that determines the amount of grout that will intake to the bricks.

Modes of failure for masonry subjected to triplet test are described in **Photo 4.5**. As could be expected, the dominant mode of fracture for masonry prisms was failure type A1, in which masonry fails due to separation of brick-mortar interface **(Photo 4.5 a)**. Because of low bond strength of brick-mortar inter face this type of failure is probable for masonry prisms in which lime mortar was used. However as demonstrated in **Photo 4.5 b,** with increasing the lateral load, failure type was changed from type A1 to type D.

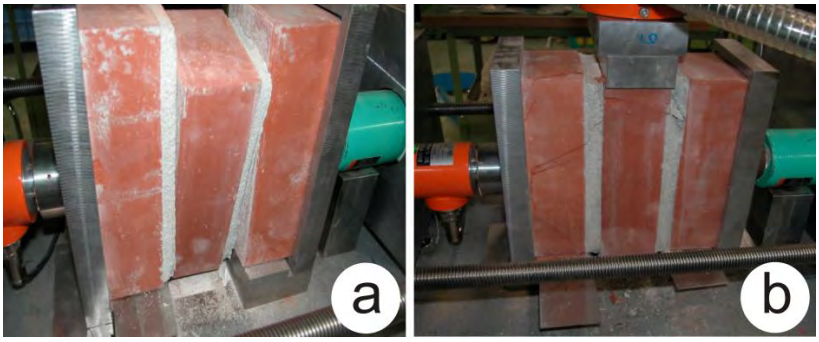

Photo 4.7. Failure modes of specimen subjected to triplet test.

4.3.4 Diagonal compression test results

Diagonal compression test procedure calls for the testing of small masonry walls with height-length (H/L) ratio of 1 in diagonal compression. In this study diagonal compression tests were performed according to ASTM E 519 [19] in order to extract the shear strength, shear strain and shear elastic modulus of 1.2 by 1.2m masonry assemblage. This experiment usually consists of square prisms by compression along one direction with a resulting of failure in diagonal tension. In this test, diagonal monotonic compression load gradually applies to the corner of the wall via hydraulic actuator until rupture of the specimen.

Test setup is composed of two steel loading shoes, which were produced by recommendation of related standard and fixed on two opposite corners of the panels. These shoes have function of distributing the load on the edges of the panels. Four specimens in scale 1:1 of 1265×1255mm^2 and thickness of 375mm size (code URM1-2 for unreinforced and CRM1-2 for reinforced panels) were performed and placed precisely along the vertical direction and loaded in compression parallel to this direction (See **Figure 4.6**).

Two kinds of apparatuses were attached to the each specimen on both sides. Linear Variable Differential Transducer (LVDT) by capacity of 50 mm (Tokyo Sokki Kenkyujo Co.Ltd, Japan) were utilizes to measure shortening of vertical diagonal and lengthening of the horizontal diagonal and strain gauge which measured strains in the center of panel, parallel to the load orientation and transverse direction. A squared area in the center of all panels was produced using a thin layer of gypsum in order to make a flat zone to paste the strain gauges. Each of these apparatuses has been installed on one side of every specimen

(**Photo 4.6**). In **Table 4.5** the result of diagonal test including three different interpretations along with shear strain, shear module and failure mode are summarized. With regard to the failure modes, two types of failure observed for masonry panels subjected to diagonal compression test as can be expected. Masonry without concrete cores, demonstrated non-diagonal brittle failure in which cracks developed through brick mortar interface without crushing the bricks (**Photo 4.7 a**) while reinforced specimen showed diagonal failure in which cracks developed from bottom to top of the specimens dividing the sample in two parts, almost symmetrically (**Photo 4.7 b**).

Non-diagonal failure counts as a brittle failure in against diagonal type. In contrast to unreinforced panels, reinforced panels preserved the monolithic after the failure and they present a less brittle failure than the unreinforced one. Mentioned difference and points can be observed on load-displacement diagrams as illustrated on **Figure 4.7, Figure 4.8**. As it can be seen, the diagram recorded for coreless panels shows a brittle failure while the diagram concerning the reinforced specimen with concrete core shows descending path after the maximum load. It should be specified that in the case of CRM 1, load-displacement diagram does not describe post peak behavior because the execution of performed test was interrupted after reaching the maximum load value. It is worth noting that in the case of specimens without cores, failure occurs because shear stress exceeds shear strength of the mortar used to realize the joints while specimen with concrete cores fails because tensile stress of the panel exceeds ultimate tensile strength of masonry.

Table 4.6 Diagonal compression test results.

Specimen Name	P_{max} (kN)	τ_1 (MPa)	τ_2 (MPa)	τ_3 (MPa)	τ_1/f_{vok}	τ_2/f_{vok}	τ_3/f_{vok}	γ	G (MPa)	FM
URM1	319.7	0.56	0.40	0.26	3.08	2.20	1.43	0.00033	1688	ND
URM 2	345.9	0.61	0.43	0.28	3.35	2.36	1.54	0.00042	1428	ND
AVGE	332.8	0.59	0.42	0.27	3.24	2.31	1.48	0.00038	1558	-
CRM1	622.4	0.94	0.66	0.44	/	/	/	0.00038	2464	D
CRM 2	515.9	0.78	0.55	0.36	/	/	/	0.00033	2309	D
AVGE	569.3	0.88	0.60	0.40	/	/	/	0.00035	2387	-

P_{max} = Maximum vertical Load, $\tau_{1=}$ Shear strength Eq. (1), $\tau_{2=}$ Shear strength Eq. (4), $\tau_{3=}$ Shear strength Eq. (5), f_{vok} = characteristic shear strength by triplet test, γ= Shear strain, G= Modulus of rigidity, FM= Failure mode.

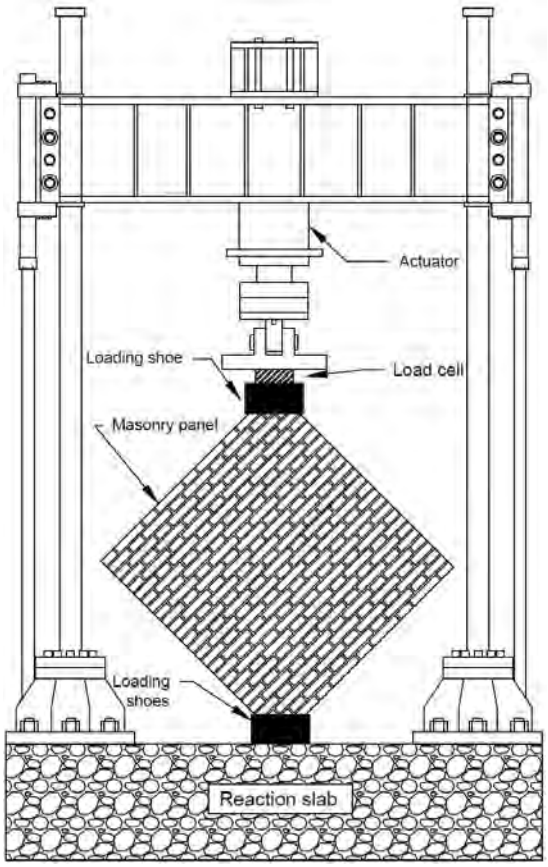

Figure 4.5 Experimental setup for diagonal compression test on masonry panels.

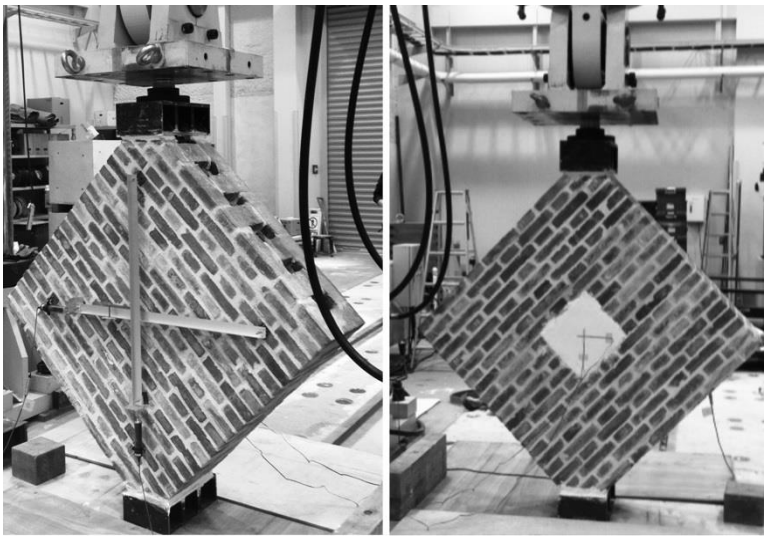

Photo 4.8. Diagonal compression test measurement devices.

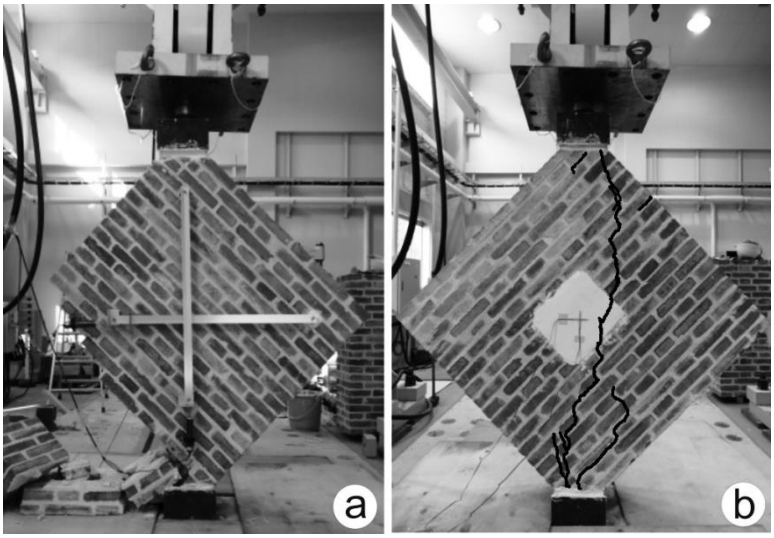

Photo 4.9. Failure modes of masonry panels subjected to diagonal compression test; (a) non-diagonal failure; (b) diagonal failure.

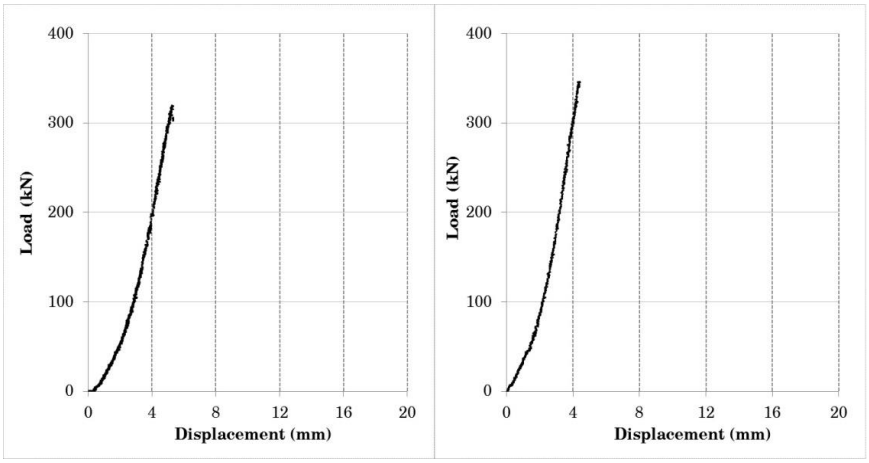

Figure 4.6 Load-displacement diagram for specimen URM1,2.

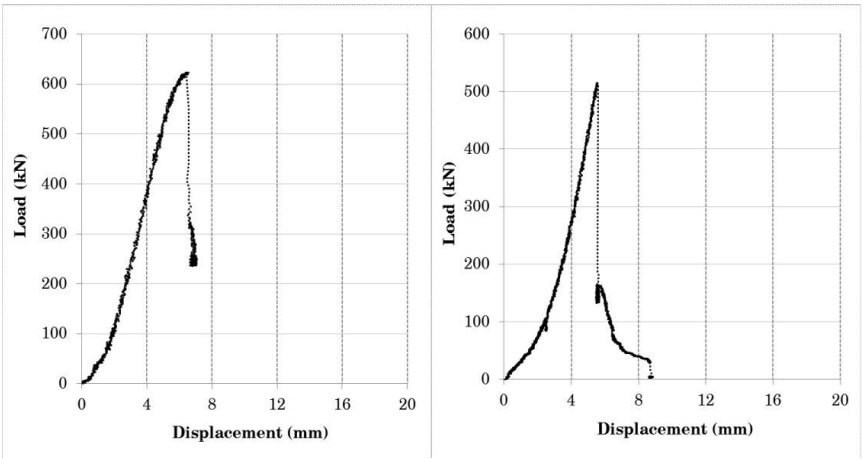

Figure 4.7 Load-displacement diagram for specimen CRM 1,2.

Relation of load applied on top of the unreinforced panels and both transverse and vertical strains in the center of specimen, under diagonal compression are included in **Figure 4.9** for comparison with those for reinforced one. As mentioned before, in some cases, the measurement equipment was removed after attaining the ultimate load to prevent it from damages due to sudden failure. It is obvious in **Figure 4.9** that although the fiber concrete reinforcement significantly increase the strength of Head-straight masonry panels, no appreciable increase in stiffness of the panels is obtained.

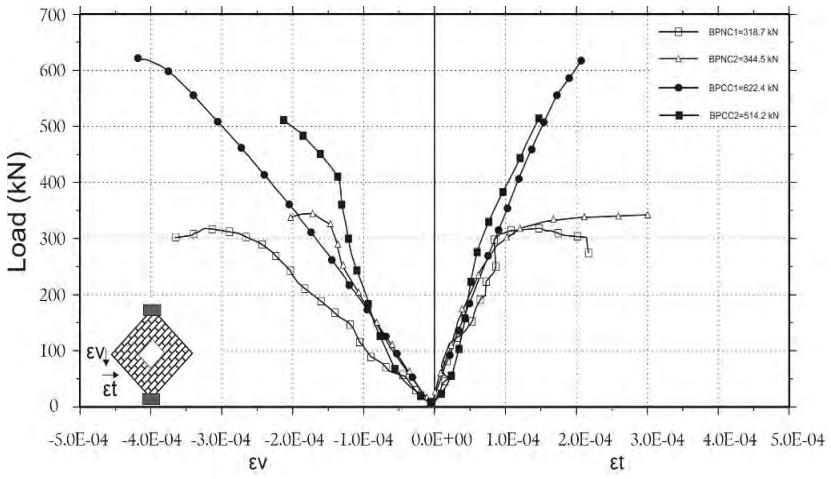

Figure 4.8 Relationship between load and both transverse ε_t and vertical ε_v strains in the center of specimens.

4.4 Cyclic test on masonry panels

In this research specimens were classified into two categories denoted by URM for the walls were laid up by Head-straight order (double Flemish texture) without in-filled fiber concrete cores and CRM for Head-straight order with inner fiber concrete cores. For each of mentioned categories two analogous specimens were built with the same masonry cohesion pattern and construction details. Out of four homological masonry walls, two of them were filled utilizing fiber concrete, after one week of curing. For performing a foundation, all specimens were placed on a mold with certain dimensions including a prefabricated mesh rebar. The foundation concrete was placed until the second layer of the wall from the bottom. Ultimately loading concrete beam (with two holes to install loading utilities) was mounted on the top of the wall. It worth noting that aspect ratio (H/L) for all specimens was considered 1 because of square shape of all masonry specimens.

The experimental program was performed in order to evaluate in-plane shear behavior and identification of shear strength, pseudo-ductility, energy dissipation and stiffness degradation of coreless and core filled head-straight masonry walls.

During cyclic test, masonry panels are subjected to reversal in-plane lateral loads such as those induced by seismic actions. In this kind of test, masonry are subjected to constant vertical forces representative of gravity dead and live load in line with horizontal cyclic displacement applied on the top of the wall. **Figure 4.10** illustrates displacement history that was applied during the test. It is known that the behavior of masonry walls when subjected to in-plane cyclic loading test is severely affected by applied vertical load [20]. Therefore in this study, tests were performed under two different levels of vertical loads. From the inspected prototype in brick masonry building one up to three stories, values for vertical stresses close to 1-2 kg/cm^2. Therefore to provide results due to general validity two vertical load levels with magnitudes of 1 and 2 kg/cm^2 were considered.

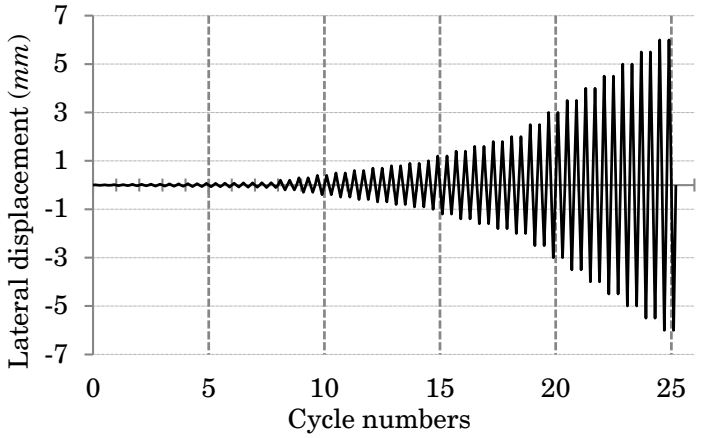

Figure 4.9 Cyclic displacement time-history.

4.4.1 Test setup and instrumentation

Test setup regarding to perform cyclic test is illustrated on **Figure 4.11** and **Photo 4.8.** Load application was manually controlled by hydraulic actuators with load capacity of 400 *kN* in horizontal direction and 3000 *kN* in vertical direction. The magnitude of vertical stress on the panel was kept constant during the test. Necessary vertical load intensity was manually tuned to the required level by use of screw-operated jack. Thereafter horizontal displacement until reaching the target displacement were imposed to the specimen in one direction and then in the opposite direction for two cycles. Details of dimension and

arrangement of main LVDTs in the tests to measure displacements is illustrated in **Figure 4.12** and **Photo 4.9** and were recorded automatically by a computer and data acquisition system. A large amount of experimental data was acquired during the test and the appearance and propagation of cracks were carefully observed by eye. The most important results are summarized and presented through the obtained failure modes, force-displacement hysteresis curves, envelope of force-displacement hysteresis curves, stiffness degradation of the walls at repeated cycles and energy dissipation capacity.

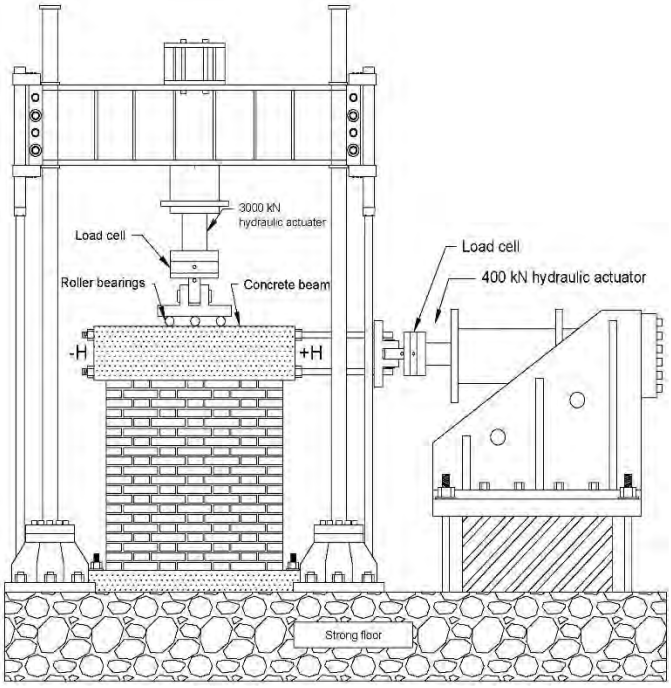

Figure 4.10 Test setup system for cyclic test on masonry panels.

Photo 4.10. Loading system in cyclic test.

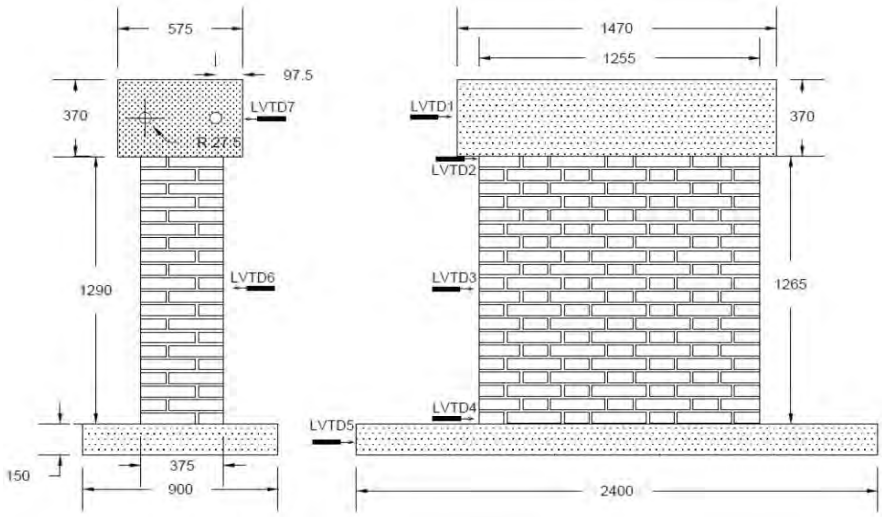

Figure 4.11 Dimensions of specimens for cyclic test and arrangement of LVDTs transducers.

Photo 4.11. Loading system in cyclic test.

4.4.2 Failure modes

Generally speaking, the walls exhibited flexural failure mode. In process of loading the flexural moment at the bottom of the panel accumulated as the load increased. Once the tensile stress associated with the flexural moment exceeded the tensile strength of the mortar, the first horizontal cracks appeared at the margin of the first or second from the bottom and tend to develop to the center of the panel. After the cracks on the sides of the

specimens joined together in the center, all the walls started to demonstrate rocking behavior revolves around the center (see **Photo 4.10**).

With present research, it was confirmed that behavior of internal concrete columns was highly integrated with the behavior of masonry components with aspect ratio less than 1.0. No bulged phenomenon was observed during the tests. For all the specimens no diagonal cracks were observed throughout the test and the failure of the walls caused by separation from the bottom. It was observed that the cracks on both front and back side developed synchronously, indicating symmetrical precision of construction and loading condition.

Photo 4.12. Cracking pattern and failure modes of the specimens.

4.4.3 Result of horizontal load and displacement

After performing load-displacement test on masonry walls a large amount of experimental data was acquired. The most important results are summarized and presented in **Table 4.6**, including cracking load P_{cr}, peak load P_{peak}, failure load P_u and their corresponding displacements. According to rocking behavior of all specimens failure load was considered corresponding load on displacement of 3 *mm*. Based on the results, a significant improvement of shear capacity of CRM walls compared with URM walls was achieved. The maximum forces obtained for each load step in the core filled specimens, were higher than the corresponding load obtained in the unreinforced specimens, varying within the range of 24 to 106%. Same effects were achieved in the other two limit states. Beside this in term of deformation capacity, the data expressed an interesting effect related to the crack limit (Δcr). The data presented **Table 5** revealed a higher amount of cracking limit of unreinforced walls loaded with vertical stress of 1.0 kg/cm^2 than that of the strengthened walls. Reverse consequence was achieved in conjunction with peak displacement (Δ_{peak}).As mentioned the deformation capacity in ultimate limit state of the all specimens was decided 3*mm* in order to rocking behavior.

Table 4.7 Specimen parameters and results of load-displacement.

Specimen	Length *L[mm]*	Height *L[mm]*	*H/L*	σo Vertical stress [kg/cm^2]	*σo /fk*	P_{cr}*(kN)*	Δ_{cr} *(mm)*	θ_{cr}%	P_{peak}*(kN)*	Δ_{peak} *(mm)*	*Pu (kN)*	Δ_u *(mm)*
URM 1	1255	1265	1	1	0.031	17.61	0.183	0.014	30.26	0.57	26.86	3.0
URM 2	1255	1265	1	2	0.063	19.93	0.193	0.015	35.06	0.60	47.79	3.0
CRM 1	1255	1265	1	1	0.031	21.09	0.133	0.010	45.12	0.81	52.80	3.0
CRM 2	1255	1265	1	2	0.063	31.18	0.150	0.012	72.56	1.20	79.95	3.0

4.4.4 Hysteresis diagrams and envelope curves

Hysteresis diagrams as well as envelope curves can trace the development of horizontal displacement on top of the wall during the cyclic loads. The hysteresis diagrams and

envelope curves for each specimen are shown in **Figure 4.13** and **Figure 4.14.** Envelope curves comprehensively reflect the shear capacity and seismic response of the wall.

From the envelope curves and hysteresis diagrams, loading process of all the walls can be divided into three steps:

1-*Elastic phase*:

This step starts from the beginning of the experiment to the appearance of the first limit state. Hysteresis curves as well as envelope curves remained linear and the residual displacement of the specimens was small. Load was applied to the specimens in all stages under displacement control. At the end, cracks were appeared on the sides of the specimens on the margin of the bottom. The hysteresis loops is narrow and its area is negligible.

2-*Plastic phase*:

This stage starts from cracking of the specimen to the peak load. As was expectable, rocking behavior was occurred for masonry walls after the load reached to a certain amount. Therefore corresponding load to 0.017% of lateral drift was defined as peak load for all the obtained results. There was an obvious increase in this stage on residual displacement as well as hysteresis loop area. In the first or second margin from the bottom horizontal cracks developed inward and tend to join up.

3-*Failure and rocking phase*:

This stage starts from peak load (plastic stage) to the load corresponding to displacement 3 *mm* (Drift ≈ 0.023%). The peak value of the cyclic load for almost all specimens remained unchanged due to wobbling of the wall revolving around the center and the residual displacement was increased significantly. The area under the hysteresis loops increased sharply. Generally speaking hereinafter the specimens demonstrate consistent reaction against horizontal lateral loads.

As is noticeable from **Figure 4.13**, hysteresis loop of specimens CRM 1 and 2 covered a larger area than specimen URM 1and 2 indicating improved energy dissipation capacity for concrete filled masonry panels which signify the role of slim fiber concrete columns on absorbing the energy imposed to the structure. This issue will be discussed in detail in the later chapters. Similarly the same conclusion can be drawn from the comparison

between the cyclic loops regarding to specimens CRM 1 and CRM 2 which indicate that the increase of vertical stress on cyclic test lead to raise of energy dissipation by the specimen. This performance was also detected in some other studies as well [20,21,22].

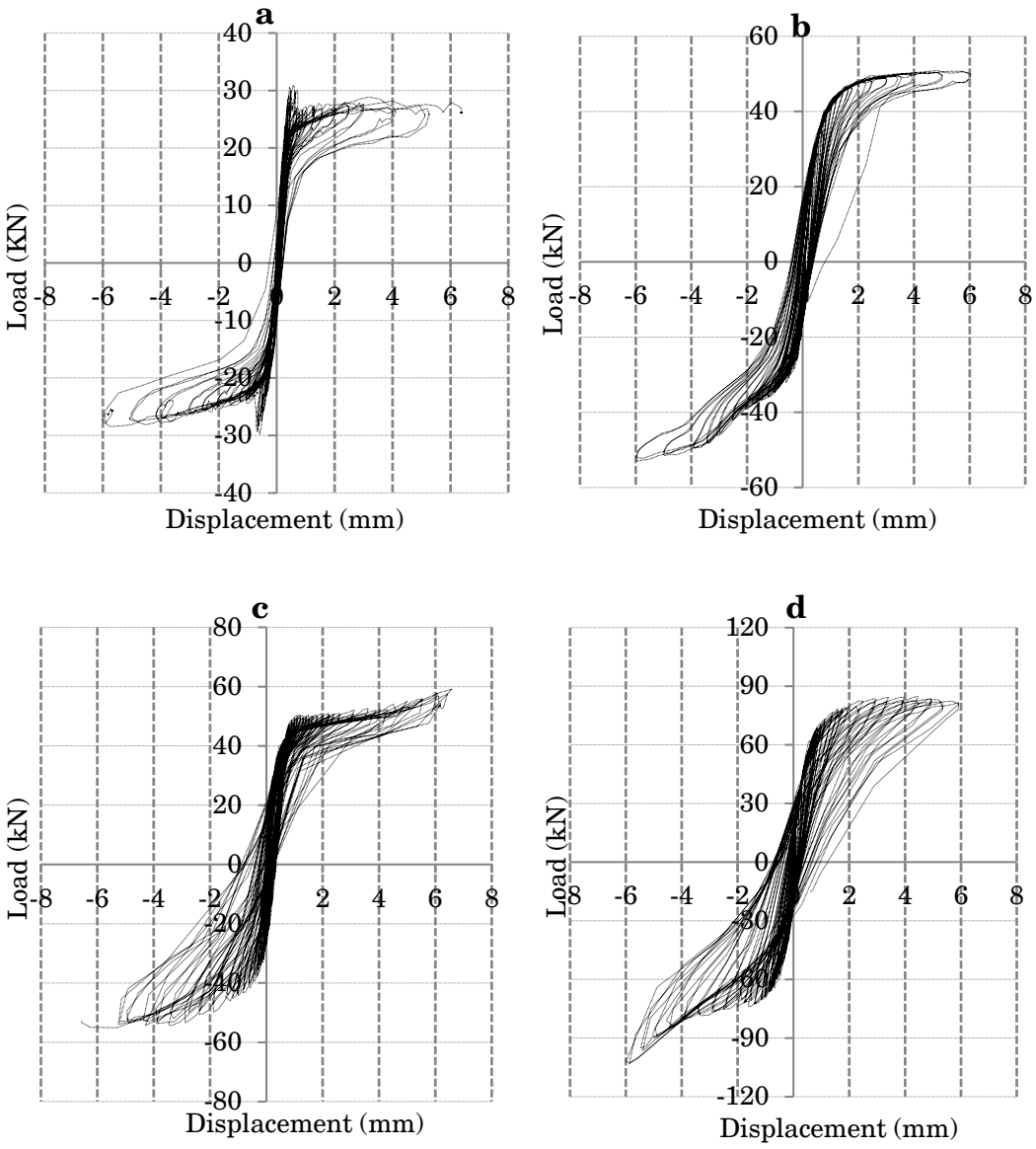

Figure 4.12 Horizontal load-displacement diagrams (hysteresis curves), (a,b) respectively for URM 1,2 and (c,d) respectively for CRM 1,2.

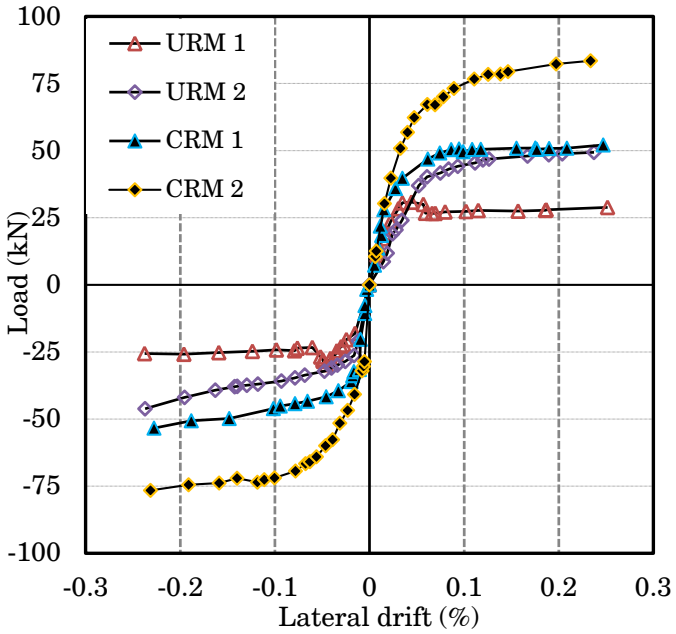

Figure 4.13 Envelope curves of hysteresis diagrams.

4.4.5 Idealization of force-displacement diagrams

In order to simplify design and analysis of masonry walls, concept of idealized force-displacement curves is presented by taking into account the equal energy dissipation capacity of the actual and the idealized wall [20]. Bilinear idealization for load-displacement diagrams that is suggested by Tomazevic [22] was used in order to evaluate the in-plane seismic performance in terms of nonlinear deformability. For this, elastic shear stiffness k_e was defined by the slope of the secant passing through the origin and a point on the observed load-displacement envelope curve where the load equals 0.4 P_{peak} (As required by ASTM E 2126-02a [23]). Thereafter according to Eq.(4.5.1), maximum yield point (P_{yield}) of the idealized envelope was calculated considering the circumscribing an area equal to the area enclosed by observed load-displacement, between the origin, the ultimate displacement and the displacement axis.

$$P_{yield} = k_e\left(\Delta_e\sqrt{\Delta_e{}^2 - 2\,\frac{A_{env}}{k_e}}\right) \qquad (4.5.1)$$

In which A_{env} is the area under the observed load-displacement envelope curve from zero to ultimate displacement.

Figure 4.15 demonstrates a comparison of the results obtained from the bilinear idealization of the observed load-displacement envelops. As it can be seen from the graph

despite strengthening significantly improves the lateral load resistance capacity of the walls, the deformation capacity of the walls was not proportionally increased in all the specimens. Also the strengthened panels loaded with higher level of vertical stress exhibited higher strength than the unreinforced one. This behavior can be described by the higher principal tensile stresses required to produce failure of the panel [20].

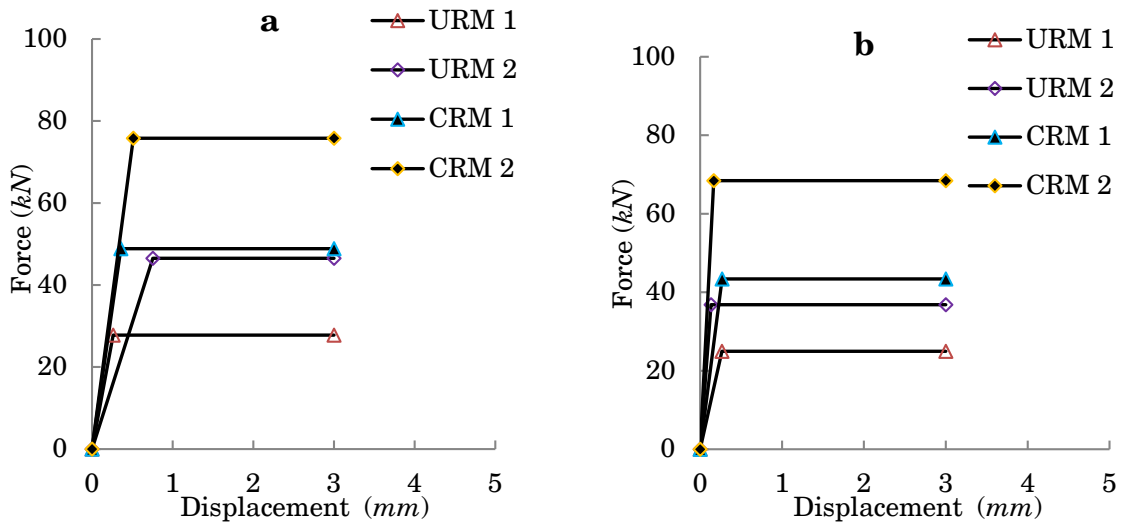

Figure 4.14 Comparison of the idealized load-displacement diagrams. (a) Positive part of the curves (b) Negative part of the curves.

4.4.6 Pseudo-ductility and stiffness degradation

With the help of bilinear idealization ductility coefficient as the most common and essential index of structures subjected to cyclic loads was calculated by the means of equation (4.5.6).

$$\mu_u = \frac{\Delta_u}{\Delta_e} \qquad (4.5.2).$$

The bilinear idealization discovered interesting consequence related to the ultimate ductility factor (μ_u). The results presented in **Table 4.7** revealed a higher ductility of URM and CRM walls loaded with the higher level of vertical pre-stressed load (2 kg/cm^2). The data show that, despite existing of concrete cores increased load capacity of the wall in all limit states, however because of reduction of the displacement in the mentioned

states, no appreciable difference between pseudo-ductility of cored masonry walls in comparison with URM specimens pre-stressed with the same level of vertical load was observed. With regard to stiffness of the specimens, the secant stiffness ($K_{s,i}$) was calculated for each load cycles according to Eq. (4.5.3).

$$K_{s,i}=\frac{F_{max,i}}{\Delta_{max,i}} \qquad \text{Eq. (4.5.3).}$$

In which $K_{s,i}$ is the secant stiffness at the ith cycle, $F_{max,i}$ is the horizontal load at maximum displacement at ith cycle and $\Delta_{max,i}$ is relative maximum displacement. The results in stages: K_e, K_{cr} ,K_{peak} and K_u (See **Table 4.7**) indicated a sharply increase between the stiffness of coreless and core filled panels. The increase varies in the range of 62ـ101%, indicating that concrete cores have significant and effective role in the increase of the stiffness of the panels. In term of deformation capacity, CRM 2 was the first that started to crack, while URM 2 was the last. Quite different and inconsistent results on displacement at elastic limit were obtained. CRM 1 exhibited its maximum load capacity in crack limit at a very low level of displacement of 0.133 *mm,* while URM 2 reached the stage of cracking load capacity at a displacement of 0.193 *mm.* As mentioned before for all specimens the ultimate displacement was decided 3 *mm* because of rocking behavior.

Table 4.8 Results of stiffness and pseudo-ductility factor

Specimen	P_{cr} (kN)	Δ_{cr} (mm)	P_{peak} (kN)	Δ_{peak} (mm)	P_u (kN)	Δ_u (mm)	P_e (kN)	Δ_e (mm))	K_{cr} (kN/mm)	K_{peak} (kN/mm)	K_u (kN/mm)	K_e (kN/mm)	μ_u
URM 1	17.61	0.18	30.26	0.57	26.87	3.0	26.36	0.26	96.23	53	8.95	99.81	11.35
URM 2	19.93	0.19	35.01	0.60	47.79	3.0	41.67	0.44	103.51	58.44	15.93	170.13	13.34
CRM 1	21.09	0.13	45.12	0.81	52.80	3.0	46.14	0.31	159.17	56.05	17.60	161.85	9.78
CRM 2	31.18	0.15	72.56	1.2	79.95	3.0	72.10	0.34	207.83	60.46	26.65	284.25	11.96

Figure 4.16 demonstrates the development of stiffness degradation with increasing of displacement cycles in the cyclic test. All the walls demonstrate similar stiffness degradation with the increase of lateral displacement. This trend of degradation complies with a power function that is not remarkably different among the walls [22]. As it is

obvious, the secant stiffness of the walls sharply decreased at the elastic limit, the degradation speed of the stiffness slow down significantly from the end of elastic stage to the plastic stage and then tend to be constant at the failure step. In case of cored panels, it seems that vertical pre-compression load level has much effectiveness on the decay of stiffness degradation slope.

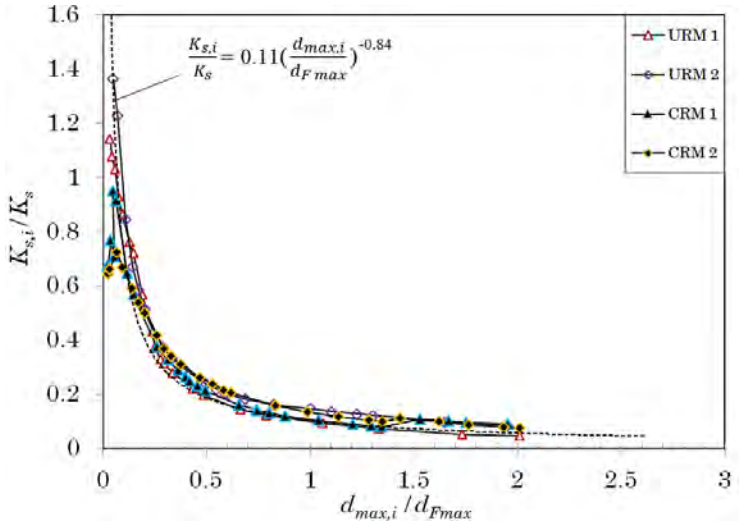

Figure 4.15 Stiffness degradation curves referring to URM and CRM walls.

Tomaževič has discovered that, this trend of degradation complies with a power function according to Eq. (4.5.4) [20,22]:

$$\frac{K_{s,i}}{K_s} = \alpha\,(\frac{d_{max,i}}{d_{Fmax}})^{\beta} \qquad \text{Eq. (4.5.4)}$$

In which, K_s is the secant stiffness at elastic limit, d_{Fmax} is the displacement at maximum horizontal, α and β are stiffness degradation parameters. These parameters depend on the horizontal load history and per-compression stress value on top of the wall. α=0.11 and β=-0.84 were obtained by regression analysis of the experimental degradation curves for all head-straight masonry walls.

4.4.7 Energy dissipation

As described in previous section the coefficient of equivalent viscous damping (ζ_e) is often selected to describe the energy dissipation in various mechanisms such as cracking, nonlinear behavior, interaction with other elements, etc., and it represent the combined effect of all the dissipation mechanisms [20]. In this study the concept of dissipated (E_{Dis}) and stored (E_{sto}) energy was employed to estimate the equivalent viscous damping. The

dissipated energy was calculated by the area enclosed by the hysteresis curves in each cycles. On the other hand stored potential energy was defined by the area under the hysteresis loops and displacement axis. In this regard, a Matlab code was developed to calculate the area enclosed by each hysteresis loop. The average values corresponding to dissipated and stored energy for each target displacement are shown in **Figure 4.17** and **Figure 4.18.**

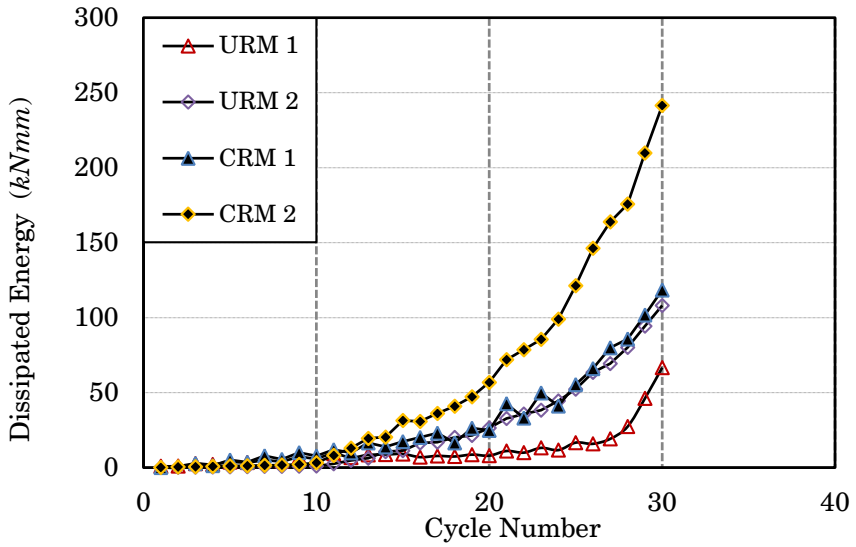

Figure 4.16 Dissipated energy in each displacement target.

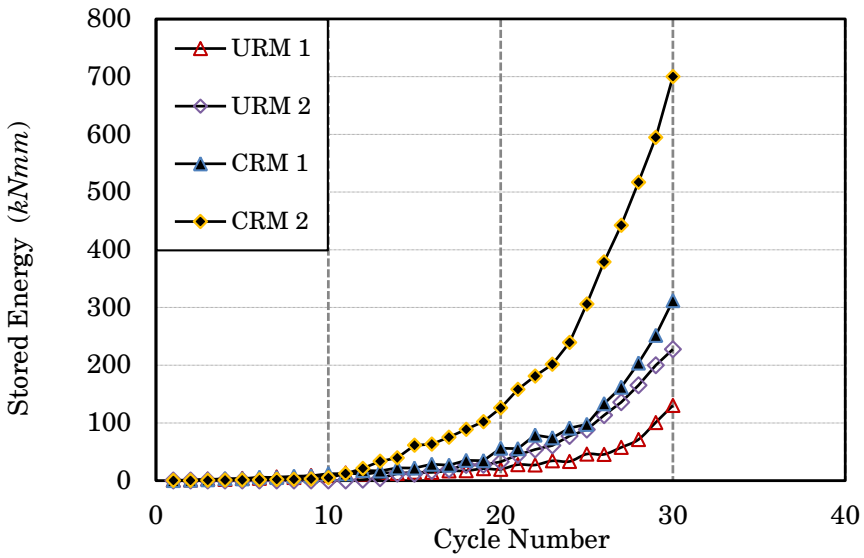

Figure 4.17 Stored energy in each displacement target.

All the masonry specimens demonstrated analogous performance in term of energy dissipation capacity. Generally the both energies increased gradually for both URM and CRM walls as the load increase, but the in case of CRM walls, the effect of pre-compression stress is very obvious on the increase of dissipated energy.

As was discussed in previous section for masonry walls under cyclic lateral loads, by equating both dissipated and stored energies, the value of the coefficient of equivalent viscous damping (CEVD) can be obtained by Eq. (4.5.5) [20].

$$\zeta_e = \zeta_{hys} = \frac{1}{4\pi}\frac{E_{Dis}}{E_{sto}} \qquad (4.5.5)$$

The coefficient of equivalent viscose damping for each specimen was estimated and presented in **Table 4.8**. Obtained results proof that vertical load has direct impact on the value of CEVD. It is interesting to note that in case of coreless panels increasing vertical stress, affect positively on the value of CEVD while this stress affect negatively for the value concerning to CRM walls. Considering URM walls the increase of CEVD was about 12% however this value for CRM walls was achieved about -16%.

Stage / Specimen	ζ_e(%)
URM 1	4.92
URM 2	5.50
CRM 1	5.64
CRM 2	4.74

Table 4.9 Coefficient of equivalent viscous damping for masonry walls.

4.5 References

[1] ASTM Committee C109/C109M-12, "Standard test method for compressive strength of hydraulic cement mortars (using 2-in. or [50-mm] cube specimens)", American Association State and Transportation Officials Standard (2012).

[2] ASTM Committee C78 / C78M-10e1, "Standard Test Method for Flexural Strength of Concrete (Using Simple Beam with Third-Point Loading)", American Association State and Transportation Officials Standard, (2010).

[3] ASTM Committee C140-12a, Standard Test Methods for Sampling and Testing Concrete Masonry Units and Related Units, American Association State and Transportation Officials Standard, (2012).

[4] ASTM Committee C469/C469M-10, Standard Test Method for Static Modulus of Elasticity and Poisson's Ratio of Concrete in Compression, American Association State and Transportation Officials Standard (2010).

[5] ASTM Committee C 67 - 12, Standard test methods for sampling and testing brick and structural clay tile, American Association State and Transportation Officials Standard (2012).

[6] ASTM Committee C 144 -11, Standard specification for aggregate for masonry mortar, American Association State and Transportation Officials Standard (2011).

[7] ASTM Committee C 1609/C 1609M ت 05, Standard Test Method for Flexural Performance of Fiber-Reinforced Concrete (Using Beam With Third-Point Loading), American Association State and Transportation Officials Standard (2010).

[8] Rilem. Technical recommendations for the testing and use of constructions materials, LUM B1, Compressive strength of small walls and prisms, (b) (1994).

[9]Eurocode 6.Design of masonry structures Part1-1: General rules for reinforced and unreinforced masonry structures. EN1996-1-1:2005,CENBrussels; (2005).

[10] EN 1052-3(E), Methods of test for masonry, Part 3: Determination of initial shear strength, European standard (2002).

[18]. Pluijm Rvd. Out of Plane Bending of Masonry Behaviour. PhD Thesis. Eindhoven University of Technology, The Netherlands, (1999).

[19] ASTM E 519-2010. Standard test method for diagonal tension (shear) in masonry assemblages. American Society for Testing Material, (2010).

[20] S. churilov, E. Dumova-Jovanoska, In-plane shear behaviour of unreinforced and jacketed brick masonry walls. Soil Dynamics and Earthquake Engineering 50 85-105 (2013).

[21] Haach VG. Development of a design method for reinforced masonry subjected to in-plane loading based on experimental and numerical analysis. PhD thesis. Universidade do Minho, Escola de Engenharia, Guimarعes, Portugal; (2009).

[22] Tomaževič M, Weiss P. Robustness as a criterion for use of hollow clay masonry units in seismic zones: an attempt to propose the measure. Materials and structures, 1:1ت 19 issn:1359-5997,(2011).

[23] ASTM E Committee 2126-02a Standard Test Methods for Cyclic (Reversed) Load Test for Shear Resistance of Framed Walls for Buildings, American Association State and Transportation Officials Standard (2002).

[24] ASTM E 518/E518 M-10 Standard Test Methods for Flexural Bond Strength of Masonry, American Association State and Transportation Officials Standard (2010).

[25]British Standards Institution (BSI), بUse of masonry: Code of practice for use of masonry, unreinforced masonry.پ BS 5628: Part 1, London (1992).

Chapter 5. Summary and conclusion

5.1 Summary

This research presents a complete experimental protocol for core less and core filled Head-straight masonry walls. Experimental program was needed as this kind of construction has been used frequently in regions of high seismic risk and there were no previous experimental information available about its seismic performance of such structures. Present study contributes to an improved insight into the in-plane behavior of masonry walls considering the influence of pre-compression load levels.

As mentioned there are different types of texture order for brick masonry construction in the world. Among these different methods, the one which is very customary especially in Middle East countries is Head-straight order. Because of special arrangement of brick units, regular interval voids appear all at the height of the wall. These kinds of brick walls due to presence of internal voids are highly susceptible to collapse in moderate to strong earthquakes.

Although shear and seismic parameters of masonry constructions were investigated in both experimental and analytical studies [1-6], there is no published data about the shear and seismic parameters of Head-straight walls with internal voids. It was hypothesized that filling mentioned voids by fiber concrete may affect positively on mechanical parameters and failure model of mentioned masonry structures. So in present study the effect of filling mentioned voids by steel fiber concrete on seismic behavior of these walls were studied. Experimental program have been established and specimens were classified into two categories denoted by URM (for the walls were laid up by Head-straight order without in-filled fiber concrete cores) and CRM (for Head-straight order with inner fiber concrete cores). For each of mentioned categories two analogous specimens were built with the same masonry cohesion pattern and construction details. Shear parameters also were investigated using Triplet and diagonal method that are two most famous and well-known standards. In contrast of diagonal test, Triplet test is a straight forward testing procedure and it has a unique formulation to calculate the value of shear strength of masonry prisms. In case of diagonal compression test the obtained data are exposed to

various kinds of interpretations. Therefore the outcomes of last testing method were discussed for all kinds of interpretations.

Static cyclic reversal loading was performed in order to investigate seismic parameters such as hysteresis diagrams and envelope curves, idealized envelope curves, pseudo-ductility, stiffness and stiffness degradation mechanism, energy dissipation capacity, and coefficient of equivalent viscous damping (CEVD) of aforementioned Head-straight oriented panels. As mentioned before, observations following past earthquakes and experimental programs have shown that piers between openings are the most vulnerable part of a masonry building and the failure of masonry construction in many cases is associated from the failure of piers. Accordingly in this study concerning height to length ratio and dimension of cyclic test specimens was considered in order to synchronize the behavior of the model with seismic response of unreinforced and reinforced masonry piers that exhibit a flexural mode of failure.

Two unreinforced and two reinforced panel was constructed and due to investigate on the effect of vertical pre-compression stress, two level of load was applied on top of the specimens. The value of pre-compression was decided in order to duplicate the stress state at bottom margin of piers in one and two story brick masonry structures. Also comparison was made among the obtained data for reinforced and unreinforced panels.

5.2 Findings and conclusions

Considering the results of diagonal test as reported on **Table 4.5,** shear strength of reinforced panels (CRM 1,2) due to existing fiber concrete was increased about 70% in comparison with unreinforced one. It is interesting to note that there was no significant difference in shear strain of URM and CRM panels. Hence module of rigidity rose by the same amount of the shear strength. Also, considering the reinforcement, existing of concrete cores, in addition to increases the ultimate strength of panels, changes the brittle behavior of specimen to a ductile one. In experiments, specimen without cores fails upon reaching ultimate shear strength of the masonry. In contrast, concrete cored panels demonstrated descending path after reaching the maximum value of the load. Furthermore, with regard to failure modes of masonry panels subjected to diagonal compression test, concrete cores changed the failure mode of the panels from non-

diagonal failure to a diagonal one. This behavior occurs because of existing of fiber concrete cores that weaves the elements of the specimen together, avoiding separation of the panel.

As mentioned and illustrated before, the results of diagonal compression test are exposed to various kinds of interpretations [7, 8]. Therefore in this research the outcomes of diagonal compression test were evaluated by the means of mentioned different formulations. The results have shown that there were substantial differences between shear strength values obtained by the three types of interpretations. However shear strength value determined by the diagonal compression test using formula (5) is very close to the one calculated by formula (2.2) on the data resulting from the triplet test. Eurocode 6 estimated and tabulated f_{vko} (shear strength of masonry) relating to different types of mortar and masonry units. The values obtained by triplet test and diagonal compression test using third interpretation (Formula 5), though not coincident, are the closest to those proposed by Eurocode 6 (0.2 *MPa*). Therefore, referring to the diagonal compression test, in order to predict shear strength of Head-straight masonry structure, it can be considered that value of the shear strength calculated by formula (5) is the most suitable and reliable one. As described in section 2.4.2 this formula is obtained by adopting the Turnaček-Cacovic criterion [9] referring to the stress state at the center of a panel which was assumed as an isotropic and homogeneous material. Thus it can be concluded that ASTM E 519 standard regulation estimates shear strength of brick panels more than the value that were obtained directly by triplet test or the one tabulated on Eurocode 6. Also this overestimation on shear strength will lead to overrating the value of module of rigidity. Concerning the choice of the more appropriate type of test, the fact that emerged from the present study permit to assert that the triplet test is very straightforward and provides reliable data results and accordingly it can be considered the more convenient as well as more suitable one.

After performing static cyclic loading test, a monographic investigation was performed to characterize seismic performance of mentioned walls, such as energy dissipation, pseudo-ductility and stiffness degradation.

From the experimental program for cyclic loading test summarized in this paper, the following observations can be made:

1- About failure category as was anticipated (because of high strength of masonry units and small amount of H/L ratio) rocking mechanism was observed in all test specimens. This phenomenon mostly occurs in masonry piers between openings. In case of URM 1 because of small amount of vertical stress, peak load was observed on hysteresis diagram as well as envelope curves.

2-experimental results proof that, internal concrete columns increased lateral resistance of the Head-straight masonry panels in all limit states. This increase of lateral resistance in case of URM 1 and CRM 1 in crack limit was 20% and in ultimate limit was 97%. It is interesting to mention that despite the increase of the load in cracking limit, corresponding displacement was decreased up to about 30%. This can be due to the effect of the cores on the increasing of the stiffness of the walls. Also for URM 2 and CRM 2 the enhancement of lateral resistance in cracking and ultimate limit states was 56% and 107% which reveal that concrete cores will affect greater if the level of vertical stress increase.

3- Level of pre-compression load showed direct correlation with the lateral resistance of the walls. For URM 1,2 and CRM 1,2 the wall loaded to a higher pre-compression load, achieved higher lateral capacity. The amount of this increase for URM walls for crack limit was 13% and for CRM walls was 48%. This kind of behavior also was observed in other studies as well [10,11]. This behavior can be explained by the higher principal tensile stresses needed to generate failure of the walls.

Figure 5.1 shows the effect of existing concrete cores and also pre-compression stress on the value of load in all limit stats. It is obvious that the value of lateral load resistance was increase in each limit states. The amount of increase in failure state is much more that the others. As is obvious from the **Figure 5.1** strengthening and the level of pre-compression has minimum effect on the value of cracking load. Therefore it can be conclude that concrete cores significantly affect post-cracking behavior of this kind of construction system.

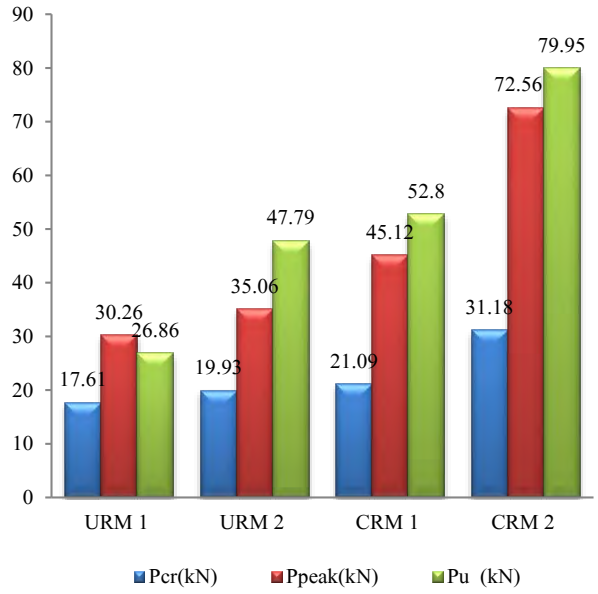

Figure 5.1 Lateral load resistance of URM and CRM panels in all limit states.

4-In conjunction with stiffness, all the panels demonstrate similar degradation process during the test. Secant stiffness of the masonry panels decreased sharply at elastic phase. The degradation speed slows down significantly from the end of the elastic phase to the plastic stage and tended to be constant at the failure phase. Coreless panels clearly exhibited lower initial stiffness than concrete cored ones, and a more rapid decrease in the first phase. Beside this, existing internal concrete cores demonstrated obviously positive effect on the development of the stiffness of the specimens in all stages. This increase in some cases was about 40%. Also in case of cored panels, it was found that the amount of vertical pre-stress value has much more impact on the enhancement of stiffness of the specimens.

Results of stiffness are summarized in **Figure 5.2**. As it is obvious with the progress of the test value of stiffness in all limit state was decreased. Also the effect of pre-compression on the stiffness in case of concrete core panels is much more considerable. Beside this the value of elastic stiffness and cracking limit stiffness in low level of per-compression are very close together indicating that the bilinear idealization become more accurate if the value of vertical load is not high.

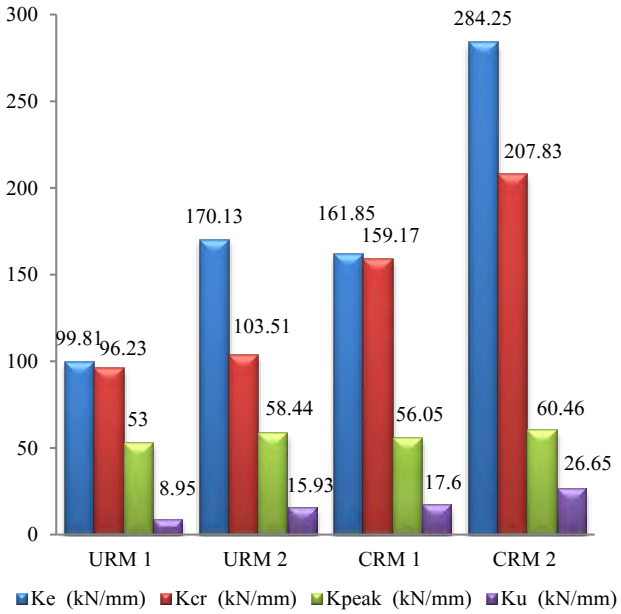

Figure 5.2 Value stiffness of URM and CRM panels in all limit states.

5-Analysis of energy revealed that with the progress of the experiment energy dissipation capacity at elastic stage was negligible (about 2% of ultimate dissipated energy at failure stage). This value was constantly increased in plastic limit but in the failure stage the slope was more sharply and in the final step reaches its maximum value. Also the results showed that the wall with a higher pre-compression level demonstrate higher energy dissipation capacity. It is interesting to note that for URM 1 despite other specimens, the amount of dissipated energy was almost constant in two firs limit stages. Coefficient of viscose damping (CEVD) was calculated and analyzed in this report. The value of CEVD for URM walls was increased up to about 12% as the load increased. On contrary for CRM walls this amount was decreased about -16%. Beside this for masonry with low level of pre-compression load, existing concrete columns increased the value of CEVD up to about 15%. But in case of high level of vertical load mentioned amount become -14%. This behavior can be describe by high amount of the stiffness of the specimen CRM 2 that results from the existing of internal concrete cores. **Figure 5.3** graphically illustrates the value of CEVD and pseudo-ductility factor for all URM and CRM panels.

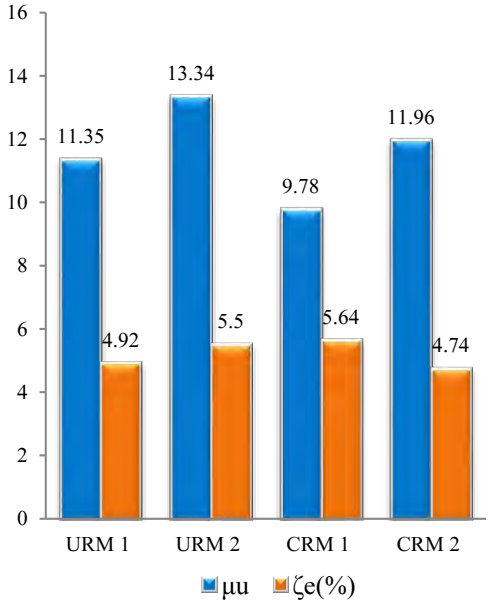

Figure 5.3 Value of pseudo-ductility and CEVD of URM and CRM panels.

Eventually as the result of this research work, it was concluded that head-straight masonry construction (with internal concrete cores) can be considered as suitable methods for in-plane enhancement of URM walls. The experimental study clearly indicated that strengthened system not only had excellent strength, stiffness and pseudo-ductility, it also controlled the damage to brittle wall piers, thus providing safety against sudden failure. Moreover referring to the diagonal compression test, in order to predict shear strength of Head-straight masonry structure, it should be considered that value of the shear strength calculated by adopting Turna$_{c}$ek-Cacovic criterion [9] referring to the stress state at the center of panels, is the most suitable and reliable one and is very close to the one calculated resulting from the triplet test.

Regarding to the out of plane characteristics of cored and coreless panels, it can be anticipated that thin fiber concrete columns by maintaining the integrity of masonry elements will positively affect the out of plane behavior of the walls.

In this context, further theoretical research should be conducted not only on the characterization of concrete cores but also on the description of the out-of-plane behavior under simulated seismic load. Hence, we can succeed to results that can provide accurate guidelines for design and implementation of this kind of masonry constructions.

5.3 Future works

Some issues in this research work which needs more investigation are presented here and recommended as the extension of this study:

1. Developing numerical analysis to generate FEM model of Head-straight texture order masonry walls in order to investigate more about the role of internal concrete columns on shear and seismic parameters of this kind masonry walls.

2. Further experimental test must be accomplished in order to evaluate the effect of H/L ratio on seismic performance of this kind of construction system.

3. Experimental study must be performed in order to investigate the effect of concrete cores on out of plane behavior of concrete filled masonry walls.

4. Analytical study should be prepared due to formulate the lateral resistance of mentioned masonry walls.

5. Further experimental test can be accomplished in order to investigate the effect using steel rebar instead of steel fibers inside to voids of Head-straight masonry walls.

5.4 References

[1] A. Gabor, E. Ferrier, E. Jacquelin, P. Hamelin, Analysis and modelling of the in-plane shear behavior of hollow brick masonry panels, Construction and Building Materials 20, 308-321, (2006).

[2] P. Medeiros, G. Vasconcelos, P.B. Lourenغo, J. Gouveia, Numerical modelling of non-confined and confined masonry walls. Construction and Building Materials 41, 968-976, (2013).

[3] V.G. Haach, G. Vasconcelos, P.B. Lourenغo, Parametrical study of masonry walls subjected to in-plane loading through numerical modeling. Engineering Structures 33, 1377-1389, (2011).

[4] S. churilov, E. Dumova-Jovanoska, In-plane shear behavior of unreinforced and jacketed brick masonry walls. Soil Dynamics and Earthquake Engineering 50, 85-105, (2013).

[5] F. da Porto, G. Guidi, E. Garbin, C. Modena, In-Plane behavior of clay masonry walls: experimental testing and finite-element modeling, Journal of Structural Engineering 136;11, 1379-1392 (2010).

[6] A. Tena-Colunga, A. Juعrez-Ángeles, V.H. Salinas-Vallejo, Cyclic behavior of combined and confined masonry walls, Engineering Structures 311 , 240-259 (2009).

[7] L. Binda, G. Cardani, G. Castori, M. Corradi, A. Saisi, C. Tedeschi, Procedure sperimentali per la determinazione delle caratteristiche della muratura, In: Borri A, editor. Manuale delle murature storiche , vol. I. Roma, Tipografia del Genio Civile, 316ت8, (2011).

[8] S. Chiostrini, L. Galano, A. Vignoli, On the determination of strength of ancient masonry walls via experimental tests, In: Proc. 12th world conference on earthquake, (2000).

[9] V. Turnaچek, F. Cacovic, Some experimental results on the strength of brick masonry walls, In: Proc. of the 2nd international brick masonry conference United Kingdom Stoke-on-Trent, 149ـ56 , (1971).

[10] ASTM Committee C78 / C78M-10e1, Standard Test Method for Flexural Strength of Concrete (Using Simple Beam with Third-Point Loading), American Association State and Transportation Officials Standard, (2010).

[11] ASTM Committee C140-12a, Standard Test Methods for Sampling and Testing Concrete Masonry Units and Related Units, American Association State and Transportation Officials Standard, (2012).